NASA Technical Memorandum 58223 NASA-TM-58223 19800016876

Orbiter/Shuttle Carrier Aircraft Separation: Wind Tunnel, Simulation, and Flight Test Overview and Results

D. J. Homan, D. E. Denison,
and K. C. Elchert

May 1980

NASA
National Aeronautics and
Space Administration

Lyndon B. Johnson Space Center
Houston, Texas 77058

NASA Technical Memorandum 58223

Orbiter/Shuttle Carrier Aircraft Separation: Wind Tunnel, Simulation, and Flight Test Overview and Results

D. J. Homan
Lyndon B. Johnson Space Center
Houston, Texas

D. E. Denison and K. C. Elchert
Rockwell International Space Division
Downey, California

NASA
National Aeronautics and Space Administration

Scientific and Technical Information Office

1980

CONTENTS

TABLES

FIGURES

SUMMARY

The approach and landing test phase of the Space Shuttle Program presented the problem of carrying the Orbiter aloft atop the Shuttle Carrier Aircraft, a modified Boeing 747, and separating the two vehicles in a safe and reliable manner. Five Orbiter free flights were flown using basically the same separation procedures. These separation procedures were designed using analytical prediction techniques and mathematical modeling that were the result of 3 years of scale-model wind tunnel testing, engineering analysis, engineering simulations, and vehicle flight testing. The wind tunnel testing provided the initial information for building a separation aerodynamic data base to support both off-line digital simulations and man-in-the-loop simulations. The simulations served as a starting point for separation procedure formulation and crew training. Verification of the aerodynamic data base and mathematical modeling techniques was accomplished with flight test data retrieved through the Shuttle Carrier Aircraft load measurement system. The load measurement system also provided data for real-time assessment of separation parameters during the actual flights. Comparison of actual separation trajectories and analytically predicted trajectories revealed excellent agreement between the two and instilled confidence in testing and prediction techniques to be used to support the orbital flight test phase of the program.

INTRODUCTION

During the approach and landing tests conducted at the NASA Dryden Flight Research Center (DFRC), Edwards, California, the Orbiter was required to separate unpowered from the Shuttle Carrier Aircraft (SCA), relying only on the lift generated by its wings. The mere size of the Orbiter (figs. 1(a) and 1(b)) created the problem of finding an aircraft capable of carrying it to a suitable altitude for release. This problem was solved by modifying a Boeing 747 specifically for carrying and launching the Orbiter. The solution to the problem of separating the unpowered Orbiter from the SCA is the subject of this report.

This paper discusses (1) the wind tunnel testing and engineering simulations used to generate the aerodynamic data base and flight test procedures, (2) the load measurement system (LMS) and flight test program used to generate flight data for comparison and verification of predictions, and (3) the results of the Orbiter/SCA separations performed during the approach and landing test (ALT) program. The appendix is an analytic discussion of the computer program.

It should be noted that Alan L. Carter, DFRC, was responsible not only for the successful incorporation of the LMS into the flight test program but also for the acquisition of the SCA data required by the NASA Lyndon B.

Johnson Space Center (JSC) and Rockwell International Space Division engineers during and following each flight. The calibration data and equations for the load measurement system, along with all postflight corrections to the data, were available only through his personal efforts.

George M. Glenn, McDonnell Douglas Corporation, Houston Astronautics Division, Houston, Texas, assisted in the development of the postflight data reduction program and was instrumental in the overall success of the separation aerodynamics subsystem for the ALT program.

In compliance with NASA's publication policy, the original units of measure have been converted to the equivalent value in the Systeme International d'Unites (SI). As an aid to the reader, the SI units are written first and the original units are written parenthetically thereafter.

SYMBOLS

a	acceleration, m/sec^2
$\bar{c}$	mean aerodynamic chord, m
C_D	drag coefficient, $D/\bar{q}S$
C_L	lift coefficient, $L/\bar{q}S$
C_M	pitching moment coefficient, $M/\bar{q}S\bar{c}$
$L_{B_{ref}}$	Orbiter body reference length, m
N_Z	normal acceleration, g
$\ddot{R}$	linear acceleration, m/sec^2
T	time, sec
V	velocity, m/sec (knots) equivalent airspeed
α	angle of attack, deg
ΔN_X	relative longitudinal acceleration, g
ΔN_Z	relative normal acceleration, g
ΔX	relative longitudinal separation distance, m
ΔZ	relative vertical separation distance, m
δ_e	Orbiter elevon deflection, deg
θ	pitch attitude, deg

$\dot{\theta}$ pitch rate, deg/sec

$\ddot{\theta}$ pitch acceleration, deg/sec^2

Subscripts:

o Orbiter

c Shuttle Carrier Aircraft

cmd command

sep separation

OVERVIEW

Figure 1 shows the Orbiter mated to the Boeing 747 that was modified for use during the ALT program and gives basic vehicle dimensions and configuration details. Figure 2 is a flow diagram that traces the testing and analysis aspects of the separation problem that is discussed here in terms of wind tunnel testing, simulations, the load measurement system, inert flights, captive-active flights, and free flights.

Approximately 1400 hours of wind tunnel testing provided the aerodynamic data base from which analyses and off-line simulations were used to generate the first procedures required for separation. This initial look at procedures determined the data requirements and planning for the captive phase of the flight test program. Man-in-the-loop simulations incorporated the results from previous analyses with the experience of the respective flightcrews to (1) optimize the separation procedures and techniques, (2) generate simulated flight data to debug and exercise postflight data reduction programs, and (3) give some insight into the implementation of the information to be gained during the actual flight program. Four of the eight captive flights produced useful separation data that were incorporated into previous analyses to obtain the final set of separation conditions and procedures to be used on the five ALT flights. The final section of the report contains a discussion of the free-flight test results.

WIND TUNNEL TESTING

The Orbiter/SCA data base was developed through an abbreviated schedule of wind tunnel tests performed during a 22-month period. The final Separation Aerodynamic Data Book was published in November 1976 (ref. 1). The tests were divided into four major categories as shown in table I.

The first category, configuration development, involved a set of tests designed to gather data on various proposed configurations as a first approximation at optimizing both mated vehicle climb performance and Orbiter/SCA

separation performance. Two basic Orbiter configurations (with and without the tailcone[1]) were tested; a range of Orbiter incidence angles and Orbiter elevon deflections was covered; and various drag-reducing attach structure fairings were assessed. The tests were conducted using two model scales, two facilities, and a range of Mach numbers and Reynolds numbers to provide a means for correlating and abbreviating future tests throughout the program.

The "mated data base" test provided performance, stability, and control data for the mated vehicles in the launch configuration. The test also provided basic isolated SCA data and proximity data for both vehicles at a separation distance of zero meters, or at the instant of separation. The tailcone-on Orbiter configuration was used for the entire test. Orbiter elevon and body flap effects and SCA stabilizer effects on the proximity data were obtained during this test. Data from this test were used as a basis for establishing initial target conditions for separation.

The "mated verification" test used the same model as the mated data base test but was performed in a different facility. This test replicated runs from the mated test to establish confidence in previous data and expanded the mated data base with the tailcone-off Orbiter data.

The "separation data base" test provided data for decaying the proximity effects of each vehicle on the other, from their maximum influence in the mated configuration to free stream where neither vehicle influenced the other. Data were taken with the SCA and Orbiter mounted on separate balances and stings to allow the vehicles to be positioned at various distances apart in the same tunnel at the same time.

A matrix of the basic configurations tested during the program is shown in figure 3. The amount and quality of data obtained during these tests and the sensitivity of these data permitted elimination of two complete tests from the wind tunnel test program.

SIMULATIONS

The separation aerodynamic data base developed through the wind tunnel test program was incorporated into the off-line and man-in-the-loop engineering simulations that were used to formulate the separation maneuver.

Two off-line digital simulations were implemented on computer systems at the Rockwell International Space Division and at JSC. The major emphasis of these programs was to perform parametric studies of the separation maneuver to determine how it was affected by airspeed, Orbiter elevon setting, Orbiter incidence angle, Orbiter center-of-gravity (c.g.) location, the tailcone, aerodynamic data tolerances, proximity aerodynamics, winds, turbulence,

---

[1]The tailcone was an aerodynamic fairing placed over the aft end of the Orbiter to reduce drag and SCA tail buffet and improve the performance of the mated vehicle.

nonequilibrium conditions, and premature separation of one or more attach points. The studies were also used to evaluate emergency Orbiter jettison procedures during the inert and ferry flight tests. The off-line simulations incorporated mathematical models of each vehicle's flight control system, equations of motion, and algorithms for combining the aerodynamic data needed to "fly" the simulations. The computer program that was run at Rockwell International Space Division was formulated and checked out at McDonnell Douglas Corporation, St. Louis, whereas the program run at JSC was a modification of the existing space vehicle dynamics simulation (SVDS) program. The SVDS program was modified (with Orbiter/SCA data, mass properties, etc.) by McDonnell Douglas Astronautics Company, Houston (MDAC-H), and both programs were compared for compatibility of results.

Five man-in-the-loop simulations were run to obtain engineering data on the best way to proceed with the mated and separation sections of the flight test program. These simulations introduced, into the analysis and planning, the pilot techniques required to assure good separation of the two vehicles.

The first of the simulations was a two-body, six-degree-of-freedom, man-in-the-loop real-time flight simulation. The SCA crew station was a fixed-base simulator with an out-the-window display of the horizon, whereas the Orbiter crew station was a moving-base fighter cockpit station that was modified to include a rotational hand controller (RHC) and dedicated separation switches and displays. The simulator had the capability of representing the flight characteristics of the SCA and the Orbiter during the mated flight, the separation transient, and the free flight of each vehicle.

The next three simulations were flown in fixed-base simulators. Two of the simulations used a manned Orbiter crew station with a "canned" SCA trajectory, and the third used a manned SCA crew station with a canned Orbiter trajectory. The canned portion of each simulation was computer generated using mathematical models of the flight control system and equations of motion similar to those used in the off-line simulations. The SCA simulation was flown by the SCA pilots and was used to investigate pilot capabilities for attaining separation initial conditions, optimum procedures to minimize altitude loss during the "pushover" maneuver, and procedures for acquiring separation data during the captive-inert and captive-active flight phases the of ALT.

The Orbiter simulations were run in the avionics development laboratory at Rockwell International Space Division, Downey, California, and in the crew procedures evaluation simulator at JSC. These simulations investigated the effects of pilot steering techniques, aerodynamic variations, configuration variations, winds, gusts, and turbulence on the Orbiter separation.

The fifth simulation was flown at DFRC in conjunction with a wake vortex study that used the Boeing 747 before it was modified to carry the Orbiter. The 747 was equipped with smoke generators on each wingtip to mark the vortices created by the wings. F-104 and T-38 aircraft were flown by the Orbiter crews and DFRC test pilots in formation with the 747 to simulate a nominal separation maneuver, from SCA pushover through Orbiter separation.

The Orbiter was simulated by the smaller planes that flew in the same vertical and horizontal position as the mated Orbiter during the pushover, but it was laterally displaced about 60 meters to the right of the 747. When the SCA pilot called "launch ready," the simulated Orbiter (F-104 or T-38) performed the nominal separation steering and the SCA performed its postseparation bank maneuver. The flights were designed to obtain qualitative data on postseparation clearances between the two vehicles and to obtain vortex avoidance distances.

LOAD MEASUREMENT SYSTEM

The LMS for the Orbiter/SCA was developed by the Boeing Company, Aerospace Division, Kent, Washington. The LMS was designed to measure and record the attach forces between the two vehicles during the mated portion of each flight. An overall view of the LMS is shown in figure 4. The load cells were thin-walled cylinders instrumented with strain gages to measure axial and shear forces, and were located on each of the three Orbiter/SCA attach struts (fig. 5).

Figure 6 shows an exploded view of the aft load cell. The forward load cell measured the relative vertical and side forces at the forward attach point. The left aft load cell measured the relative vertical and drag forces at the left aft attach point, whereas the right aft load cell measured the relative vertical, drag, and side forces at the right aft attach point. These forces were recorded onboard the SCA and also telemetered to the DFRC control room, where they were displayed in real time on strip-chart recorders. The forces were also combined mathematically to display the relative normal (ΔN_Z) and axial (ΔN_X) accelerations between the Orbiter and the SCA and the instantaneous Orbiter pitch acceleration ($\ddot{\theta}$). These strip-chart data provided quick-look information for rapid postflight analysis and provided a basis for making a real-time decision to separate on the initial tailcone-off free flight.

The recorded forces were used in conjunction with recorded time histories of the SCA attitudes, rates, and accelerations as input to a computer program. The program was designed to take this information and calculate (for specified portions of each flight) the aerodynamic coefficients for the Orbiter in proximity to the SCA, the SCA in proximity to the Orbiter, and the mated vehicles. The Ground Reduced Aerodynamic Coefficients and Instrumentation Errors (GRACIE) program was used to verify and adjust the aerodynamic data base provided by the early wind tunnel testing with actual flight data. (See the appendix for a description of the GRACIE program.)

INERT FLIGHTS

The inert-captive phase of the ALT program was flown with two separation objectives: first, to demonstrate the Orbiter/SCA airworthiness within the operational envelope required to accomplish the ALT and, second, to conduct

a preliminary evaluation of the Orbiter launch profile and procedures. Three taxi tests and five flights were performed with the Orbiter unmanned and unpowered and with all control surfaces locked in position. The Orbiter was configured as follows for all five flights.

Weight	638 764 newtons
c.g.	64.5 percent $L_{B_{ref}}$
Tailcone	On
Incidence angle	6°
Elevon	-1° (up)
Body flap	-11.7°
Rudder	0°
Speed brake	0°

The taxi tests were performed with the mated Orbiter/SCA configuration to evaluate handling qualities during the takeoff roll, and braking and steering performance during the landing roll.

Following these tests, the mated configuration was flown five times. The first four inert flights were flown to obtain takeoff and climb performance data; to investigate stability and control envelopes, flutter response, and buffet and loads boundaries; and to perform airspeed calibration checks.

Inert flight 4 focused on evaluating configuration variables associated with the launch maneuver, as reflected by the buffet levels and aircraft handling characteristics. During this flight, the SCA inflight spoilers were deployed for the first time and the aircraft performance was assessed based on the special thrust ratings on the engines. These two items were of major importance to the separation maneuver because the special rated thrust (SRT) increased the climb ceiling for the mated configuration, allowing separation to occur at a higher altitude, and the inflight spoilers decreased the lift on the SCA just prior to separation, creating a high relative normal acceleration between the two vehicles at separation. This flight provided engineers their first look at a separation-related parameter in the form of the incremental effect of the inflight spoilers on each vehicle in close proximity.

Inert flight 5 obtained data during two simulated launch maneuvers starting at ceiling altitude and terminating after approximately 20 seconds of steady-state data following the "launch ready" call by the SCA pilot. Both vehicles were configured as they would be for an actual separation with the exception of the Orbiter elevon, which was locked at -1° (up). This elevon position was chosen as the optimum position for jettisoning the unmanned Orbiter in the event of an emergency and for providing flight data

with the Orbiter elevon close to the predicted position for separation. The emergency jettison capability was never confirmed or required.

During the launch maneuvers, "launch ready" was called when the SCA had reached equilibrium glide conditions with the inflight spoilers deployed, the engines in idle thrust, and the airspeed at 139 m/sec (270 knots) equivalent airspeed (EAS). Acceptable launch conditions were actually considered to be a velocity at separation of 139 ± 2.6 m/sec (270 ± 5 knots) EAS and a normal acceleration of 1g ± 0.3g. The SCA pilot was able to control the mated vehicle well within these constraints throughout the entire data acquisition period on both launch attempts.

Data obtained during this flight (using the LMS and GRACIE) are shown in figures 7(a) to 7(g). Based on these flight data, it was discovered that there was some confusion about the correct SCA data base. The problem was traced to incorrect use of wind tunnel incremental data, and the separation aerodynamic data were updated to reflect the actual flight data.

The inert-captive flight program was accomplished with a total flight time of approximately 11 hours 36 minutes, and all flight test requirements were satisfied within the flight envelope tested. The simulated launch maneuvers on inert flight 5 verified that (1) the Orbiter/SCA configuration could achieve and stabilize on the separation parameters using the prescribed procedures without exceeding Orbiter or SCA constraints, (2) safe separation initial conditions could be achieved with the baseline separation configuration and airspeed, and (3) the mated configuration could recover from an aborted separation maneuver within the vehicle constraints.

CAPTIVE-ACTIVE FLIGHTS

Three captive-active flights were flown with the Orbiter manned. The objectives of these flights were to verify (1) the separation configuration and procedures; (2) the integrated structure, aerodynamics, and flight control system; and (3) the Orbiter integrated system operations.

The first flight in this series, designated CA-1A, was limited to an airspeed of 93 m/sec (180 knots), which required the SCA flaps to be lowered throughout the entire flight and thus precluded the acquisition of any useful LMS data for separation analysis. With the flaps in any position other than completely retracted, the SCA developed enough added lift to overcome the lift generated by the Orbiter, resulting in the attach struts and load cells always remaining in compression. The speed restriction and flap position also created a problem in jettisoning the Orbiter in the event of an emergency. Therefore, the procedures for emergency separation required that the flaps be retracted and the airspeed be greater than 113 m/sec (220 knots) EAS with the SCA inflight spoilers deployed. Based on studies using the off-line simulations, emergency separation procedures were devised to allow a safe separation for both vehicles. The procedure called for the SCA pilot to accelerate while retracting the flaps. Once the flaps were retracted and the airspeed was in excess of 113 m/sec (220 knots) EAS, the engines were to be idled

and the spoilers deployed, followed by a "launch ready" call from the SCA pilot. At that time, the Orbiter crew could command separation and use the nominal steering procedures. If emergency separation was time critical, the procedure would have been for the SCA pilot to retract the flaps, deploy the spoilers, and pitch over to $N_{Z_{mated}} \leq 0.3g$; then the Orbiter crew would be cleared to separate.

The second captive-active flight, CA-1, expanded the flight envelope for both vehicles and provided a range of Orbiter elevon position data in the launch configuration. After clearing the vehicles for flutter and buffet through an airspeed of 139 m/sec (270 knots) EAS, the mated pair performed a separation run to gather data for analysis of separation configurations for the upcoming tailcone-on free-flight tests. At approximately 40 minutes into the flight, the Orbiter/SCA configured for the separation data run. The SCA started a gradual pushover to accelerate to a 139 m/sec (270 knots) EAS equilibrium target condition. When the airspeed increased to approximately 2.6 m/sec (5 knots) less than the target speed, the SCA pilot put the engines in idle thrust and deployed the inflight spoilers to achieve the equilibrium glide conditions required for the data run. The Orbiter was configured as follows.

Weight	667 233 newtons
c.g.	63.8 percent $L_{B_{ref}}$
Tailcone	On
Incidence angle	6°
Body flap	-9.7°
Rudder	0°
Speed brake	5°

The Orbiter elevon was trimmed to 0° for the first data point and held for 5 seconds. The RHC was then moved full forward and held for approximately 5 seconds of steady-state data. (Elevon software limits during this portion of the flight restricted the elevon travel between -1.5° (up) and +1.5° (down) only; therefore, moving the RHC full forward drove the elevon to the +1.5° (down) position.) In a similar manner, the elevon was positioned at -1.5° by moving the RHC full aft and holding it for approximately 5 seconds of data. The RHC was then returned to the detent position (0°) followed by a full right movement to put in 1° of right aileron for approximately 10 seconds, after which the Orbiter commander terminated the separation data run. The SCA pilot then performed a gradual recovery and reconfigured for landing.

Data retrieved from the flight, using the LMS and the GRACIE program, are presented in figures 8, 9, and 10. The primary separation parameters, relative normal load factor (ΔN_Z) and Orbiter pitch acceleration ($\ddot{\theta}_o$, are

shown in figure 8 for the elevon positions tested. These data and the aerodynamic coefficient data presented in figures 9 and 10 indicate a shift between the predicted values and the flight test data. The shift seemed to be equivalent to an approximately -1° bias in the Orbiter elevon position; i.e., the data indicated that instead of being at 0°, the elevon was actually at -1°. The data in figure 9 also show that the elevon effectiveness was in excellent agreement with the preflight predictions. The size of the separation window for the first two tailcone-on free flights was large enough to handle the -1° elevon bias without affecting the separation drastically. It was expected that data from the remaining captive-active flight and the first two free flights would give some insight as to the cause of the shift in data.

The elevon effectiveness results were used to determine the correct elevon setting for separation on the third free flight, which was flown with a more aft c.g. location and therefore required more down elevon.

The final captive-active flight, CA-3, was a dress rehearsal for free flight 1 up to the point of separation. The pushover was performed as it would be on free flight 1 with the SCA and Orbiter configured for launch. The Orbiter crew performed the preseparation functions of moving the elevon from the climb position (-2°) to the separation position (0°) and commanding a +2 deg/sec pitch rate with the RHC. At the "launch ready" call, the maneuver was aborted and the SCA recovered and reconfigured for landing.

The LMS data and the GRACIE program were used to generate the separation parameters at the time of "launch ready" for postflight analysis. A comparison of CA-1 and CA-3 data, shown in figure 11, indicates the elevon bias was not apparent on CA-3. This finding gave rise to questions regarding data repeatability and elevon position calibration accuracy. No changes to the proposed separation configuration were made because of the relative insensitivity to small elevon dispersions in the first two free-flight separation profiles. Also, two more repeat data points would result on free flights 1 and 2, from just after the "launch ready" call to the instant of separation.

All separation-related data acquired during the captive-inert and the captive-active flight test phases indicated that the desired conditions for separation would be attained by the baseline vehicle configuration and that separating the Orbiter from the SCA safely would not be a problem.

FREE FLIGHTS

The primary objectives of the free-flight phase of the ALT's were to verify (1) the handling qualities of the Orbiter vehicle, (2) the performance of the Orbiter subsystems, and (3) the Orbiter/SCA separation. The Orbiter/SCA separation is emphasized in this section. The free-flight Orbiter configurations tested are listed in table II.

Tailcone-On Flights

On the first free flight of the Orbiter "Enterprise," the flight proceeded as expected up to the time of separation. The Orbiter/SCA pushover was initiated at an altitude of 8733 meters, followed by separation at 7644 meters. All went nominally until physical separation occurred, at which time general-purpose computer number 2 (GPC 2) failed. The SCA pilot called "launch ready" at an airspeed of 138 m/sec (268.3 knots) EAS and a pitch attitude of -6.4°; within 1 second, the Orbiter commander commanded separation. At separation, the initial relative normal acceleration of the two vehicles was 0.99g and the Orbiter pitch acceleration was 3.1 deg/sec^2. The nominal steering command for the Orbiter was to have been as follows:

1. Command a pitch rate of +2 deg/sec for 3 seconds.

2. Command 0 deg/sec for 2 seconds.

3. Bank right 20°.

4. Push over at -1 deg/sec.

Figure 12(a) shows that the actual commanded pitch rate was initially about 2.5 deg/sec but peaked to about 5 deg/sec at 1 second during the transient following separation. This command resulted in a pitch rate, as shown in figure 12(b), of approximately 5 deg/sec at 1.3 seconds and a higher-than-nominal angle of attack, 11.1° maximum compared to 9.3° nominal (fig. 12(d)). The Orbiter normal load factor (fig. 12(e)) peaked at 2.1g 1.7 seconds after separation and thus violated the Orbiter constraint of $N_Z < 2.0$g. The reason for the high initial pitch rate command is unknown; however, the initial transient due to the rapid change in the normal and pitch accelerations and the master alarm triggered by the loss of GPC 2 were more than likely the major contributing factors. Also, the ALL SEP B indication and the backup separation discrete were not seen by the flight control system because of the loss of GPC 2; these are the signals from the separation switches on the aft attach points and the pilot's keyboard, respectively, that enable the primary flight control system (PFCS) normal control surface limits. Following free flight 1, the ALL SEP B and the backup separation discrete were no longer handled by the same GPC.

Postflight analysis of LMS data indicated that, as on CA-3, the elevon bias was not apparent. Reconstruction of the free flight 1 separation trajectory was performed using the off-line simulation programs with the vehicle initial conditions and the Orbiter steering command as inputs. (See figures 12(a) to 12(g).) The initial conditions were obtained from LMS and GRACIE data and from SCA flight instrumentation; the Orbiter pitch rate command was obtained from Orbiter downlist data. Also shown in figures 12(a) to 12(g) is a comparison of flight and predicted separation parameters. The predictions are based on the postflight data of pitch rate command. The off-line data show excellent agreement with the flight data. The difference seen in the SCA normal load factor (fig. 12(f)) is attributable to the difference between the postseparation steering maneuver used by the SCA pilots and that programed into the off-line simulation. Figure 12(h) is the Orbiter aft

attach point trajectory time history as reconstructed by the off-line simulation programs based on the postflight data. Photographic data obtained on free flight 1 were not sufficient for comparison with the predicted trajectory. On all subsequent flights, adequate photographic data were available.

Free flight 2 was flown with the Orbiter configured as in free flight 1. The flight itself was designed to include a number of aerosurface inputs, programed test inputs, and other data-gathering tests, but the separation procedure and configuration were identical to that of free flight 1. The Orbiter/SCA pushover maneuver was initiated at an altitude of 8887 meters, with separation occurring at 7718 meters. The Orbiter separated at an airspeed of 138.5 m/sec (269.2 knots) EAS with an initial relative normal load factor of 0.96g and a pitch acceleration of 2.4 deg/sec^2. The actual pitch rate steering command is shown in figure 13(a); figures 13(b) to 13(g) compare the values generated off-line, based on postflight data from the LMS and GRACIE. The predicted data again display excellent agreement with the flight data and, as seen in figure 13(h), the predicted Orbiter trajectory agrees with the flight photographic data. The flight photographs were taken with a motor-driven 35-millimeter camera at a speed of 2 frames per second. The first frame of the separation sequence was not necessarily taken at the instant of separation; therefore, the first point on figure 13(h) represents a time somewhere between T_{sep} and T_{sep} + 0.5 second. Subsequent points occur at 0.5-second intervals.

Free flight 3 was the third and final Orbiter free flight to be flown with the tailcone covering the aft end. This Orbiter configuration was changed by reballasting to obtain a more aft c.g. location, 65.9 percent reference length. The incidence angle remained at 6°, but the launch airspeed and the elevon position for separation were changed to accommodate the aft c.g. location. The Orbiter elevon had to be lowered from the free flight 1 and free flight 2 position to counteract the increased nose-up pitching moment caused by the more aft c.g. location. The elevon deflection originally was to have been +1.5°, but based on the apparent elevon bias noted on CA-1, the separation setting was loaded into the flight computers as +2.5°. Also, following free flight 1, the separation airspeed was lowered from 138 m/sec (268 knots) EAS to 129 m/sec (250 knots) EAS because the lower speed would provide safe separation conditions and reduce the possibility of violating the Orbiter normal load factor constraint of $N_Z < 2.0g$ as on free flight 1. When data from CA-3 and free flights 1 and 2 failed to indicate the elevon bias noted on CA-1, the elevon setting for free flight 3 was reevaluated and it was concluded that, with the lower launch speed, the elevon position of +2.5° would provide acceptable separation conditions and would not warrant reloading the flight computers with the original elevon setting.

The Orbiter/SCA pushed over at 8689 meters and the Orbiter was released at a pressure altitude of 7937 meters. The higher launch altitude was a direct result of the reduction in separation airspeed. The airspeed at the "launch ready" call was 129.9 m/sec (252.7 knots) EAS with a relative normal load factor of 0.92g and an initial Orbiter pitch acceleration of 1.0 deg/sec^2; these data were well within the separation window targeted by the SCA

pilot. Subsequent postflight analysis and trajectory reconstruction resulted in the data presented in figures 14(a) to 14(h).

The separation results from the tailcone-on free flights were in excellent agreement with the off-line predictions and well within the constraints of the separation window, as shown in figure 15. Table III summarizes the pertinent separation parameters with a comparison to both the target values and the predicted values. The predicted values are based on the actual conditions at separation, and the target values are the conditions to which the SCA pilot attempted to fly the mated vehicle.

Figure 16 shows a typical tailcone-on separation trajectory sequence as viewed from the SCA chase plane. The sequence was shot at 2 frames per second.

Tailcone-Off Flights

The last two flights of the ALT program were flown with the Orbiter configured as it would be when returning from orbit; i.e., with the tailcone removed and with the three main engine bells in place. The removal of the tailcone presented two major problems with the separation phase of the flights. First, without the tailcone, the increase in the buffet level could possibly result in an SCA cockpit environment that would make it impossible for the SCA pilot to attain the specified target conditions. Second, with the removal of the tailcone, the change in Orbiter pitching moment required $+7^{\circ}$ of down elevon, which was well outside the elevon range tested in the preceding flights. The SCA tail loads and climb performance degradation created by the increased buffet and drag levels, respectively, were also unknowns that could have terminated the flights prior to separation. A fourth captive-active flight was originally planned to investigate the flight envelope of the tailcone-off configuration but was deleted. The objectives of the canceled captive-active flight were combined with free flight 4 and were evaluated in the first half of the flight. Also, the Orbiter incidence angle was left at 6° instead of changing it to 5° as originally called for in the program. This created one less unknown to be verified for the tailcone-off flights and also relieved some of the concerns of buffet by lowering the target launch speed from 139 to 126 m/sec (270 to 245 knots) EAS.

The first portion of free flight 4 was dedicated to a real-time assessment of the buffet-induced loads and verification of the separation configuration and target conditions. A real-time GO/NO-GO decision for separation was made based on LMS data telemetered to the ground and displayed on strip-charts in the DFRC control room. The LMS data were also filtered to reduce the noise in the strip-chart parameters caused by the increased buffet levels.

The increased drag of the tailcone-off Orbiter introduced a third separation parameter, the relative axial load factor, which had been insignificant during the initial portion of the tailcone-on Orbiter separation. Two independent studies, based on the Rockwell International Space Division and the JSC off-line simulations, were performed to investigate possible combinations of the relative normal and axial load factors and Orbiter pitch accelerations

that would allow a safe separation. The resulting separation window is shown in figures 17(a) and 17(b).

A step-by-step analysis of the buffet-induced loads and vibrations from take-off through the maximum airspeed of 129 m/sec (250 knots) EAS led to the initiation of the separation data run, which provided the information necessary for the separation GO/NO-GO decision. With the Orbiter elevon positioned at $+7^{o}$, the SCA pilot deployed the inflight spoilers, idled the thrust, and attained equilibrium glide conditions at an airspeed of 127 m/sec (247 knots) EAS. Approximately 10 seconds of steady-state data was taken before the SCA and Orbiter reconfigured and began their climb to the pushover altitude for separation. During the interim, the strip-chart data were evaluated and it was concluded that the separation configuration provided adequate conditions to assure a safe separation. The "quick-look" results are shown in figures 17(a) and 17(b). (The load cells contained two sets of vernier load measurements for separation, which provided redundant readings for each parameter.) If the data had not fallen within the acceptable regions of the separation windows, the SCA/Orbiter would have performed a second separation data run to obtain data at various elevon positions, as was done on CA-1, so that the optimum setting for separation on a subsequent flight could be chosen.

Having received the "go ahead" for separation, the SCA initiated the pushover maneuver at 7397 meters, with separation occurring at approximately 6541 meters at a velocity of 127.4 m/sec (247.7 knots) EAS. The relative normal and axial accelerations were 1.04g and 0.27g,[2] respectively, and the Orbiter pitch acceleration was 0 deg/sec^2. The comparison of the flight data and the postflight off-line analysis (figs. 18(a) to 18(g)) shows excellent agreement, as does the separation trajectory data (fig. 18(h)).

The final flight in the ALT program, free flight 5, was flown with the same Orbiter configuration as in free flight 4. The prime objective of free flight 5 was to land the Orbiter on the concrete runway, which required separation to occur at a predetermined point in the sky. The separation target conditions were the same as those of free flight 4. The SCA initiated pushover at approximately 6632 meters with the SCA pilot calling "launch ready" at approximately 6041 meters. The Orbiter crew commanded separation approximately 7.5 seconds later at 5791 meters. The airspeed at that time was 128.9 m/sec (250.7 knots) EAS with a relative normal acceleration of 1.0g, a relative axial acceleration of 0.17g, and a pitch acceleration of -1.0 deg/sec^2.

The trajectory reconstruction using the actual initial conditions and vehicle configurations at separation again showed excellent agreement among flight data, off-line simulation data, and photographic data (figs. 19(a) to 19(h)).

---

[2]There was a bias in the axial load channels from the LMS as seen in the data after separation, which, if accounted for, would decrease the calculated ΔN_X from 0.27g to 0.17g at the instant of separation.

A compilation of the separation results from the tailcone-off flights is presented in figures 20(a) and 20(b) and table IV. Figure 21 shows a typical tailcone-off separation sequence. Notice the more aft relative motion of the Orbiter without the tailcone as compared to the Orbiter motion with the tailcone in figure 16.

CONCLUDING REMARKS

The analytical prediction techniques and mathematical modeling incorporated in the design of the separation procedures for the Orbiter/SCA were based on scale-model wind tunnel test data. These techniques proved to be extremely accurate and useful throughout the approach and landing test program.

The two-body man-in-the-loop simulations, with one vehicle trajectory canned, provided adequate fidelity for crew training and crew inputs to the separation procedures and configurations.

The load measurement system installed aboard the SCA provided a means for extracting the proximity aerodynamics and was a reliable source for making real-time assessments of separation and loads parameters. The load measurement system also allowed some wind tunnel tests to be deleted from the program, with actual flight data completing the aerodynamic data base. The Orbiter separated from the SCA, successfully and as predicted, five times during the approach and landing test program.

Lyndon B. Johnson Space Center
National Aeronautics and Space Administration
Houston, Texas, April 2, 1980
953-36-00-00-72

REFERENCE

1. Orbiter/747 Carrier Separation Aerodynamic Data Book - SDM Baseline. SD75-SH-0033C, Rockwell International Space Division, Nov. 1976.

TABLE I.- WIND TUNNEL TESTS

(See figure 2.)

Test objective	Test number	Location[a]	Model scale	Test date
Configuration development	CA5	BTWT	0.03	Sept. 1974
	CA6	BTWT	.03	May 1975
	CA23A	ARC	.0125	March 1975
Mated data base	CA14A	BTWT	.03	Nov. 1975
Mated verification	CA13	ARC	.03	June 1976
Separation data base	CA20	BTWT	.03	Oct. 1974
	CA23B	ARC	.0125	July 1975
	CA26	LTV	.0125	Aug. 1975

[a]Locations are as follows: ARC - Ames Research Center, Moffett Field, Calif.; BTWT - Boeing Transonic Wind Tunnel, Seattle, Wash.; and LTV - LTV Aerospace Corporation, Dallas, Tex.

TABLE II.- FREE FLIGHT ORBITER CONFIGURATIONS

Flight	Tailcone	Weight, N	c.g. location, percent reference length	Orbiter incidence angle, deg
1	On	667 411	63.80	6
2	On	667 411	63.80	6
3	On	667 055	65.90	6
4	Off	670 547	66.25	6
5	Off	670 547	66.25	6

TABLE III.- ORBITER TAILCONE-ON SEPARATION PARAMETERS

Parameter	Free flight 1	Free flight 2	Free flight 3
Orbiter c.g., percent	63.8	63.8	65.9
Orbiter elevon, deg	0	0	2.5
SCA airspeed, m/sec (knots) EAS			
Flight	138.0 (268.3)	138.5 (269.2)	129.9 (252.7)
Target	139 (270)	139 (270)	129 (250)
SCA pitch attitude, deg			
Flight	-6.38	-5.91	-2.95
Target	-6	-6	-3.5
SCA altitude (MSL)[a], m	7645	7718	7937
Relative normal loading factor, g			
Flight	0.991	0.956	0.917
Predicted	0.994	0.907	0.857
Target	0.9	0.9	0.88
Orbiter pitch acceleration, deg/sec^2			
Flight	3.1	2.4	1.0
Predicted	2.4	2.4	0.1
Target	2.5	2.5	0.6

[a]Mean sea level.

TABLE IV.- ORBITER TAILCONE-OFF SEPARATION PARAMETERS

Parameter	Flight 4	Flight 5
Orbiter c.g., percent	66.25	66.25
Orbiter elevon, deg	7	7
SCA airspeed, m/sec (knots) EAS		
Flight	127.4 (247.7)	128.9 (250.7)
Target	126 (245)	126 (245)
SCA pitch attitude, deg		
Flight	-5.25	-6.07
Target	-6	-6
SCA altitude (MSL), m	6541	5791
Relative normal loading factor, g		
Flight	1.04	1.0
Predicted	1.23	1.1
Target	1.0	1.0
Relative axial load factor, g		
Flight	0.17	0.17
Predicted	0.19	0.2
Target	0.2	0.2
Orbiter pitch acceleration, deg/sec^2		
Flight	0.0	-1.0
Predicted	-0.5	-0.5
Target	0.6	0.6

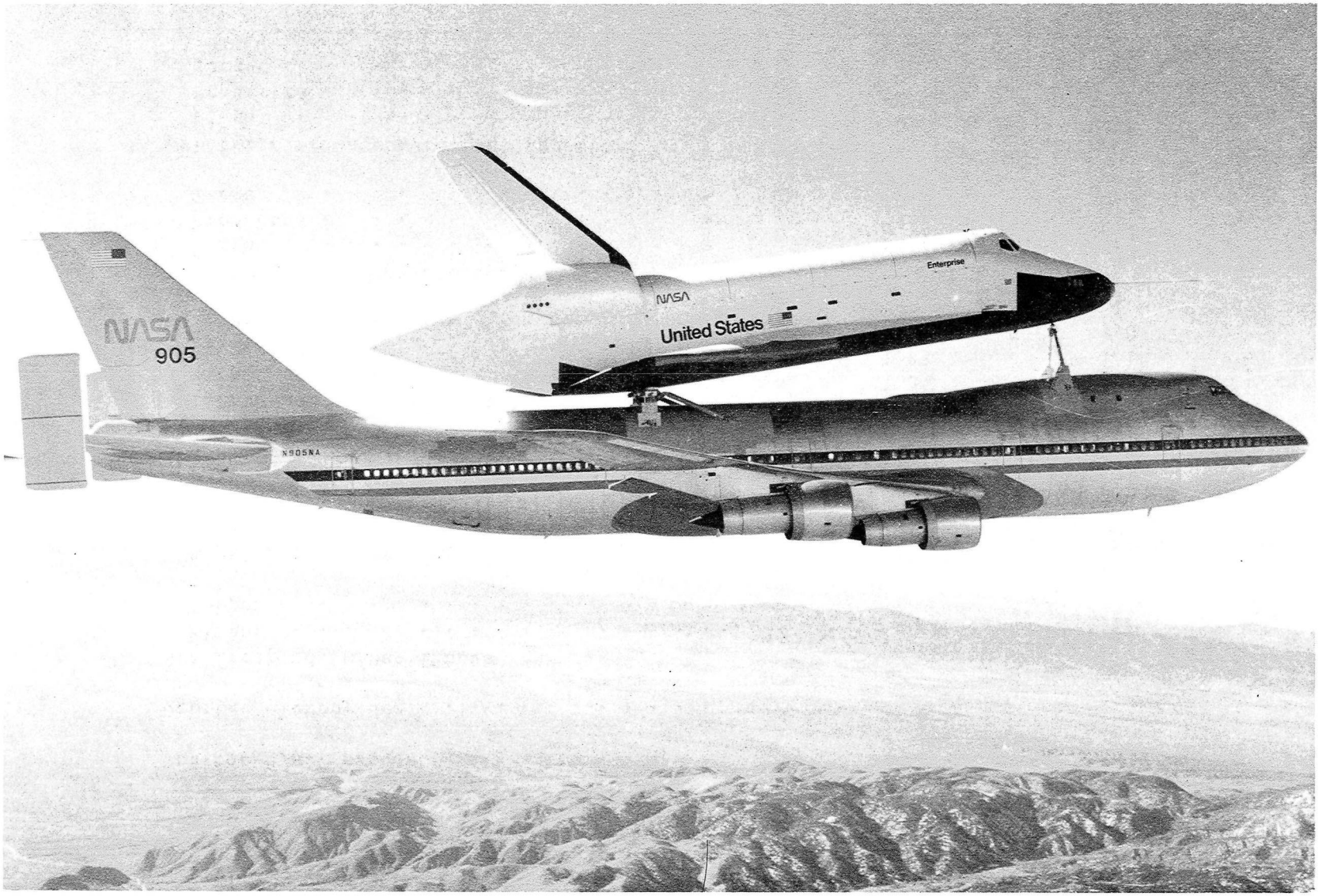

(a) Photograph.

Figure 1.- Mated Orbiter/SCA configuration.

Measurement	SCA			Orbiter	
	Wing	Vertical	Horizontal	Wing	Vertical
Area, m^2	511	77.1	136.6	249.9	38.4
Span, m	59.6	9.8	21.9	23.8	8
Aspect ratio	6.96	1.25	3.60	2.265	1.675
Taper ratio	0.356	0.340	0.250	0.200	0.404
Sweep, deg	37.5 (1/4 $\bar{c}$)	45.0 (1/4 $\bar{c}$)	37.5 (1/4 $\bar{c}$)	[a]45	[a]45
Dihedral, deg	7.0	-	7.0	[b]3.5	-
Incidence, deg	2.0	-	+5 to -10	0.5	-
MAC, [c] m	8.3	8.5	6.9	12.1	5.1

[a]Leading edge.

[b]Trailing edge.

[c]Mean aerodynamic chord.

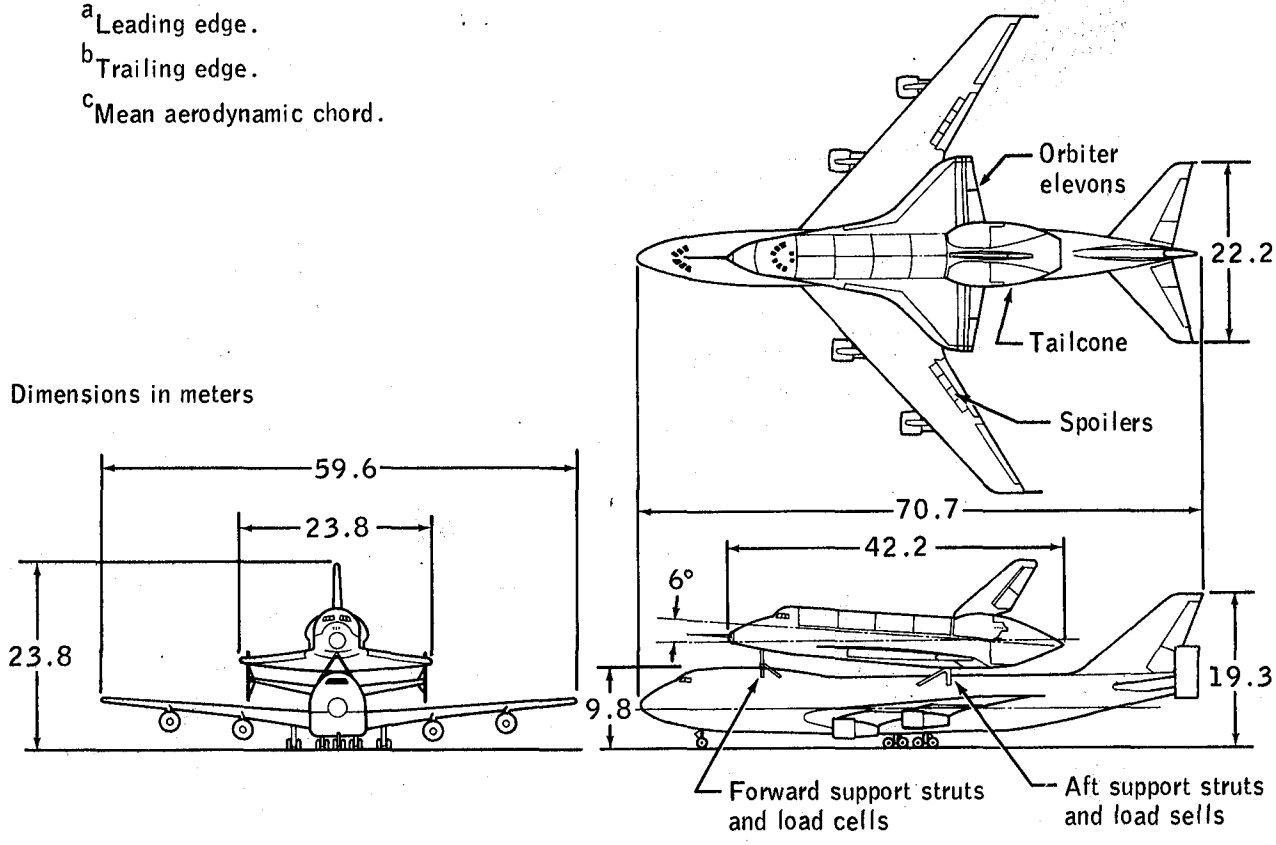

(b) Basic vehicle dimensions and configuration details.

Figure 1.- Concluded.

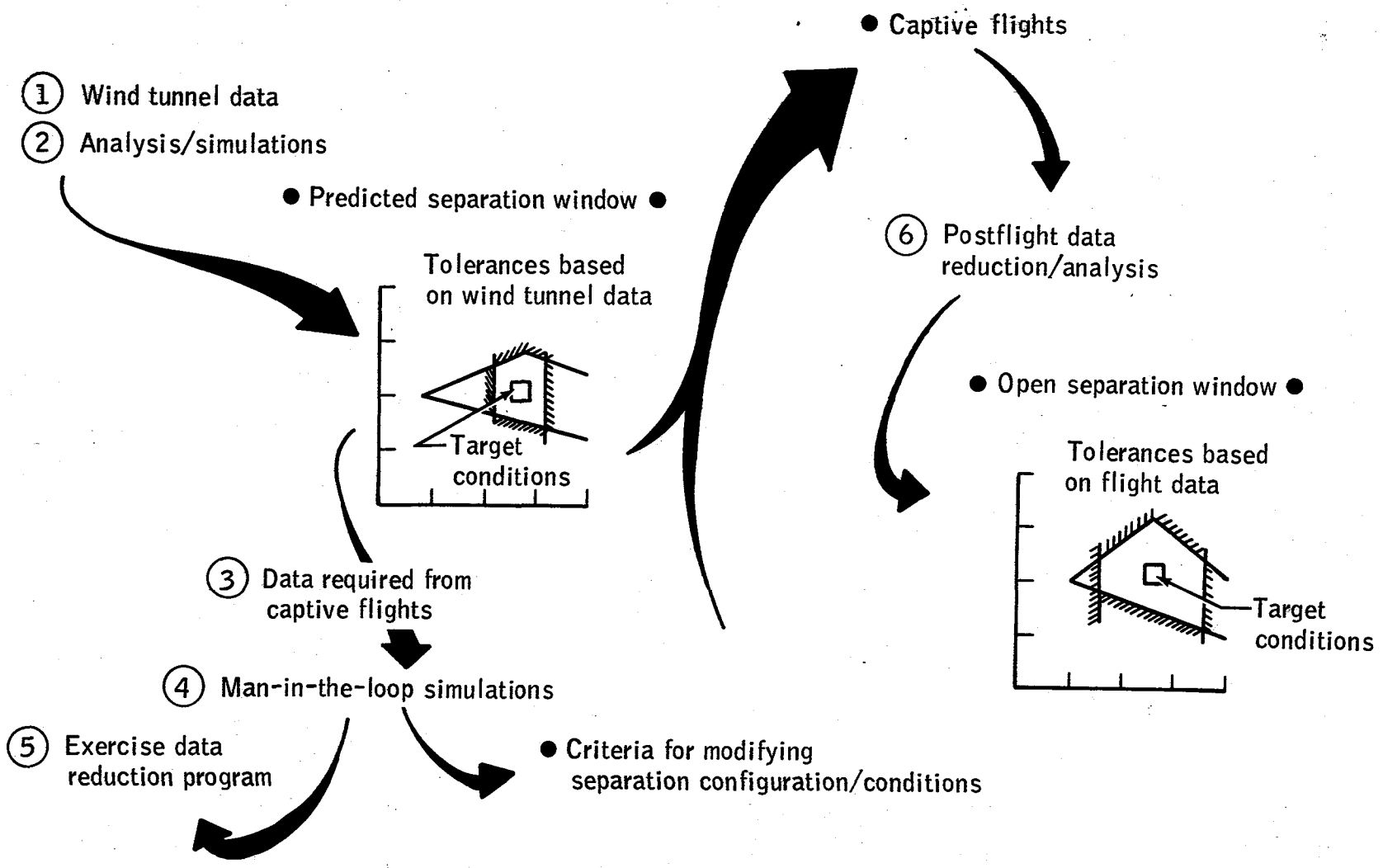

Figure 2.- Separation analysis flow chart.

Test configuration	1974												1975												1976											
	J	F	M	A	M	J	J	A	S	O	N	D	J	F	M	A	M	J	J	A	S	O	N	D	J	F	M	A	M	J	J	A	S	O	N	D
									11	1, 16	19			6			8	5		20			7				12	1		18					12	
Isolated carrier	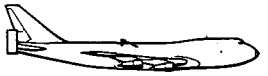								CA 5	CA 20				CA 23A				CA 23B																		
Isolated Orbiter									CA 5	CA 20							CA 6						CA 14A													
Mated (Tailcone on)	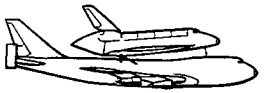								CA 5								CA 6						CA 14A						CA 13						
Mated (Tailcone off)	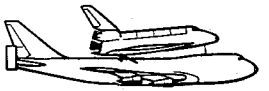								CA 5	CA 20				CA 23A			CA 6												CA 13						
Separation	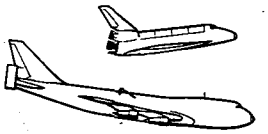									CA 20									CA 23B	CA 26																

Figure 3.- Wind tunnel configuration matrix.

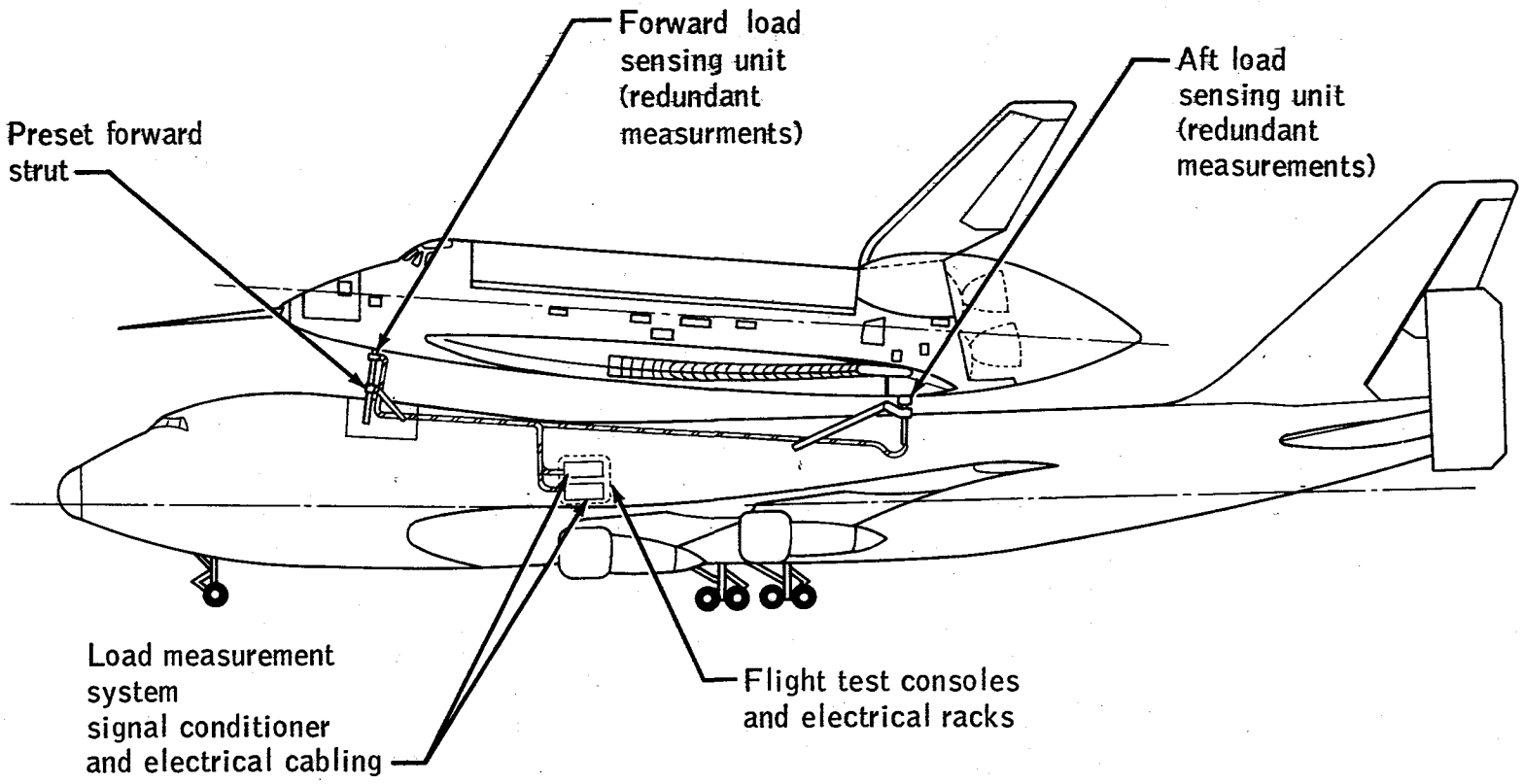

Figure 4.- Orbiter/SCA load measurement system.

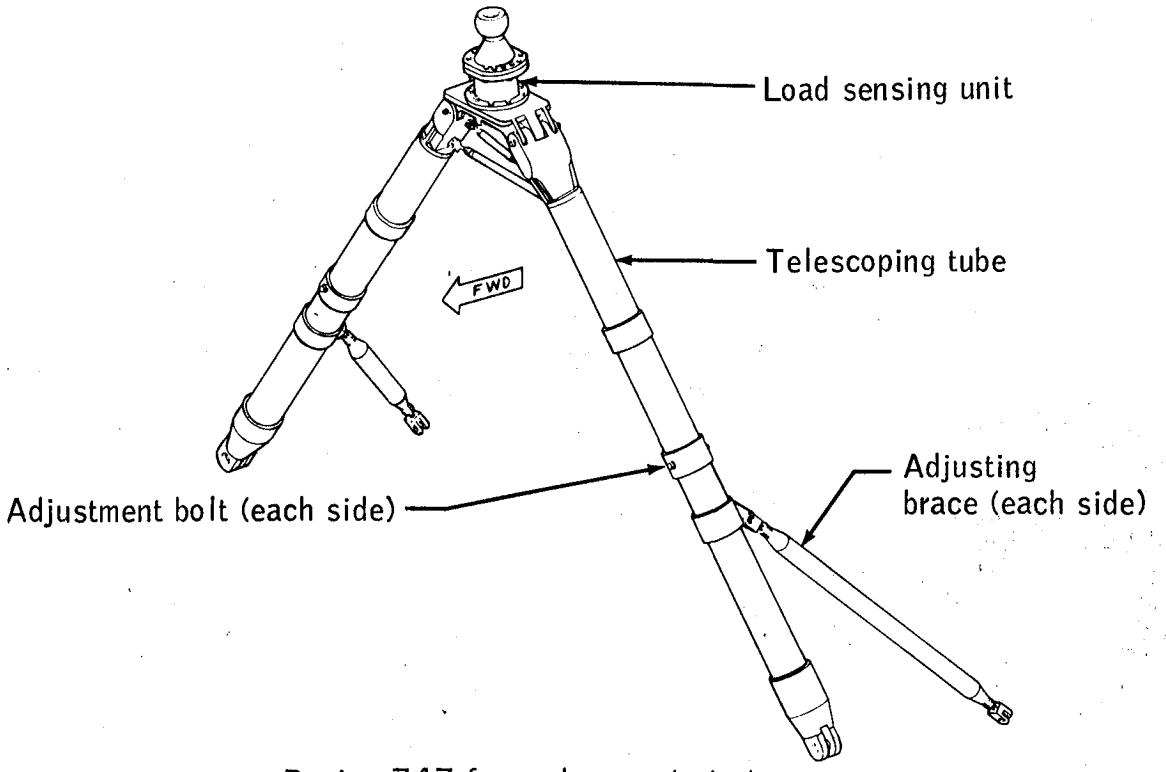

Boeing 747 forward support struts

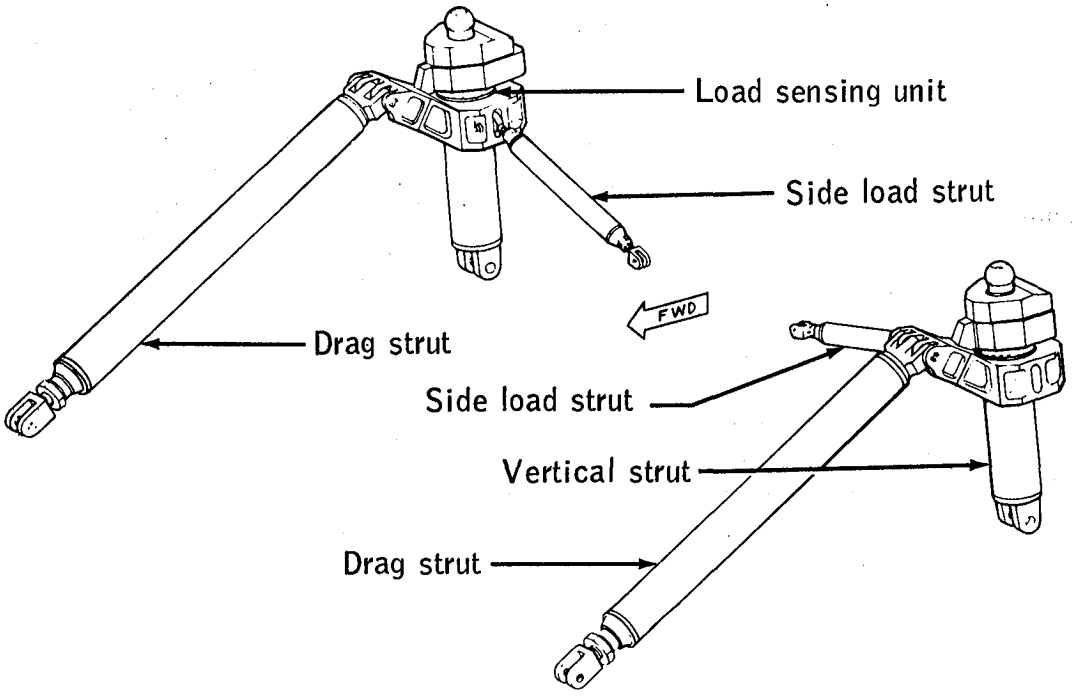

Boeing 747 aft support struts

Figure 5.- Attach strut load cell locations.

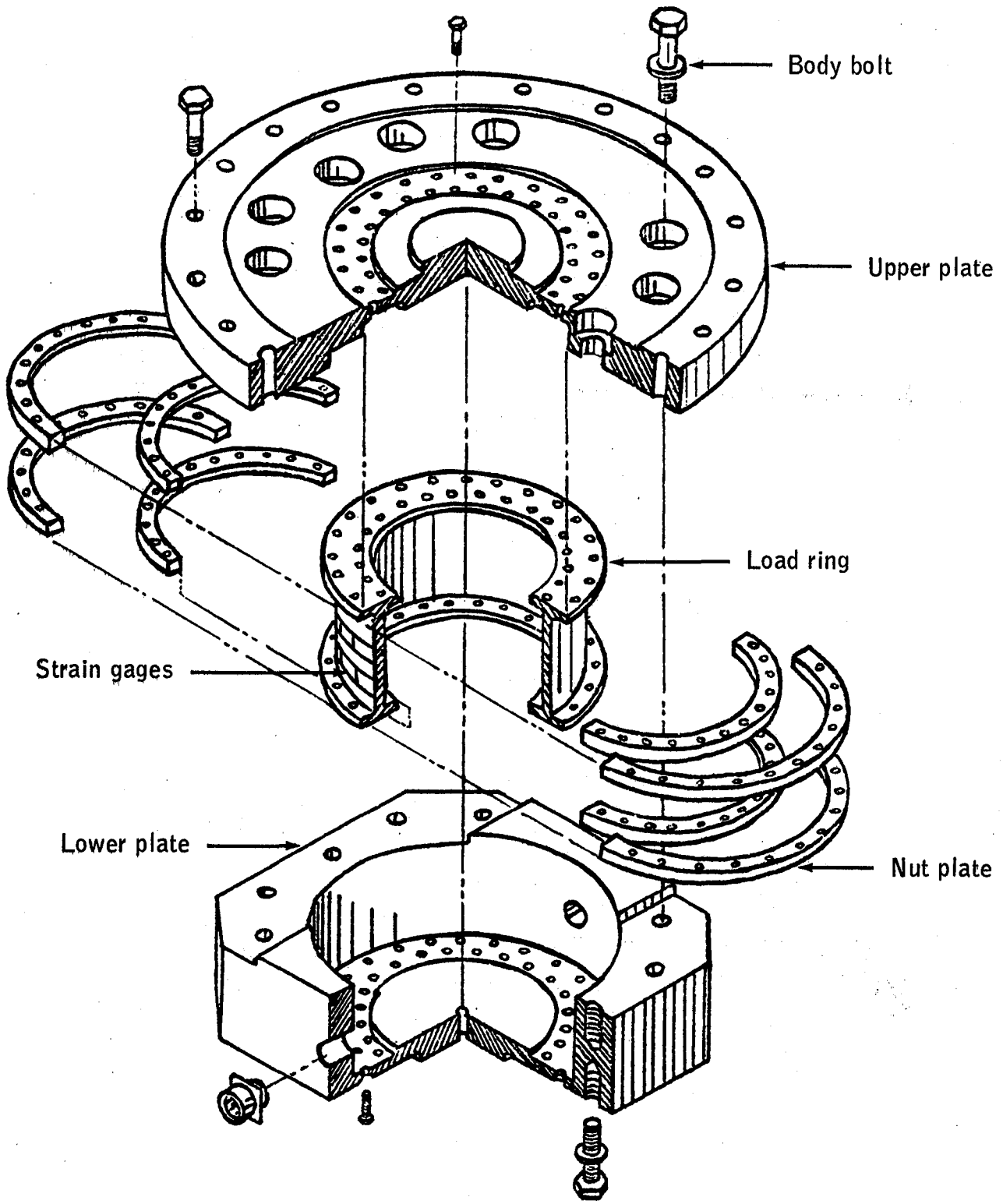

Figure 6.- Aft load cell.

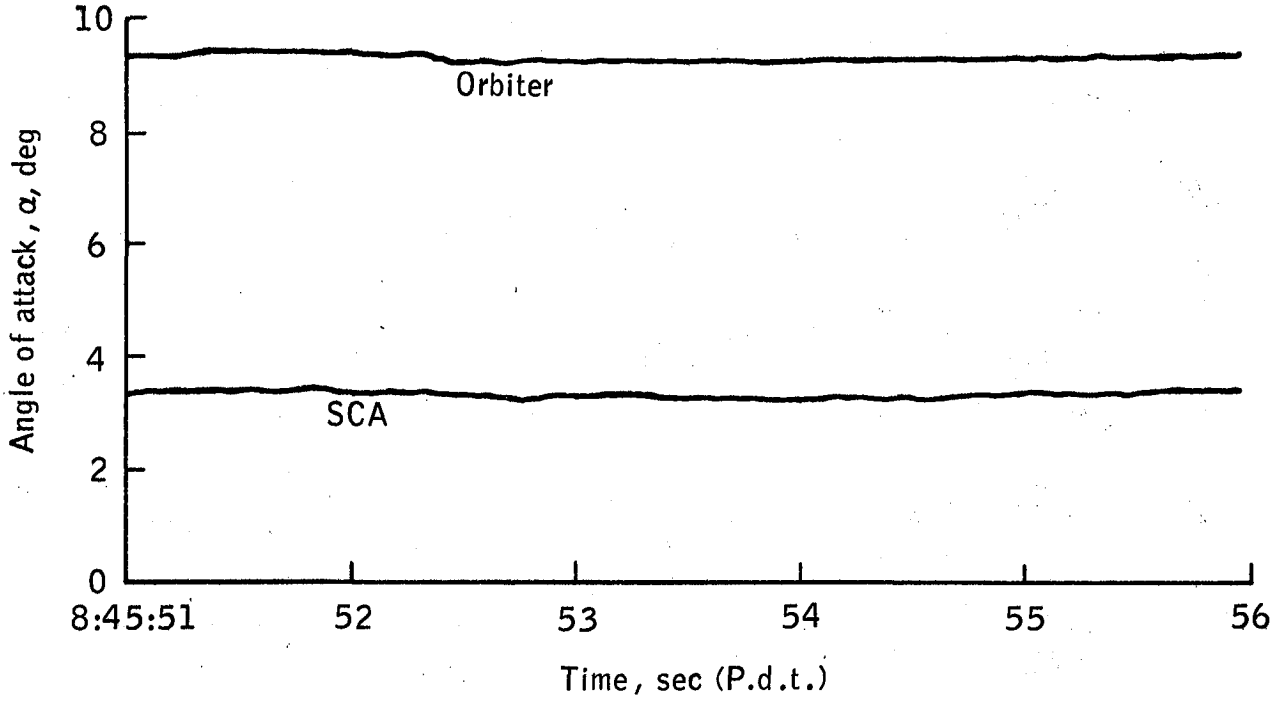

(a) Angle of attack, α, time history.

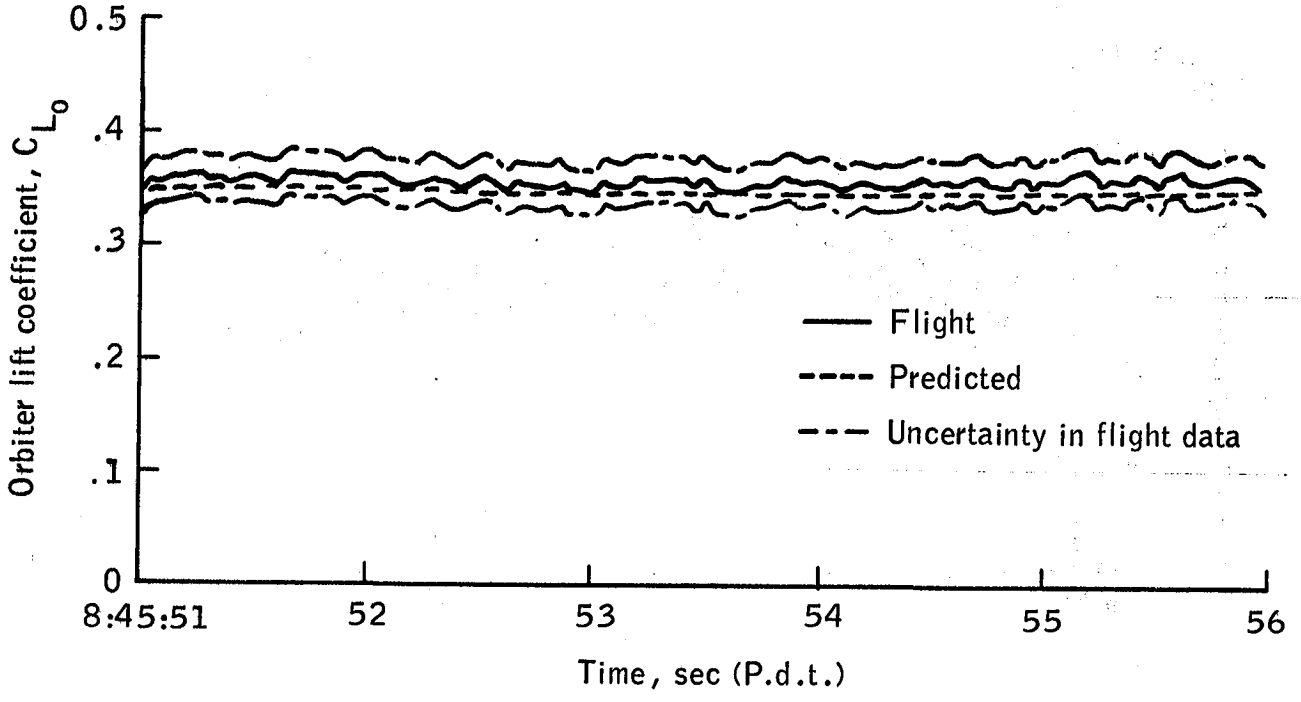

(b) Orbiter lift coefficient, C_{L_o}, time history.

Figure 7.- Inert captive flight 5, separation data run 1.

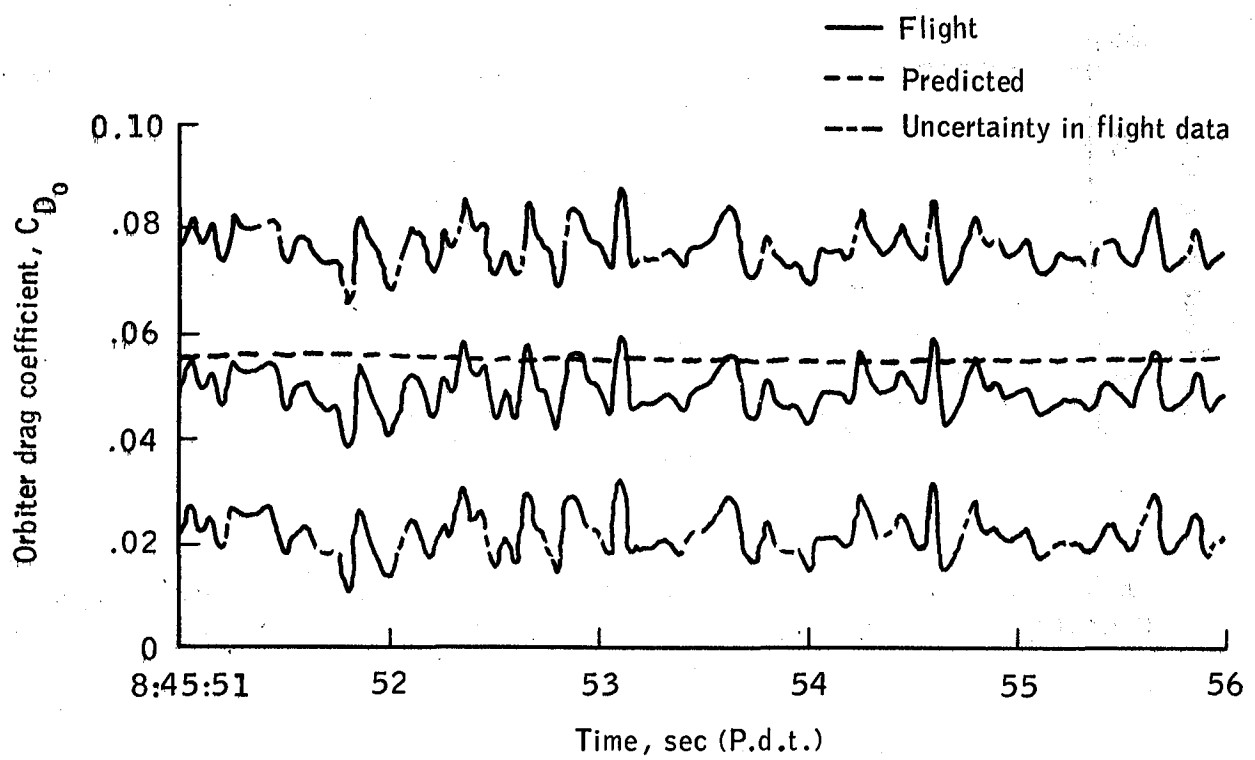

(c) Orbiter drag coefficient, C_{D_o}, time history.

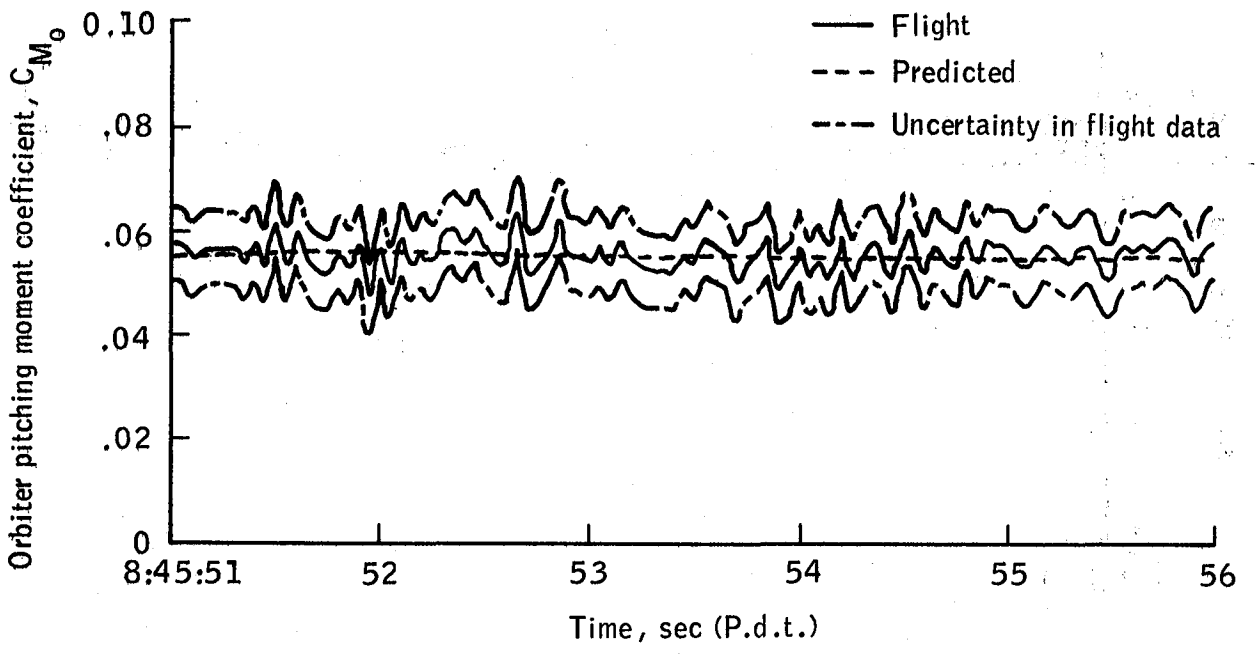

(d) Orbiter pitching moment coefficient, C_{M_o}, time history.

Figure 7.- Continued.

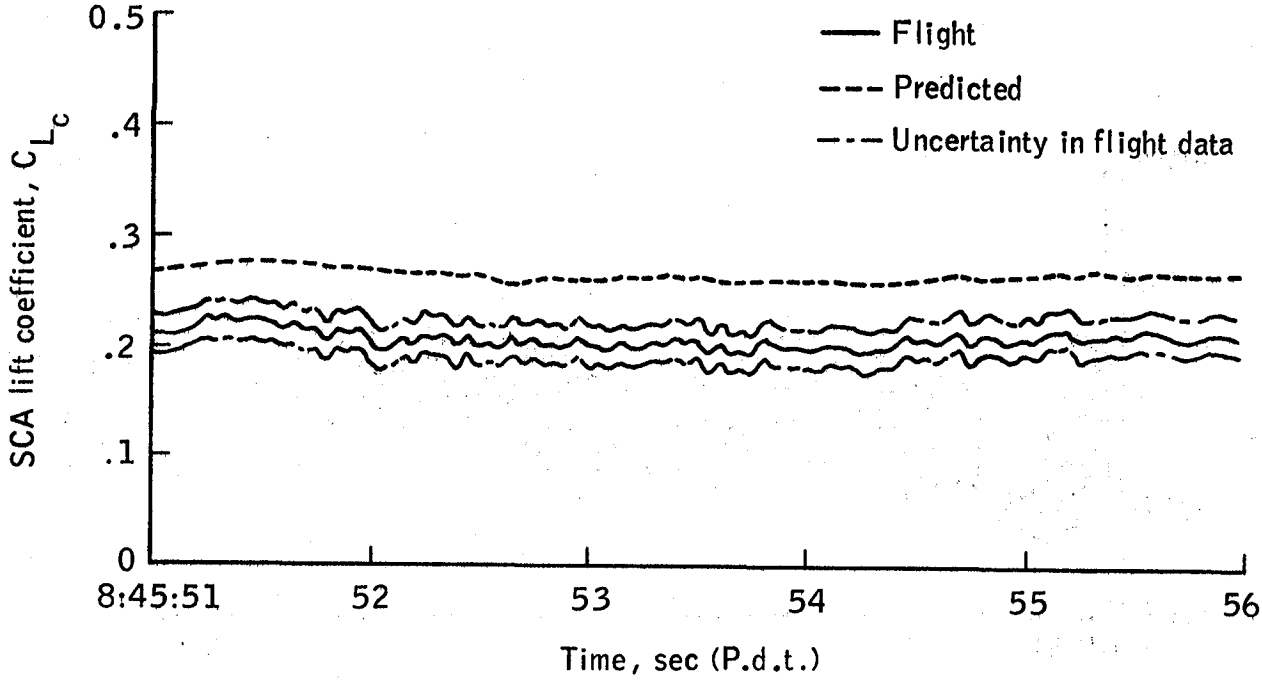

(e) SCA lift coefficient, C_{L_c}, time history.

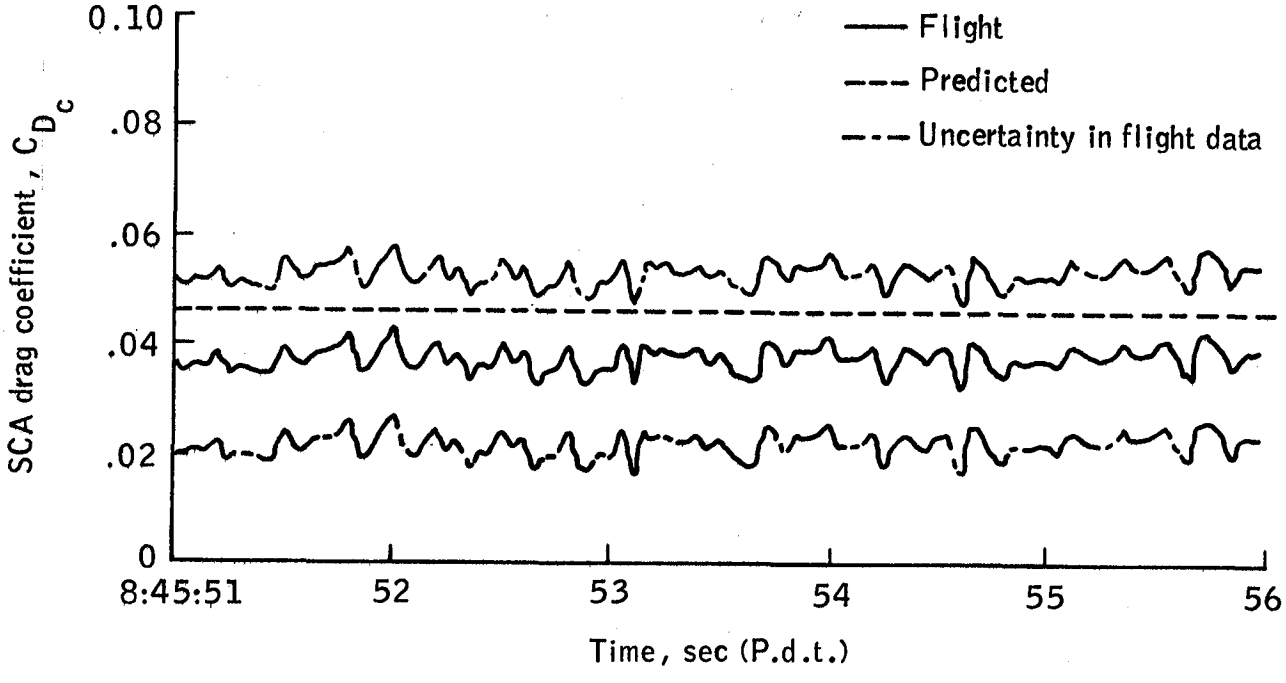

(f) SCA drag coefficient, C_{D_c}, time history.

Figure 7.- Continued.

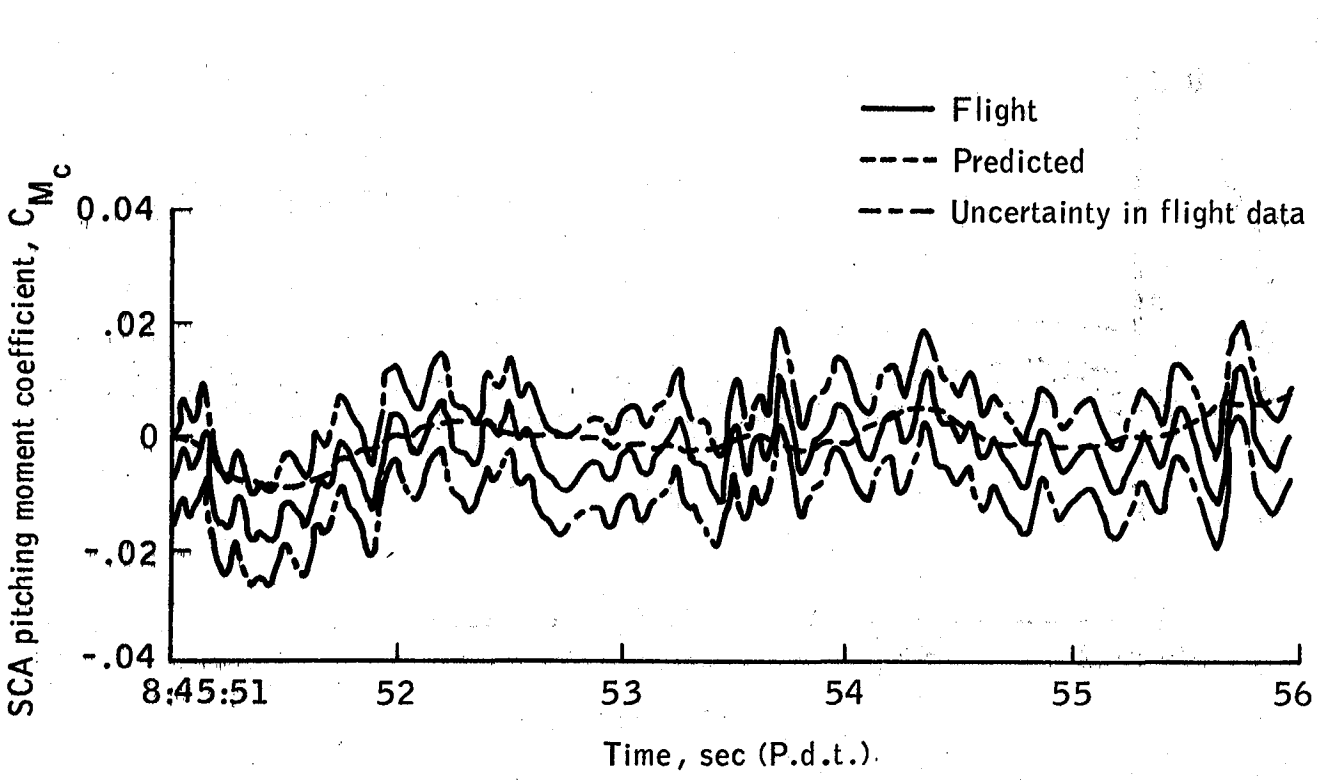

(g) SCA pitching moment coefficient, C_{M_c}, time history.

Figure 7.- Concluded.

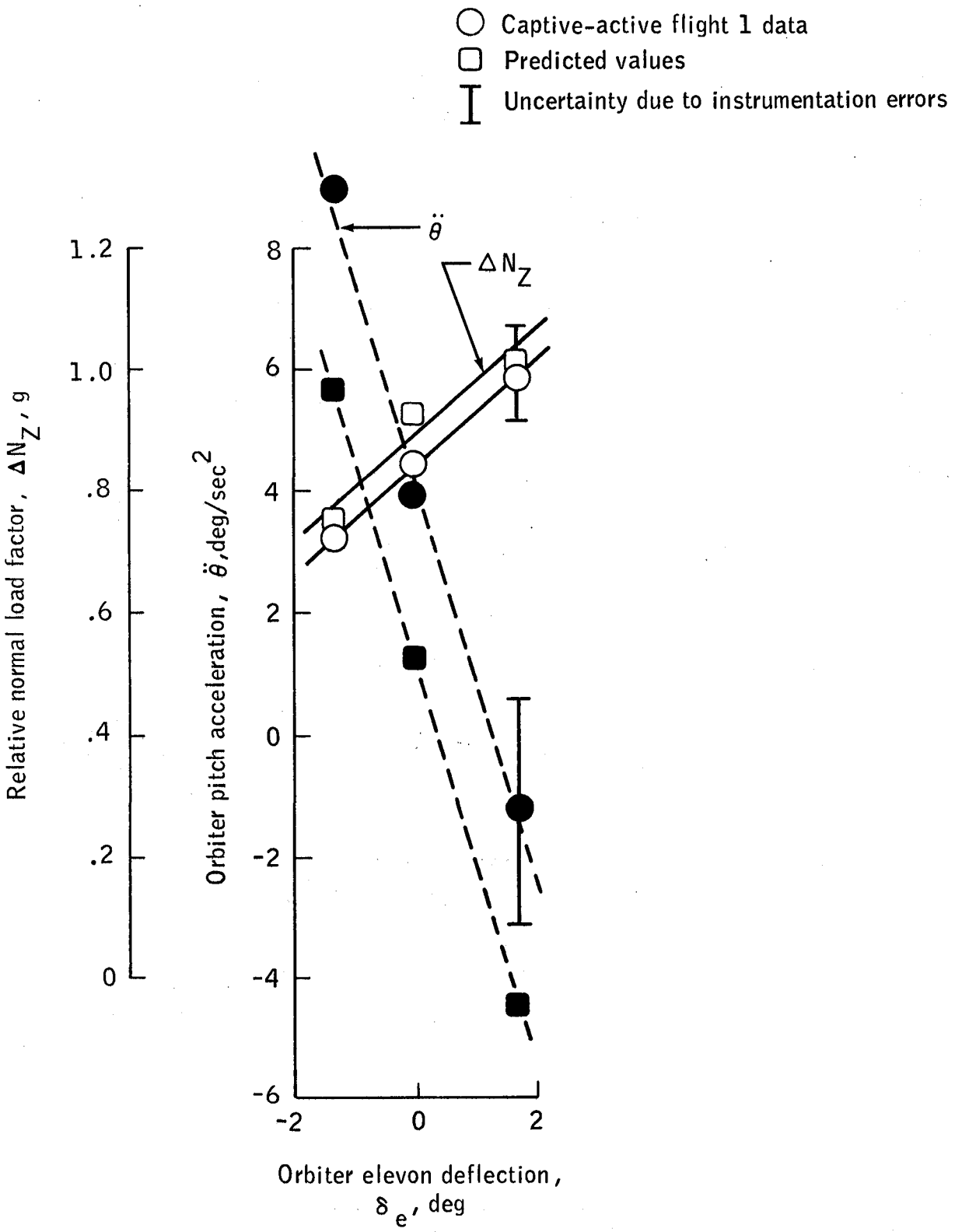

Figure 8.- Elevon bias effect on Orbiter pitch acceleration and relative normal load factor.

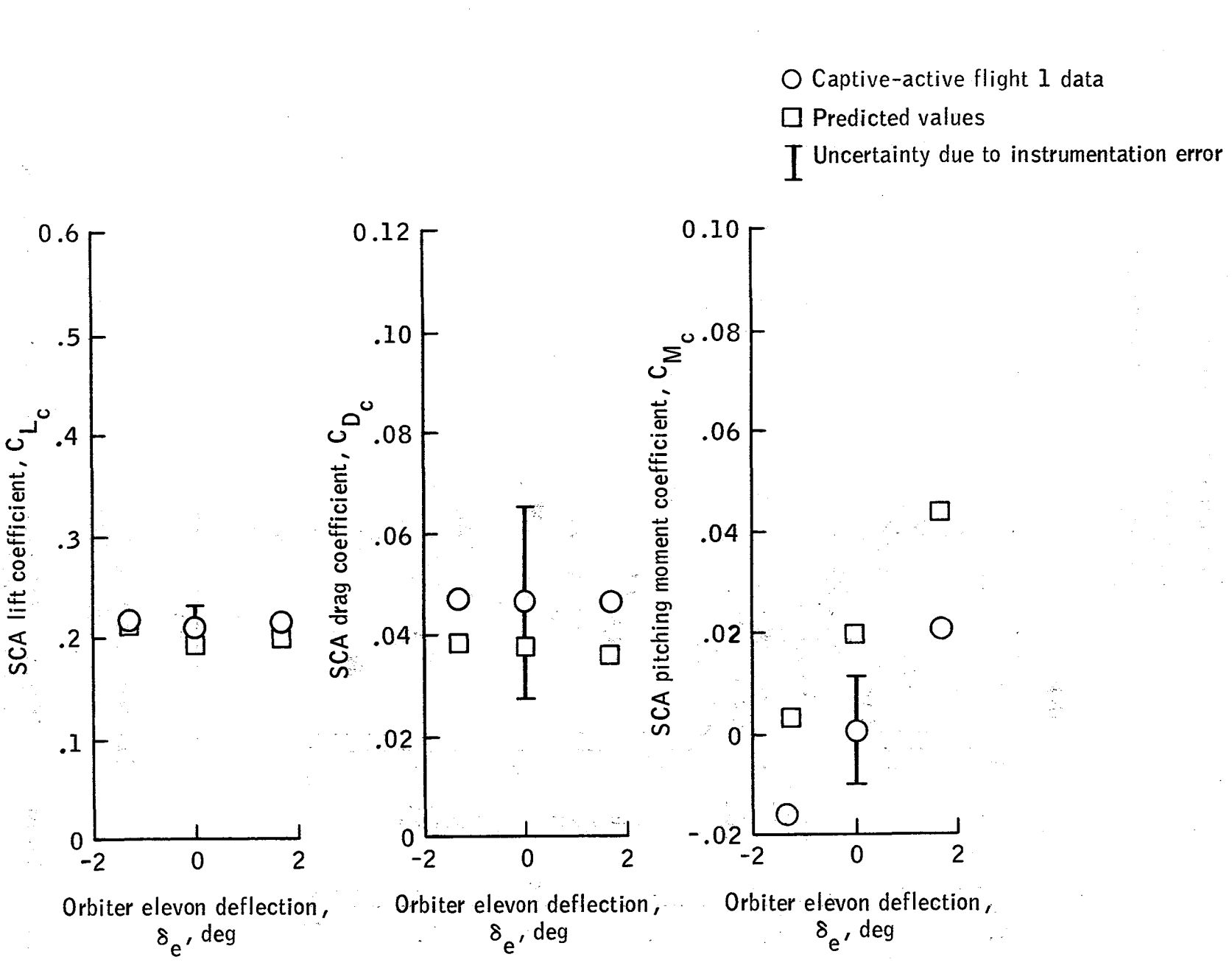

Figure 9.- SCA coefficients compared to Orbiter elevon deflection.

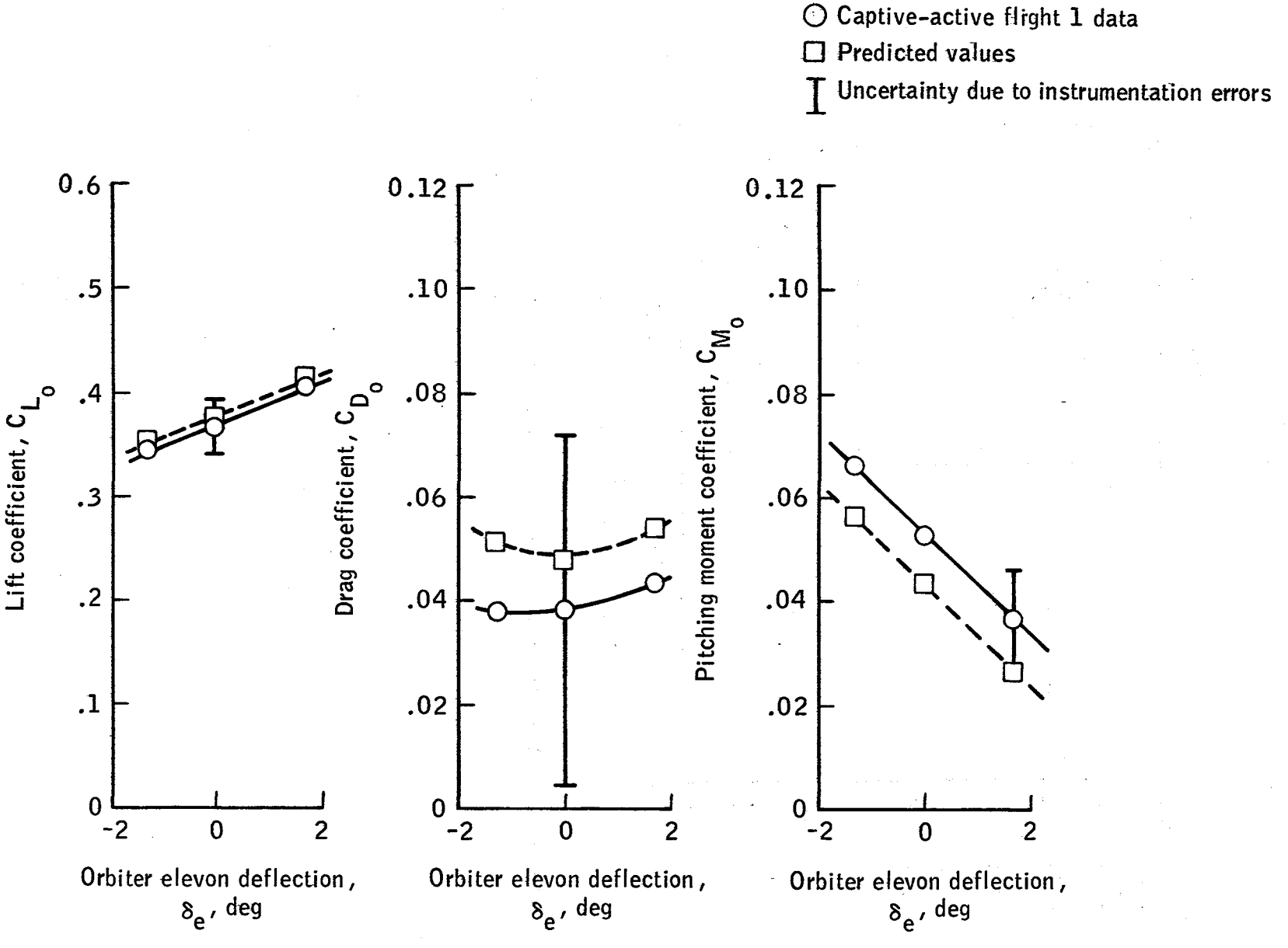

Figure 10.- Orbiter coefficients compared to elevon deflection.

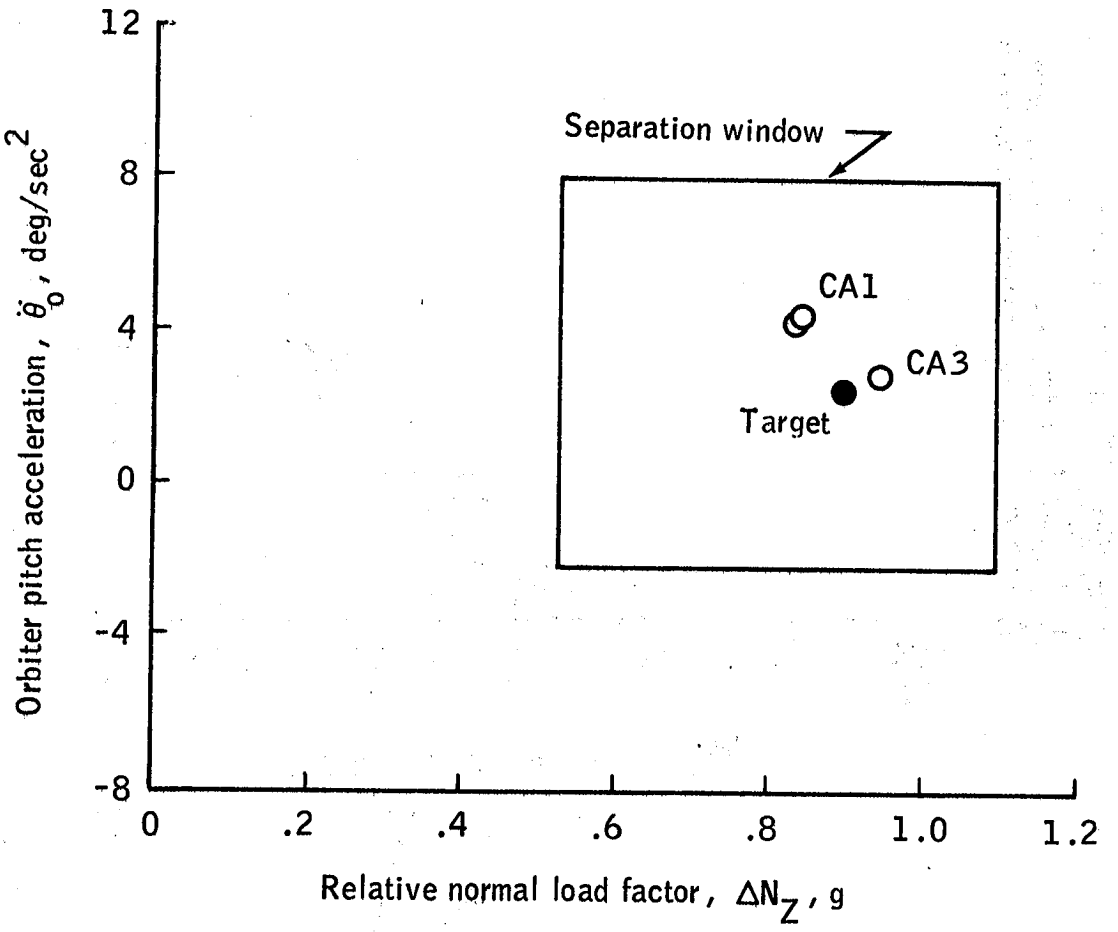

Figure 11.- Separation initial conditions from captive-active flights.

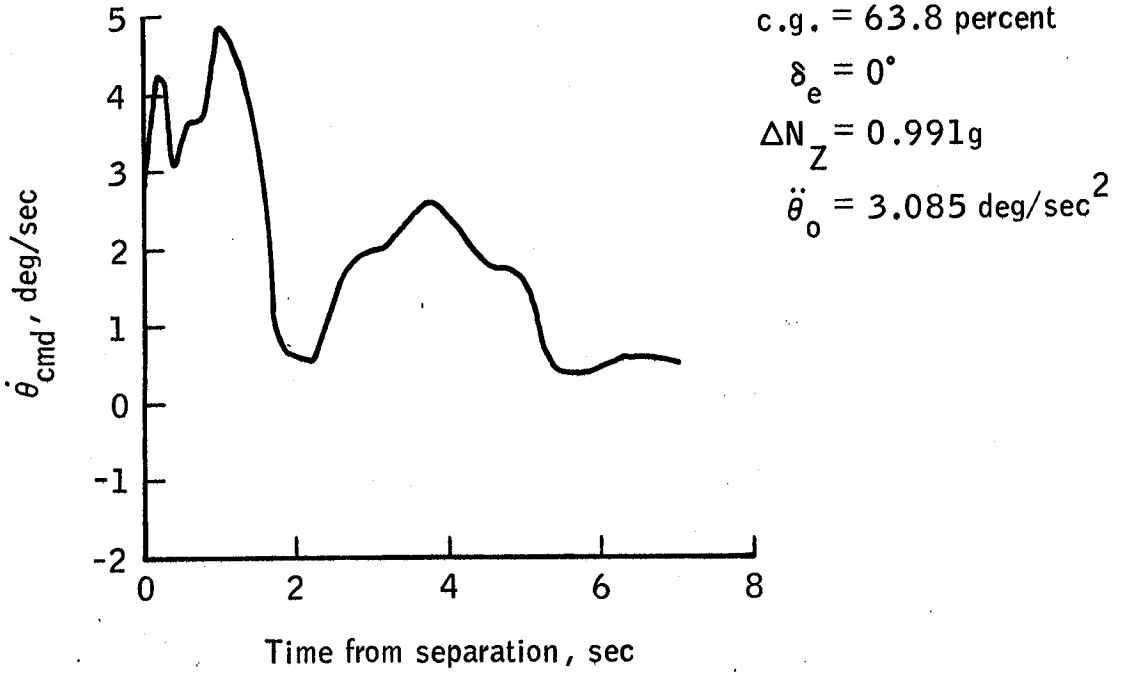

(a) Orbiter pitch rate command, $\dot{\theta}_{cmd}$, time history.

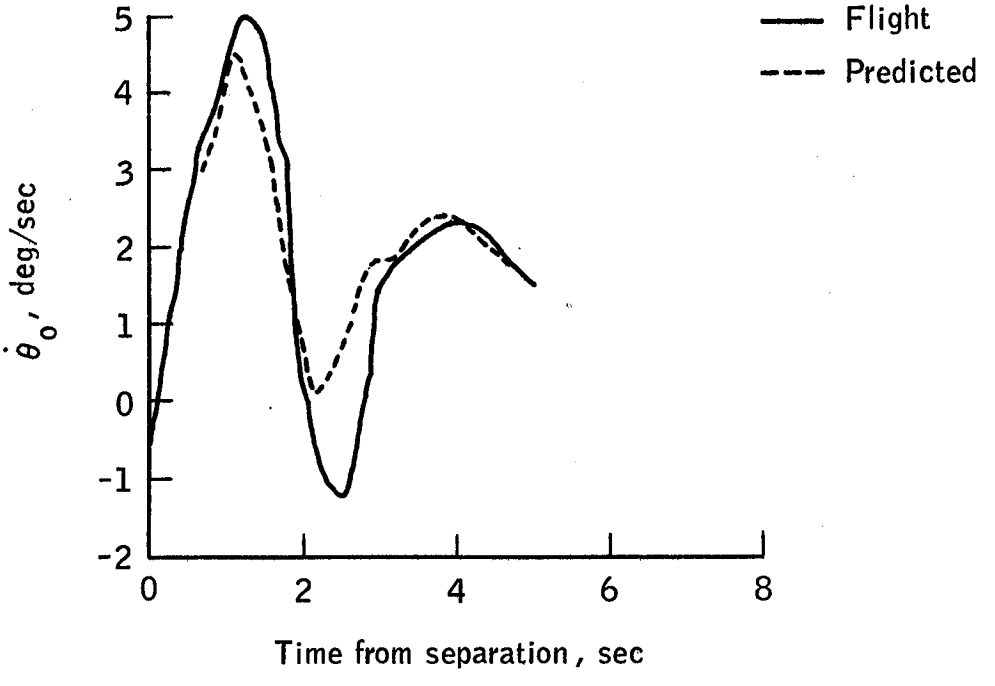

(b) Orbiter pitch rate, $\dot{\theta}_o$, time history.

Figure 12.- Free flight 1, tailcone on.

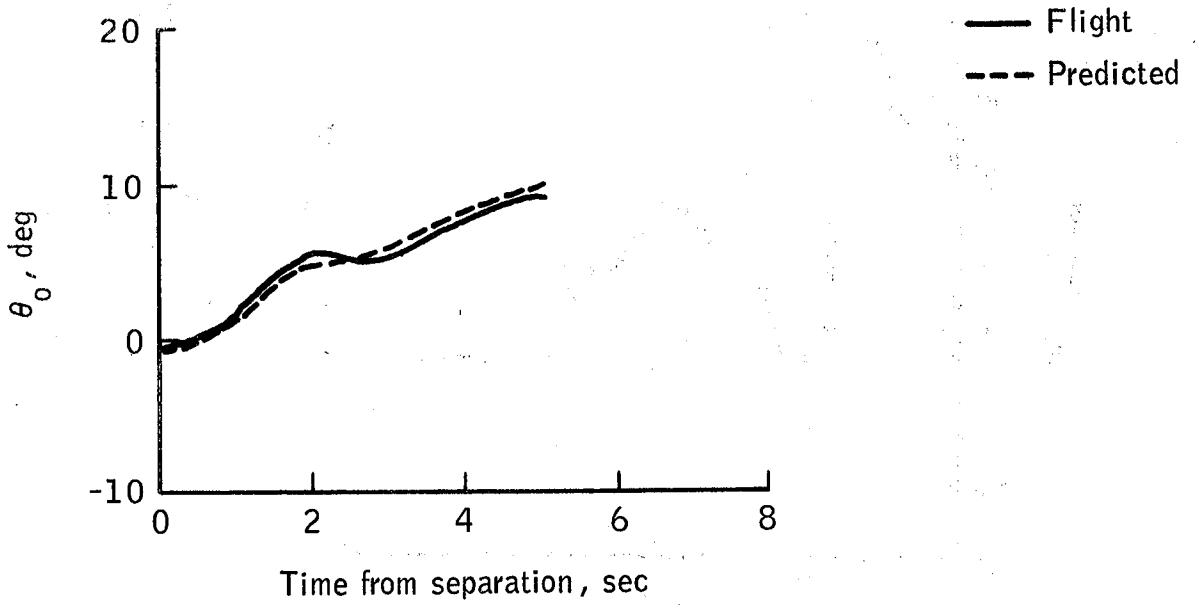

(c) Orbiter pitch attitude, θ_o, time history.

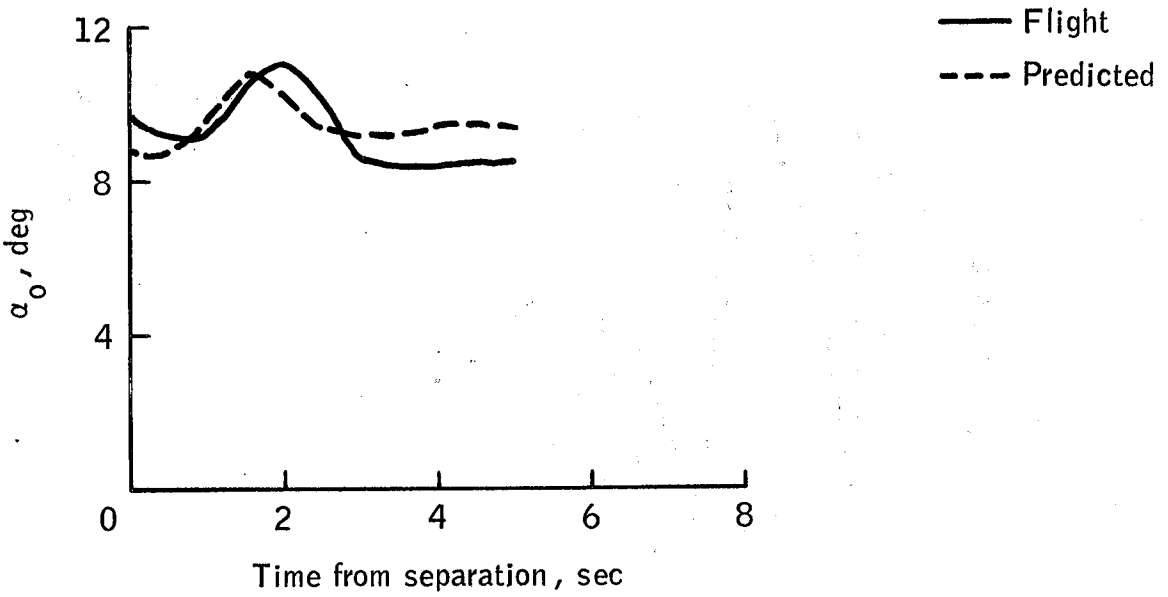

(d) Orbiter angle of attack, α_o, time history.

Figure 12.- Continued.

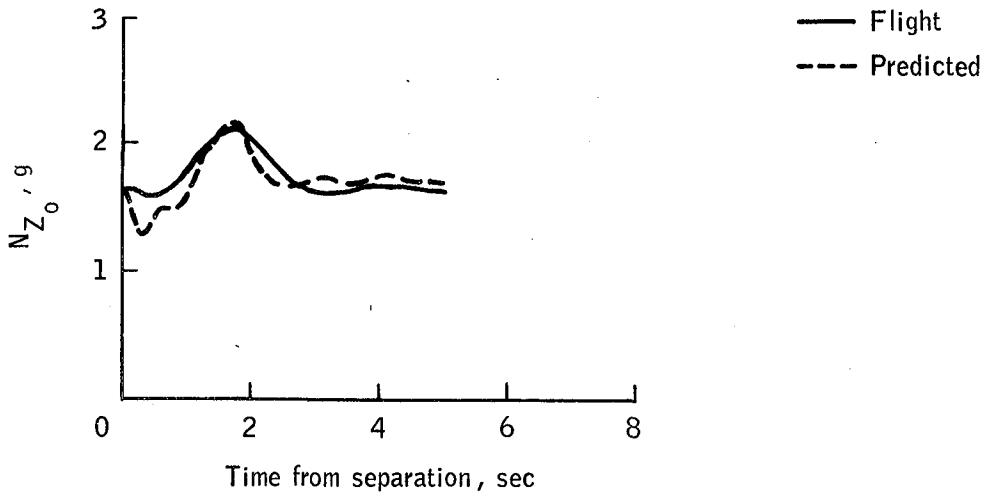

(e) Orbiter normal load factor, N_{Z_o}, time history.

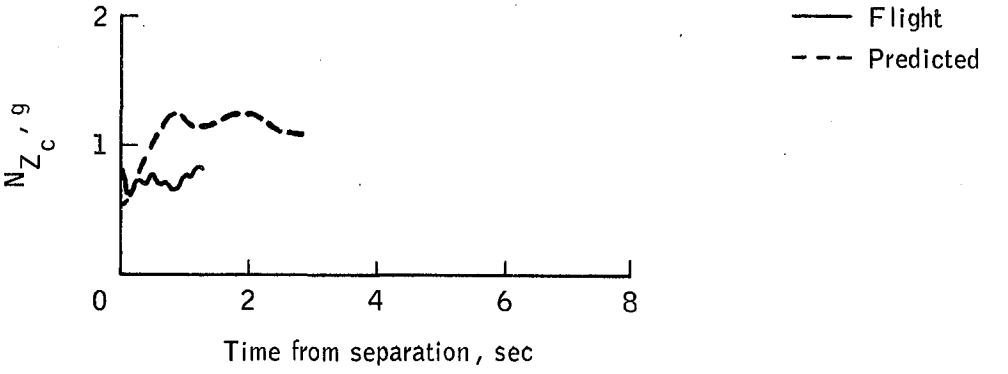

(f) SCA normal load factor, N_{Z_c}, time history.

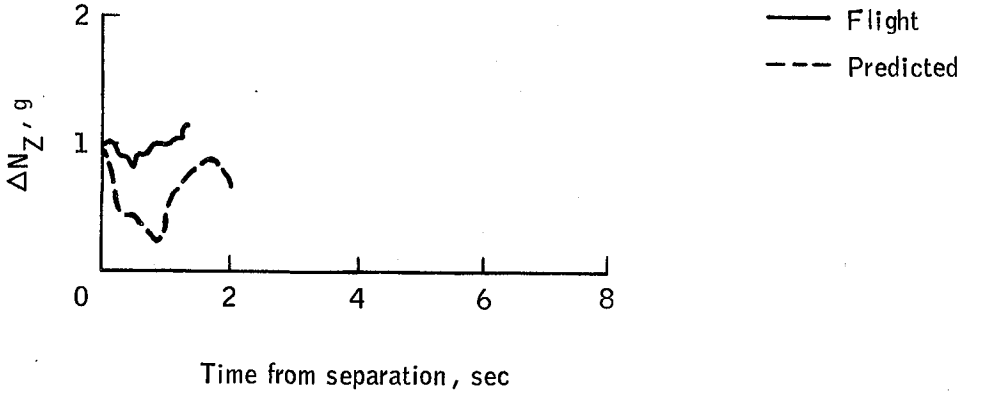

(g) Relative normal load factor, ΔN_Z, time history.

Figure 12.- Continued.

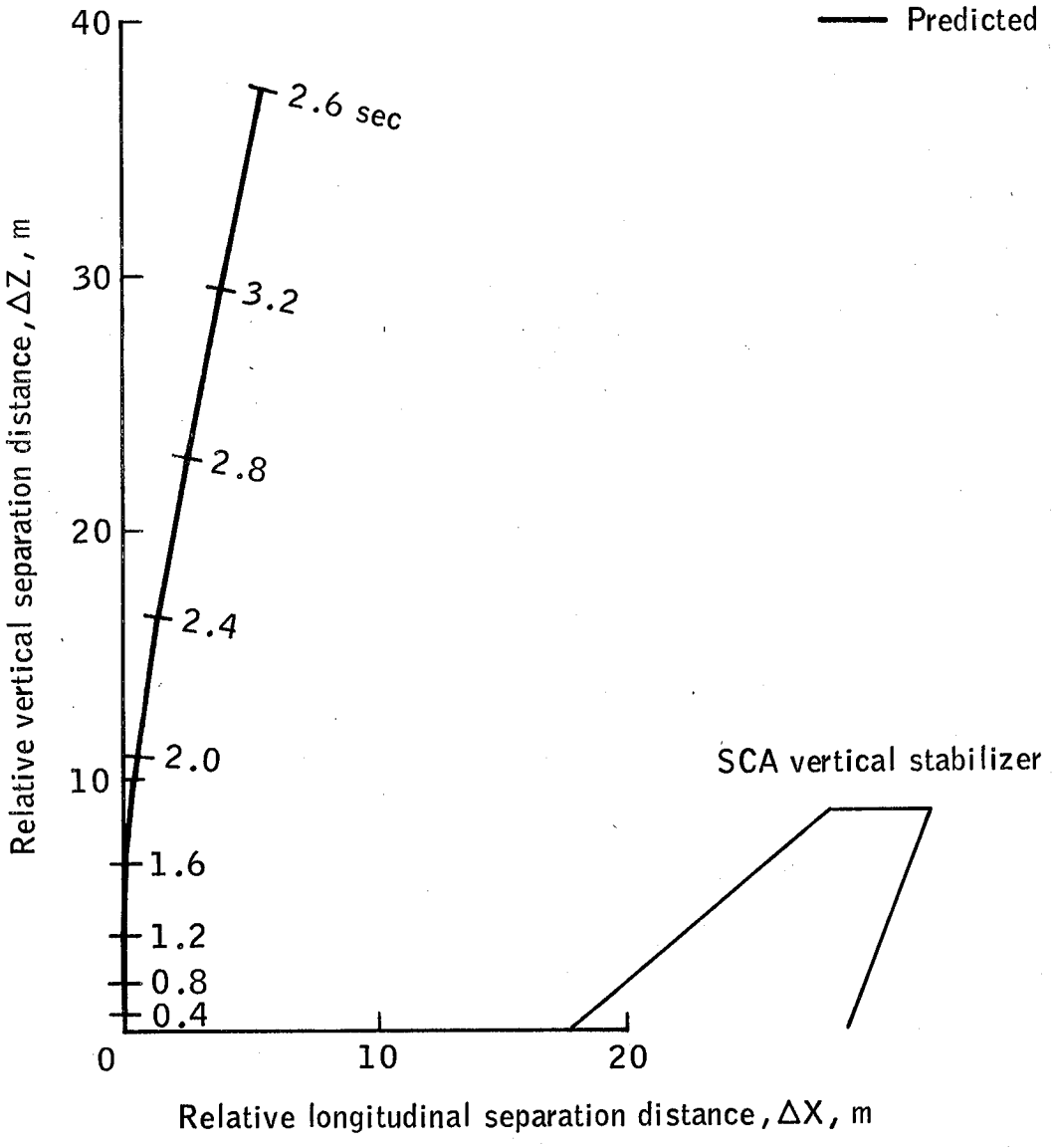

(h) Orbiter aft attach point separation trajectory. (Origin is fixed at SCA aft attach point.)

Figure 12.- Concluded.

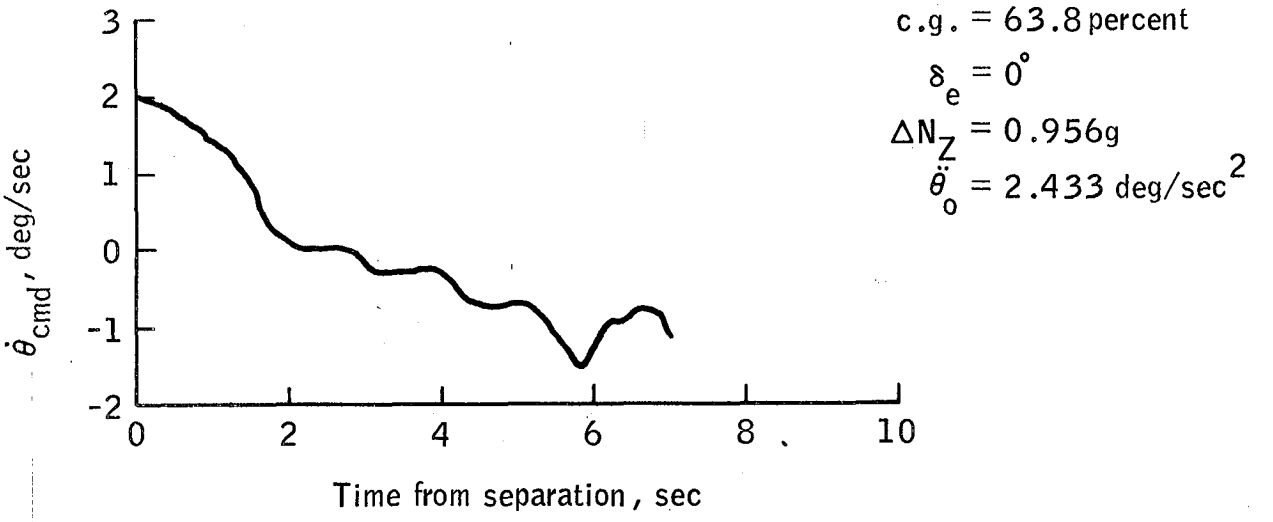

(a) Orbiter pitch rate command, $\dot{\theta}_{cmd}$, time history.

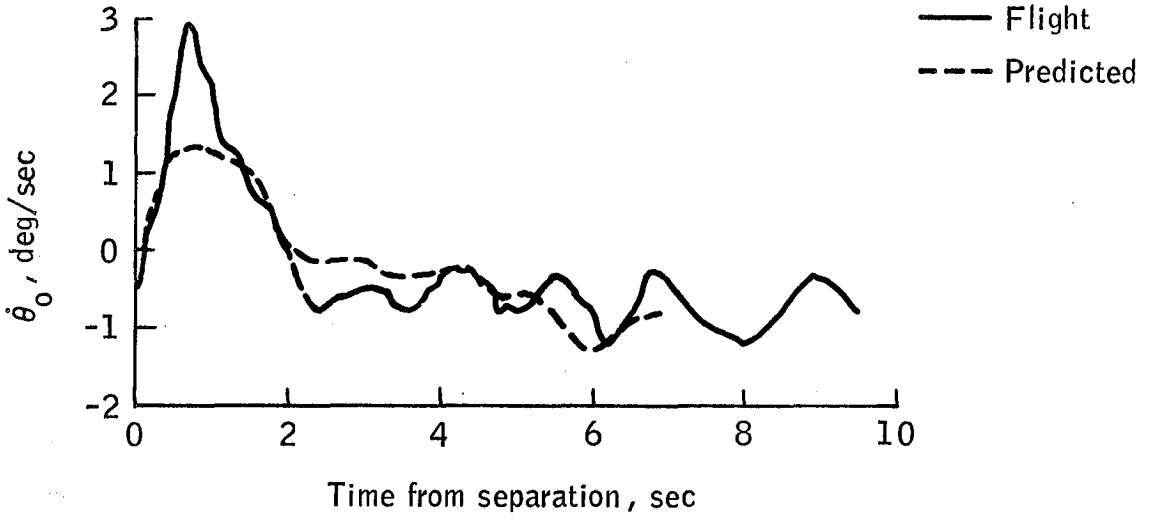

(b) Orbiter pitch rate, $\dot{\theta}_o$, time history.

Figure 13.- Free flight 2, tailcone on.

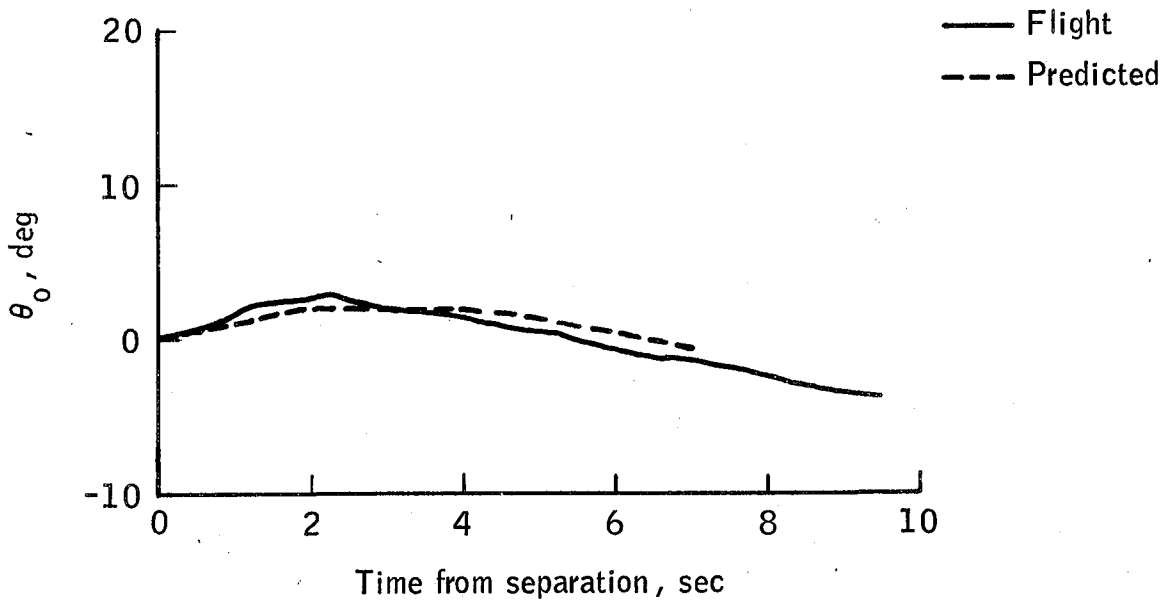

(c) Orbiter pitch attitude, θ_o, time history.

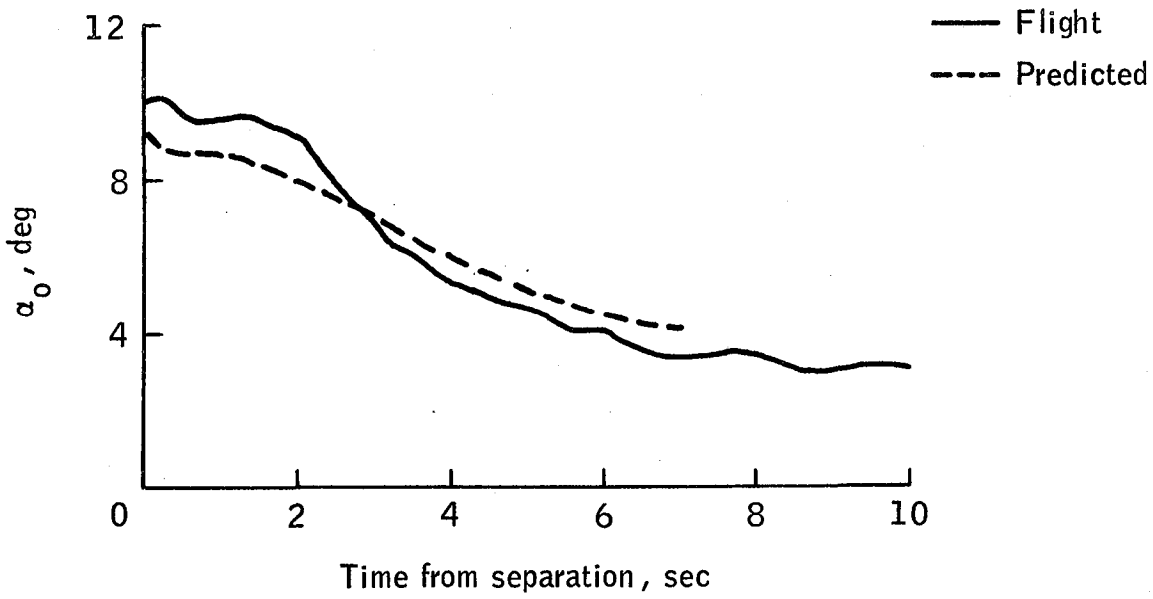

(d) Orbiter angle of attack, α_o, time history.

Figure 13.- Continued.

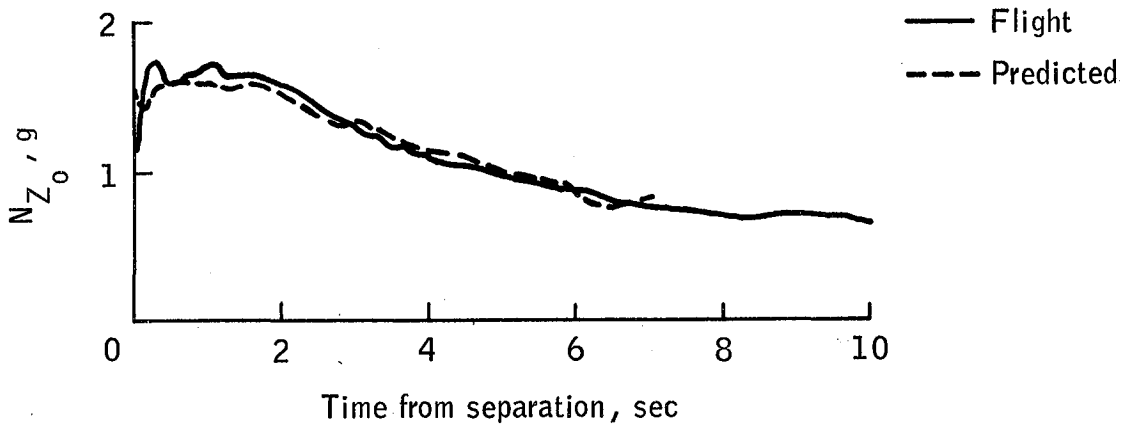

(e) Orbiter normal load factor, N_{Z_o}, time history.

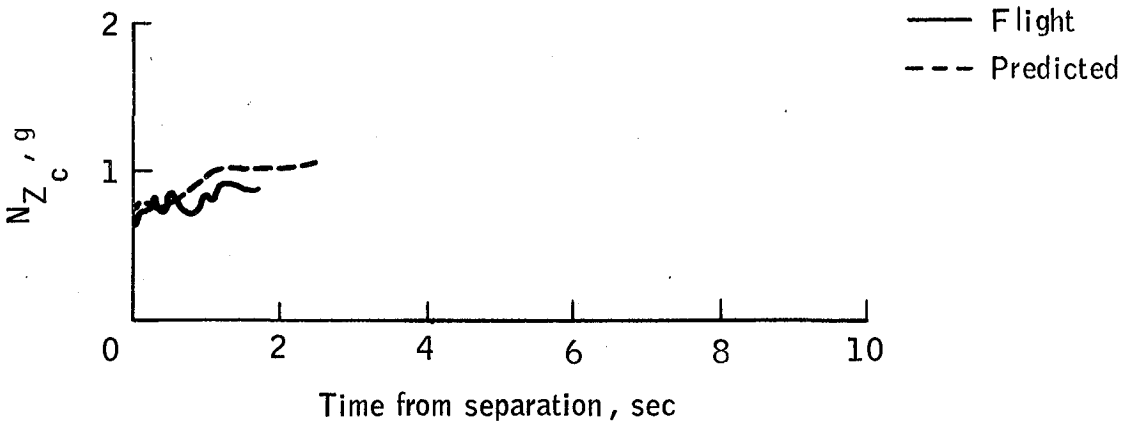

(f) SCA normal load factor, N_{Z_c}, time history.

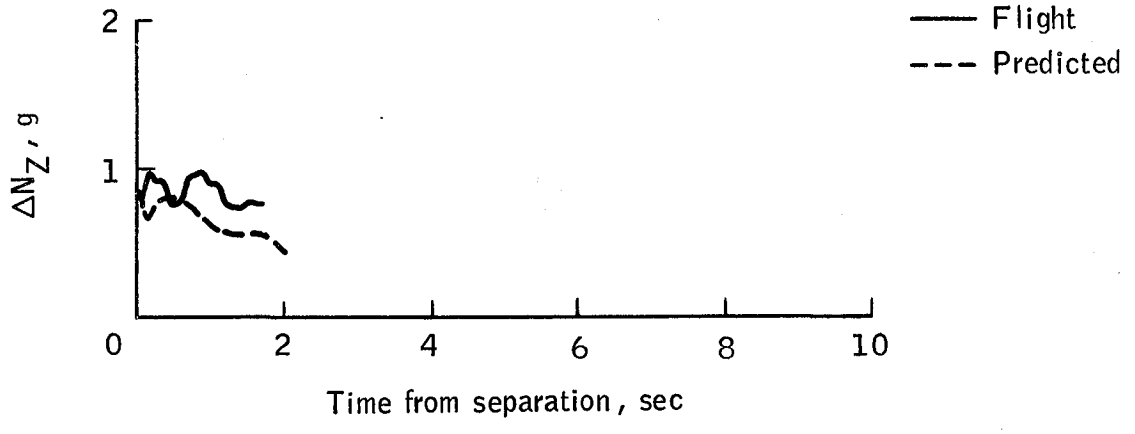

(g) Relative normal load factor, ΔN_Z, time history.

Figure 13.- Continued.

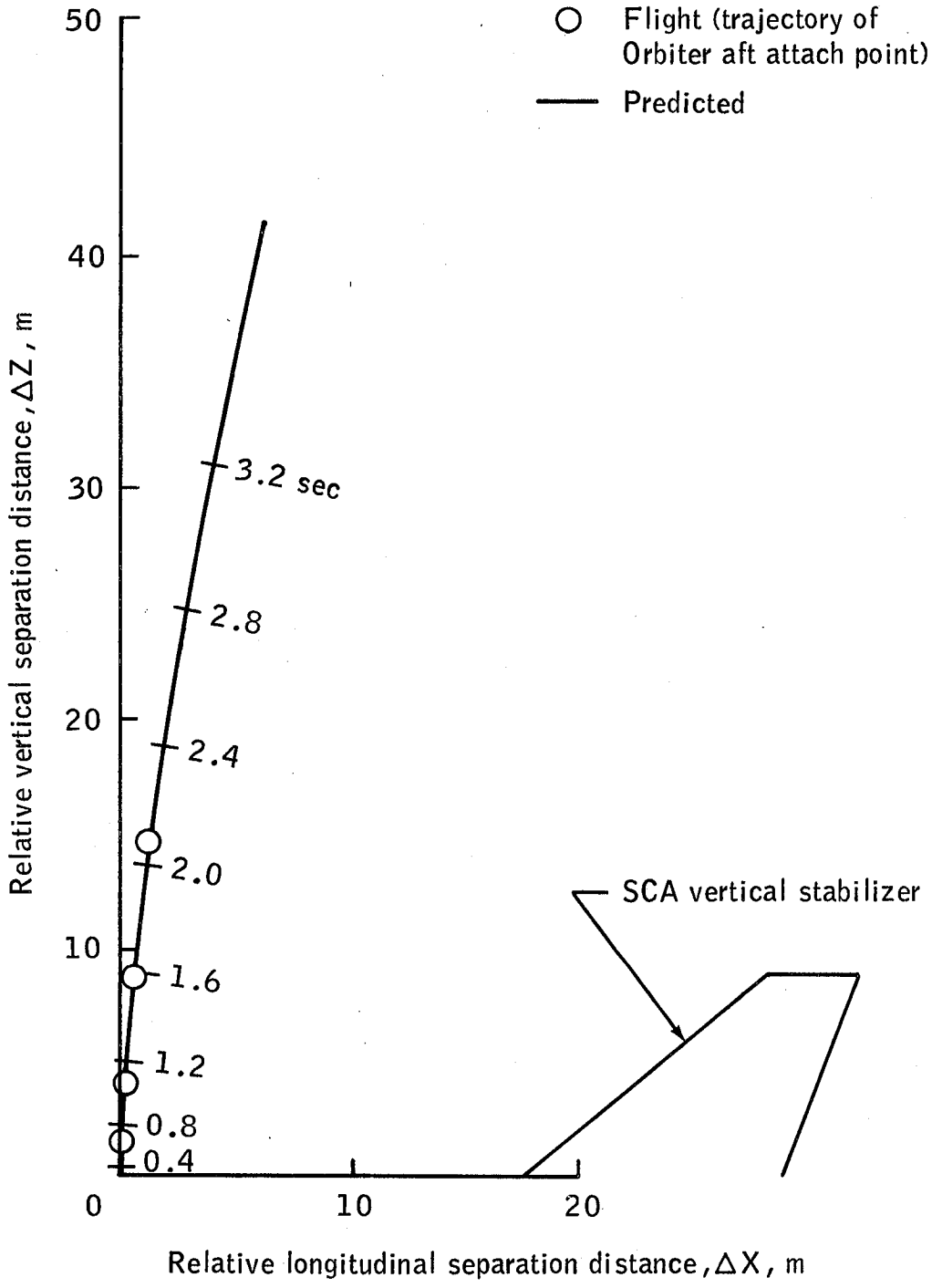

(h) Orbiter aft attach point separation trajectory. (Origin is fixed at SCA aft attach point.)

Figure 13.- Concluded.

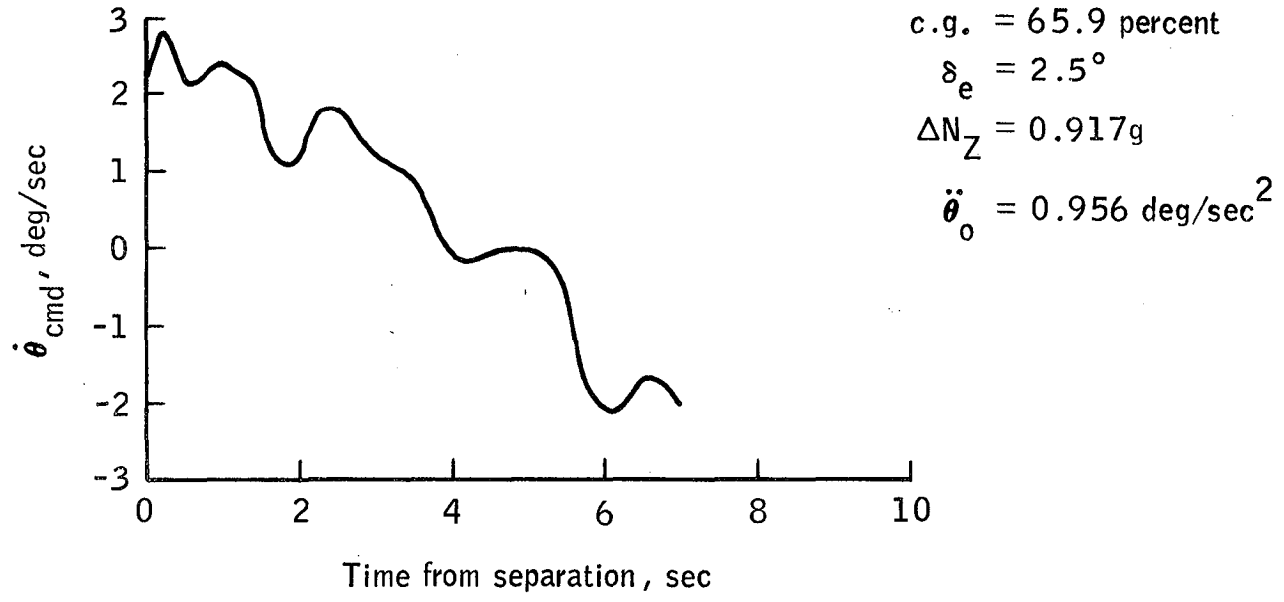

(a) Orbiter pitch rate command, $\dot{\theta}_{cmd}$, time history.

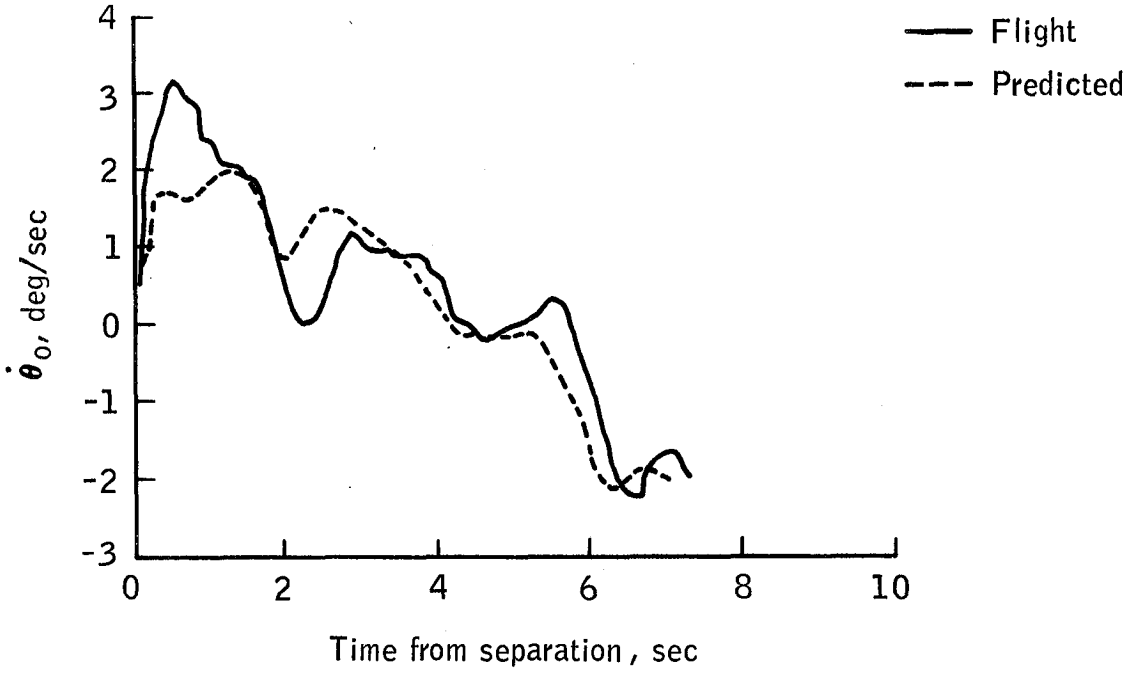

(b) Orbiter pitch rate, $\dot{\theta}_o$, time history.

Figure 14.- Free flight 3, tailcone on.

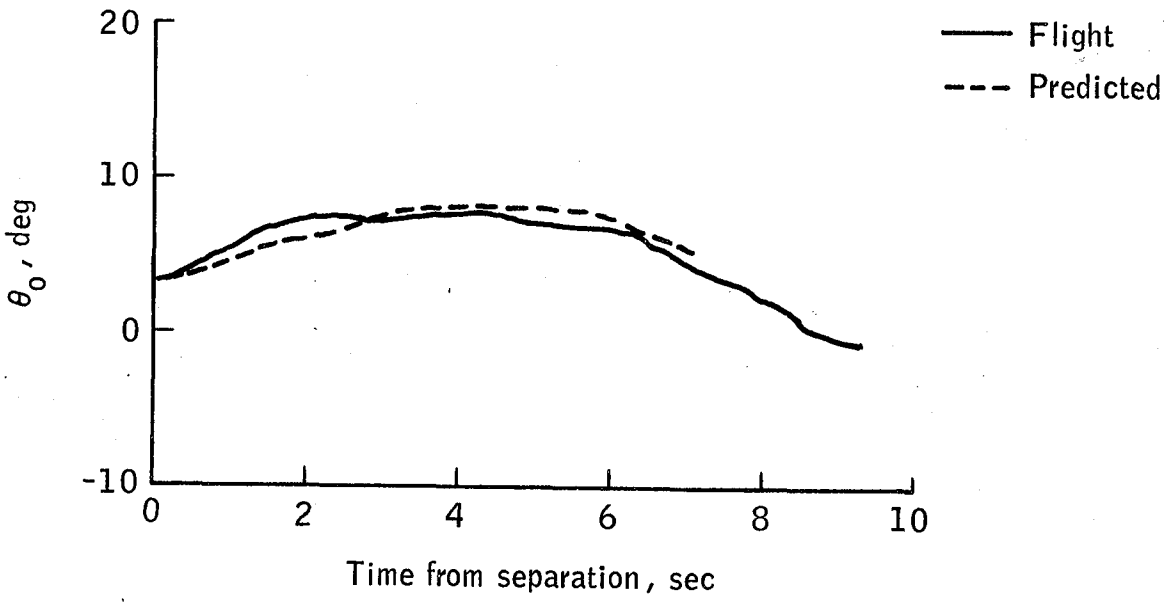

(c) Orbiter pitch attitude, θ_o, time history.

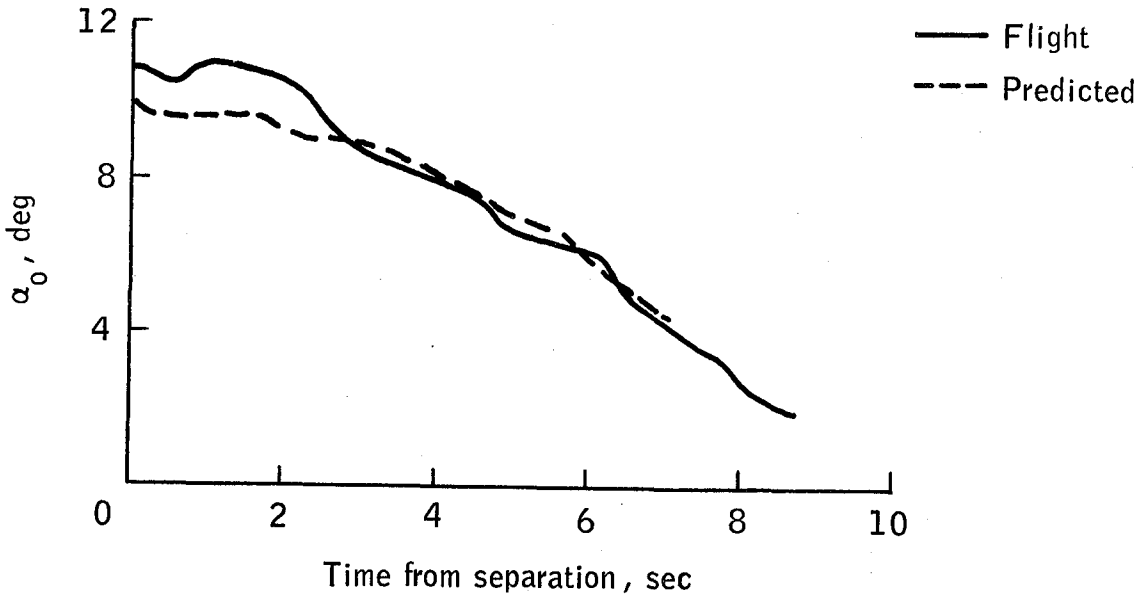

(d) Orbiter angle of attack, α_o, time history.

Figure 14.- Continued.

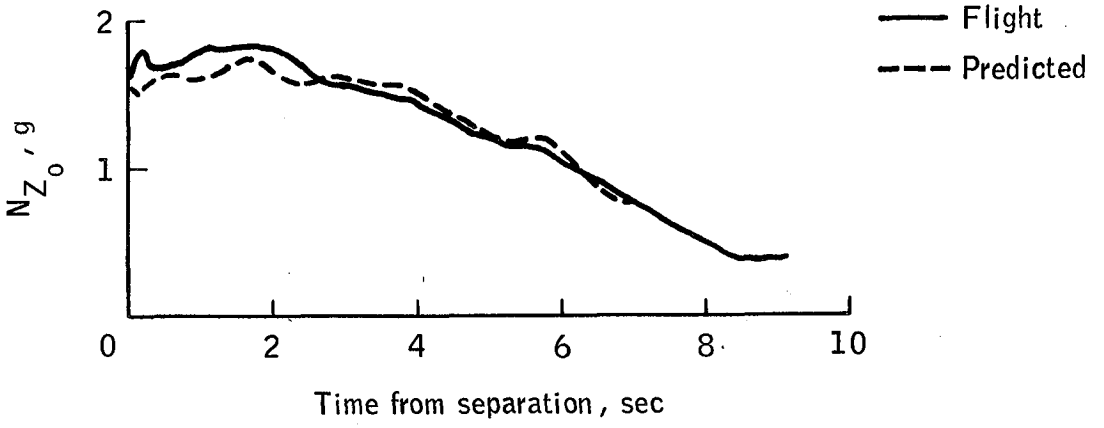

(e) Orbiter normal load factor, N_{Z_o}, time history.

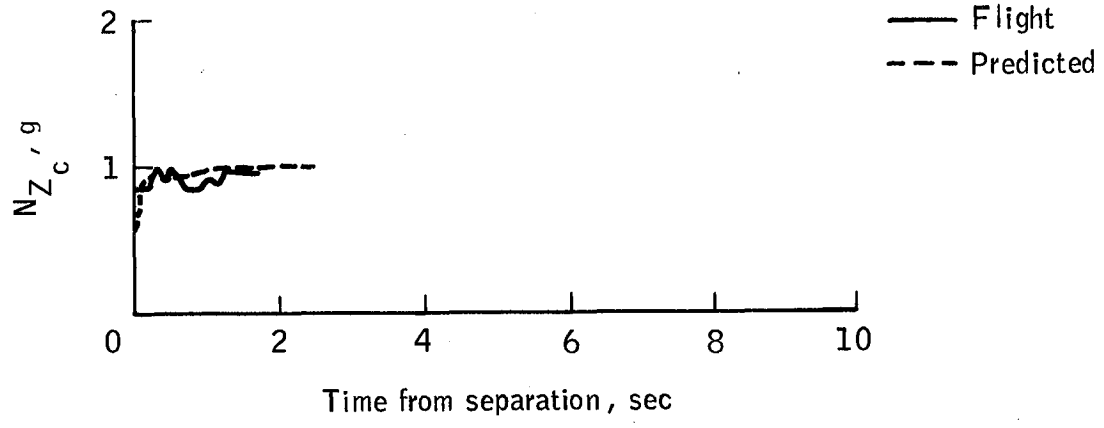

(f) SCA normal load factor, N_{Z_c}, time history.

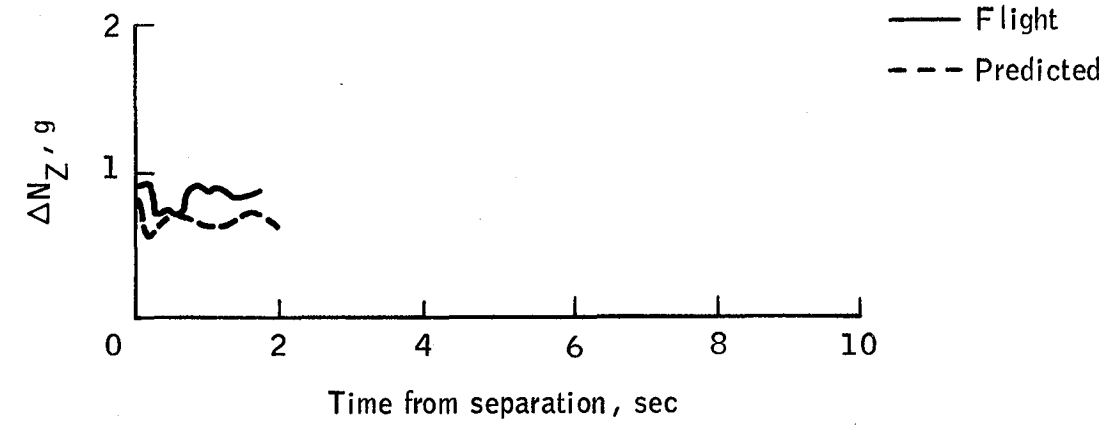

(g) Relative normal load factor, ΔN_Z, time history.

Figure 14.- Continued.

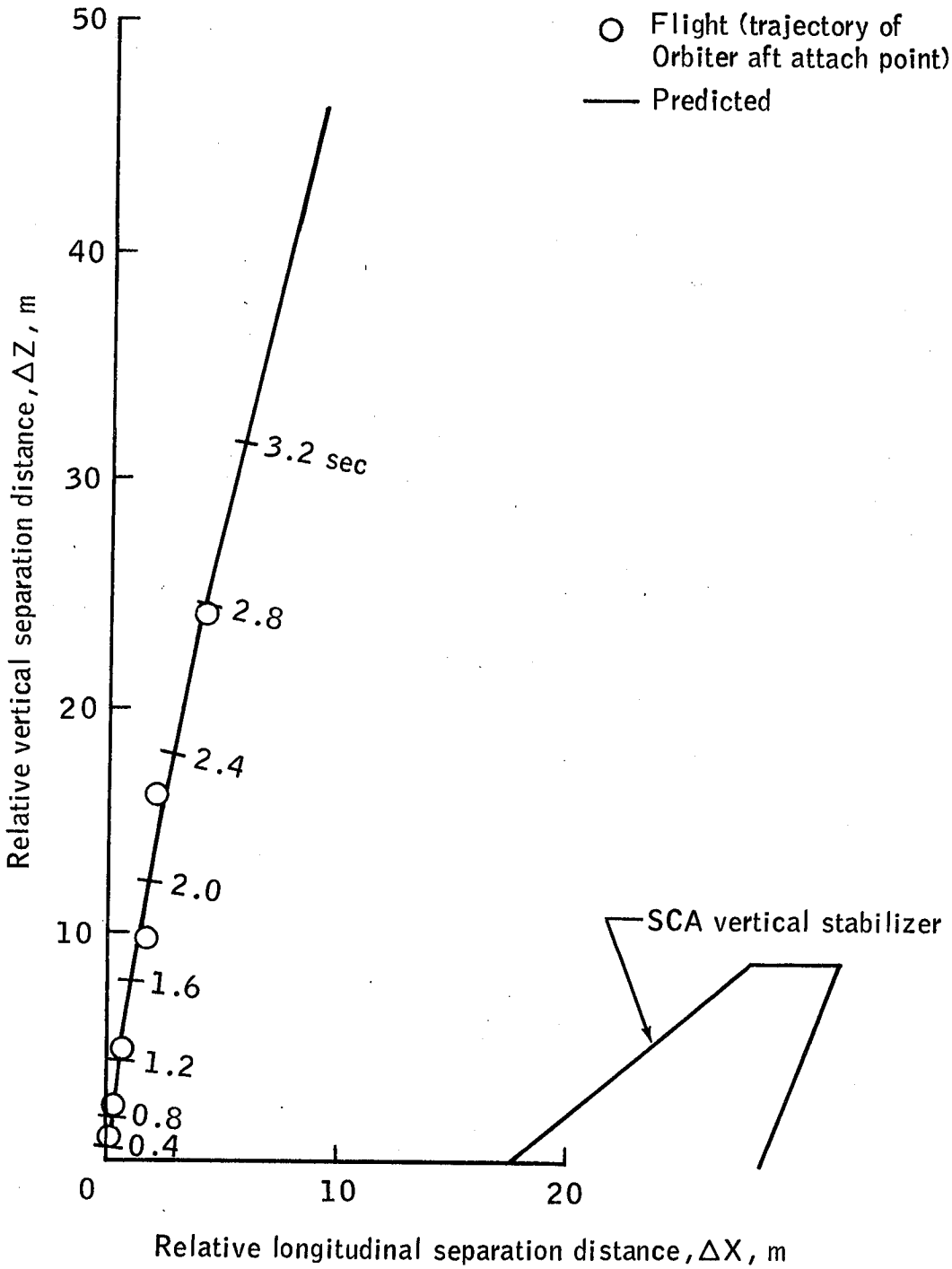

(h) Orbiter aft attach point separation trajectory. (Origin is fixed at SCA aft attach point.)

Figure 14.- Concluded.

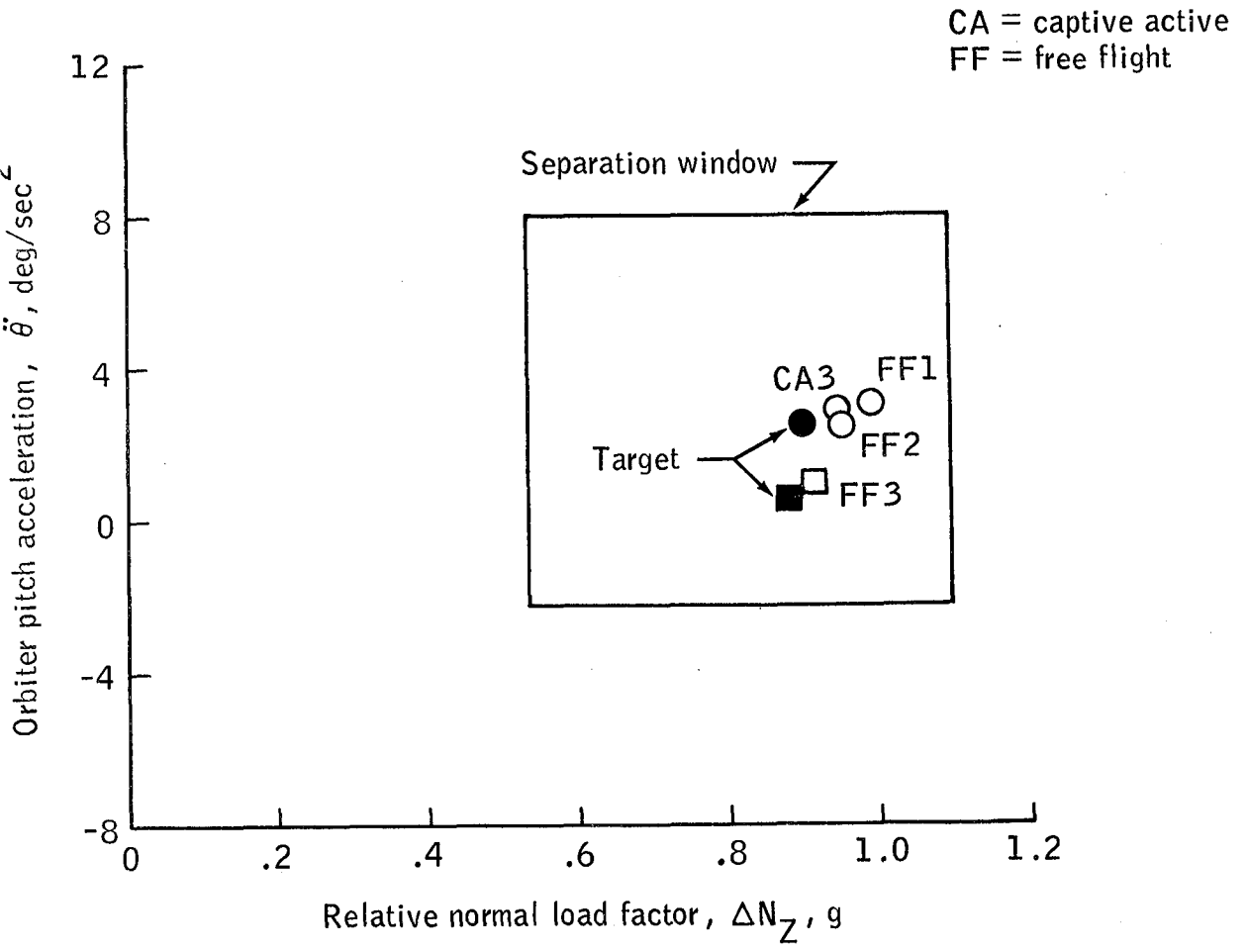

Figure 15.- Orbiter tailcone-on separation initial conditions. (See figure 2.)

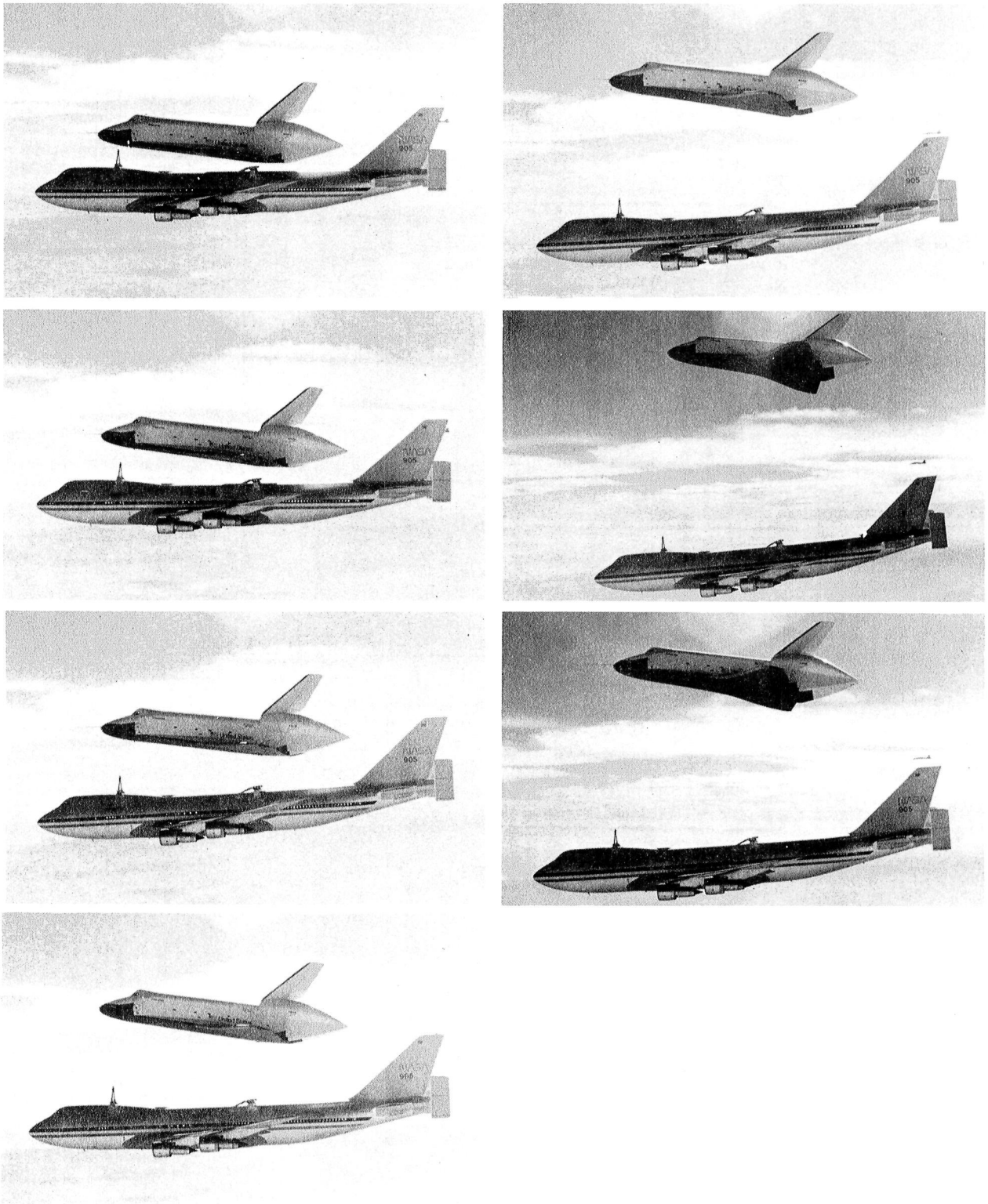

Figure 16.- Free flight 3, SCA/Orbiter tailcone-on separation trajectory (2 frames per second).

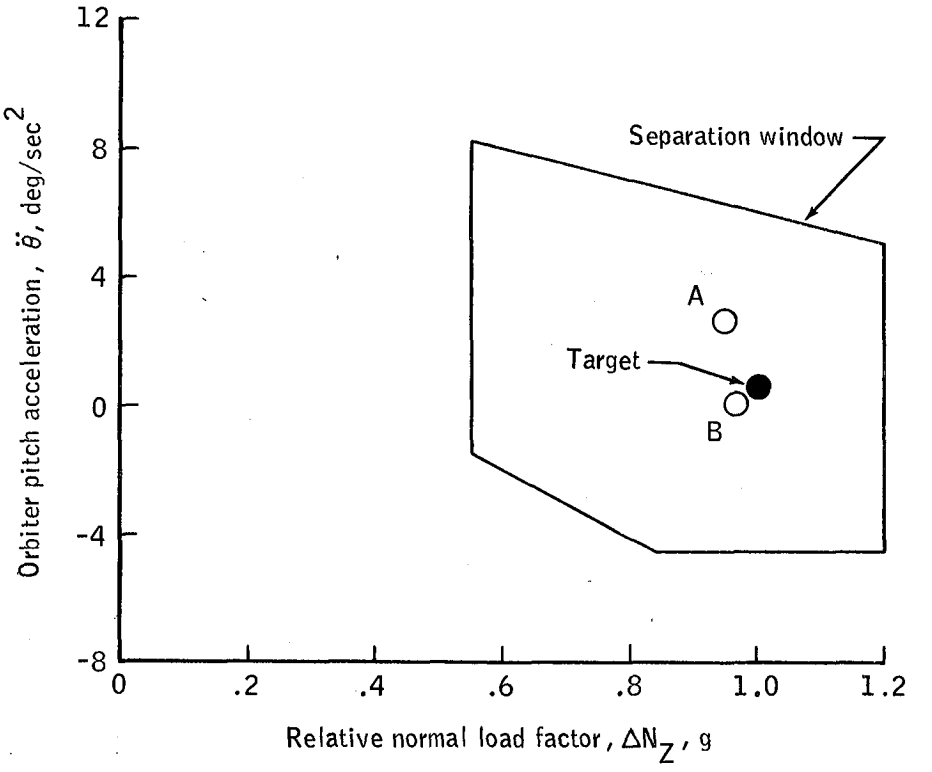

(a) Relative normal load factor compared to Orbiter pitch acceleration.

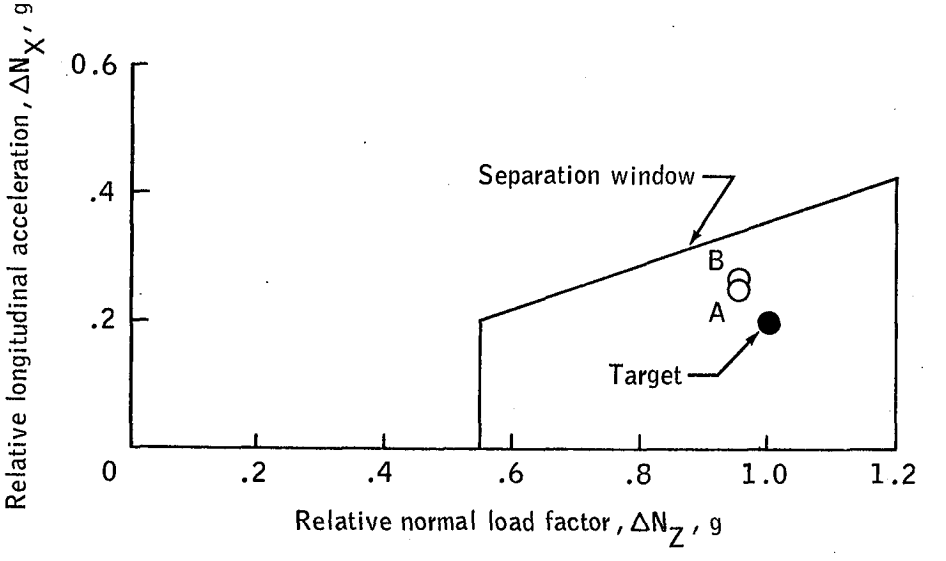

(b) Relative normal load factor compared to relative longitudinal acceleration.

Figure 17.- Free flight 4 GO/NO-GO separation window. (A and B indicate the load cell data used.)

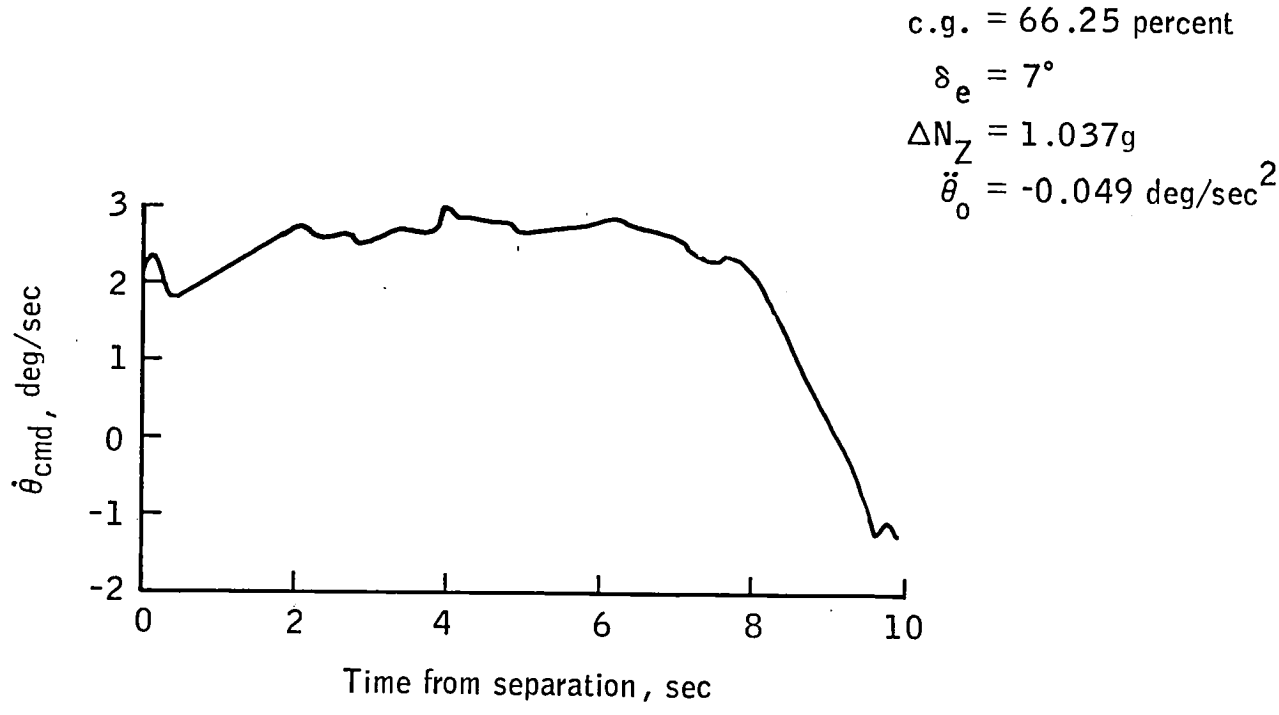

(a) Orbiter pitch rate command, $\dot{\theta}_{cmd}$, time history.

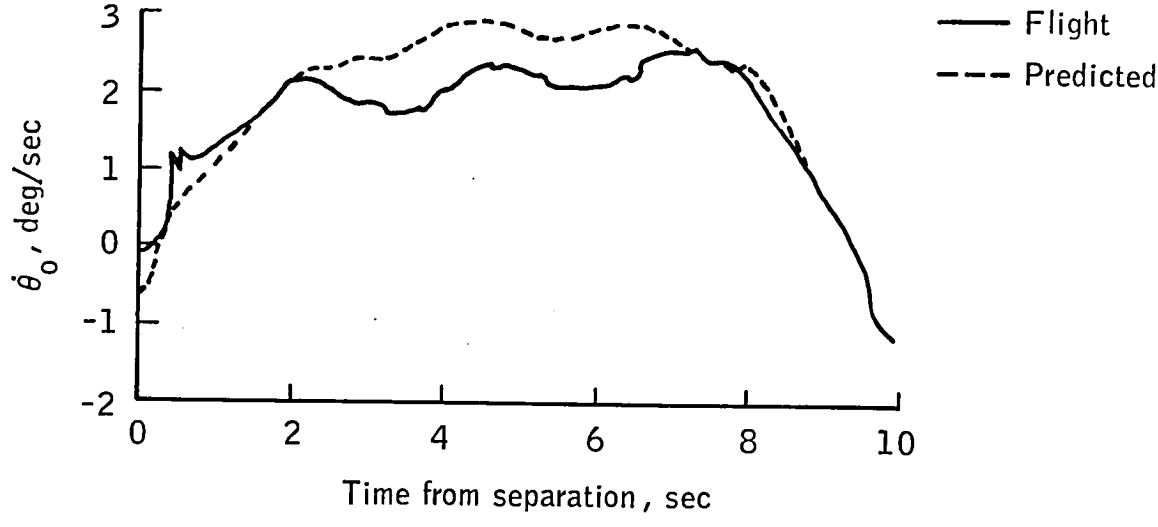

(b) Orbiter pitch rate, $\dot{\theta}_o$, time history.

Figure 18.- Free flight 4, tailcone off.

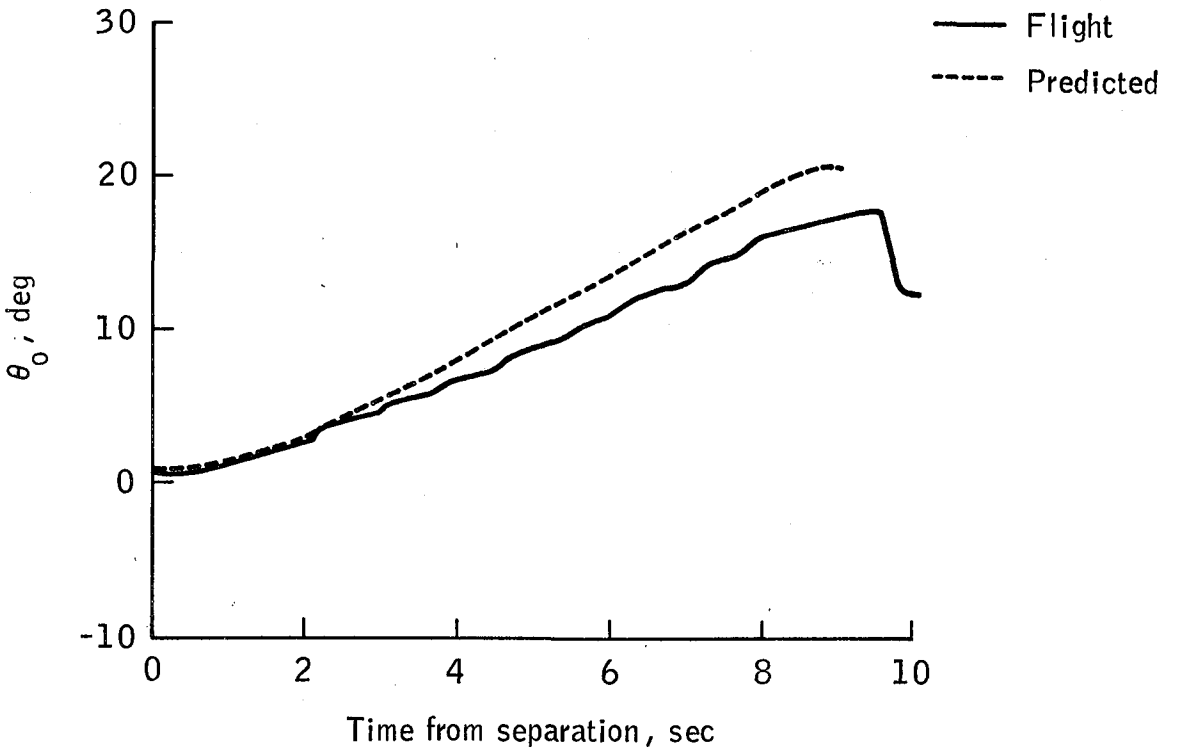

(c) Orbiter pitch attitude, θ_o, time history.

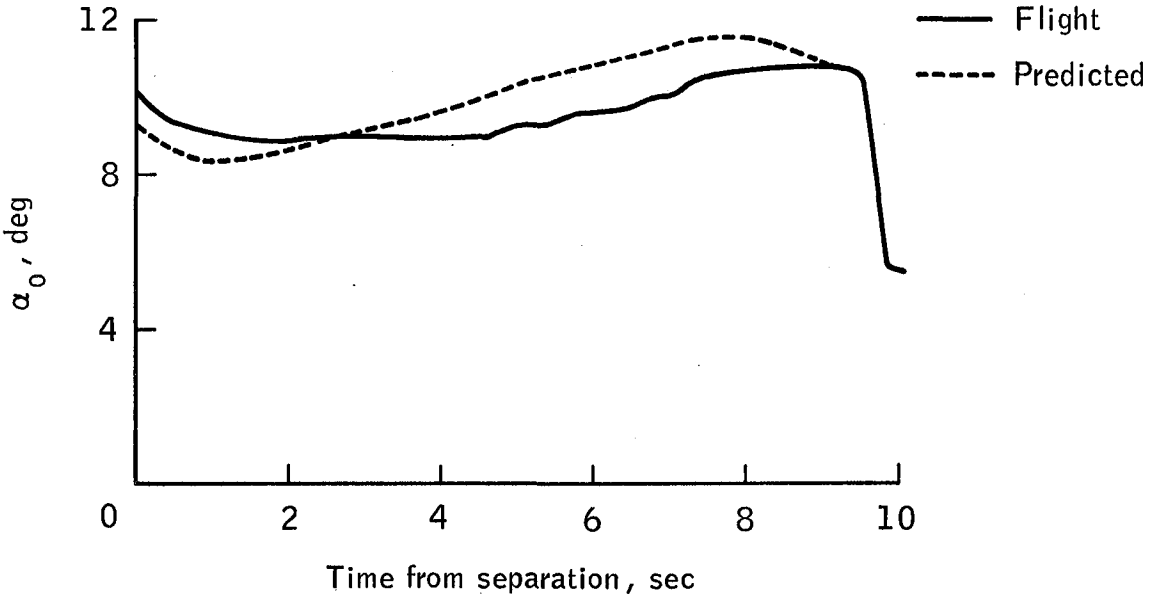

(d) Orbiter angle of attack, α_o, time history.

Figure 18.- Continued.

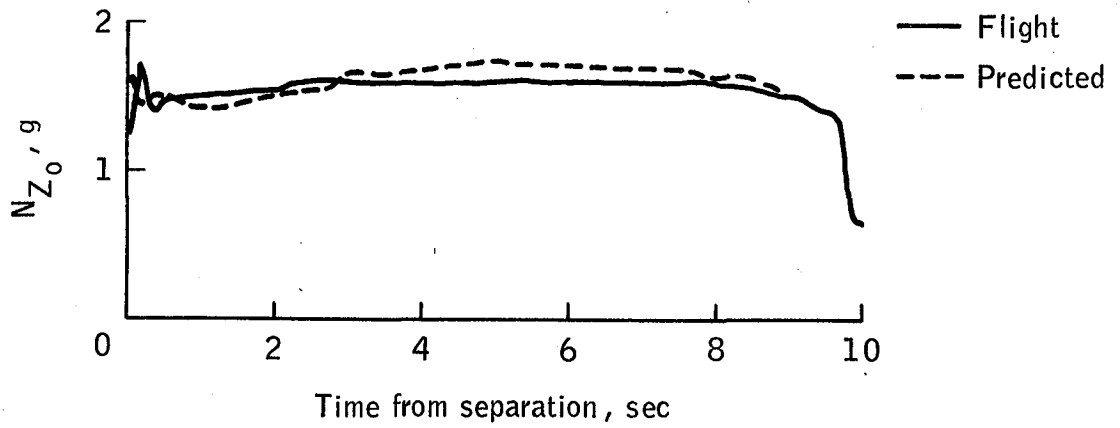

(e) Orbiter normal load factor, N_{Z_o}, time history.

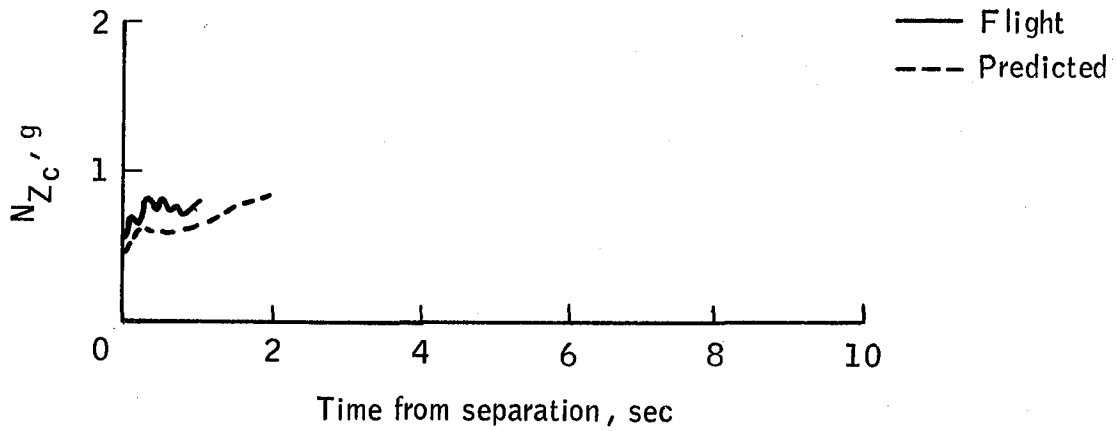

(f) SCA normal load factor, N_{Z_c}, time history.

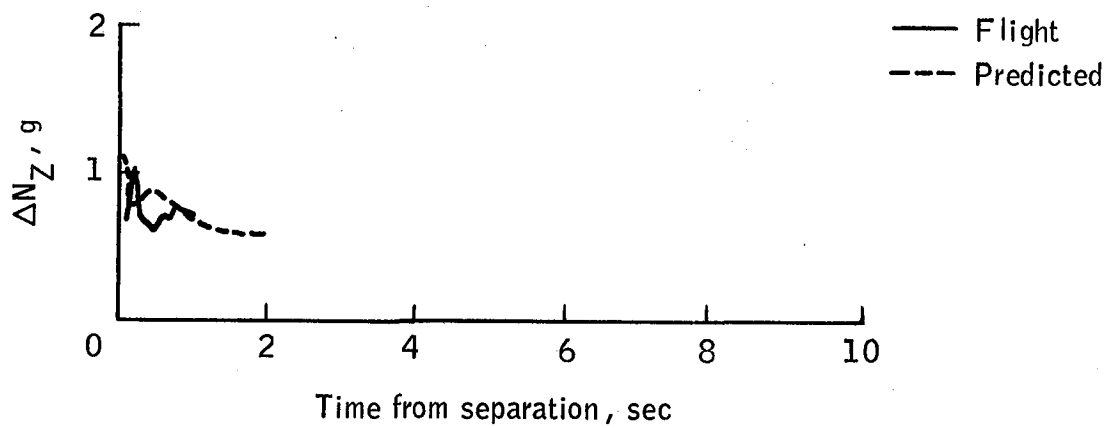

(g) Relative normal load factor, ΔN_Z, time history.

Figure 18.- Continued.

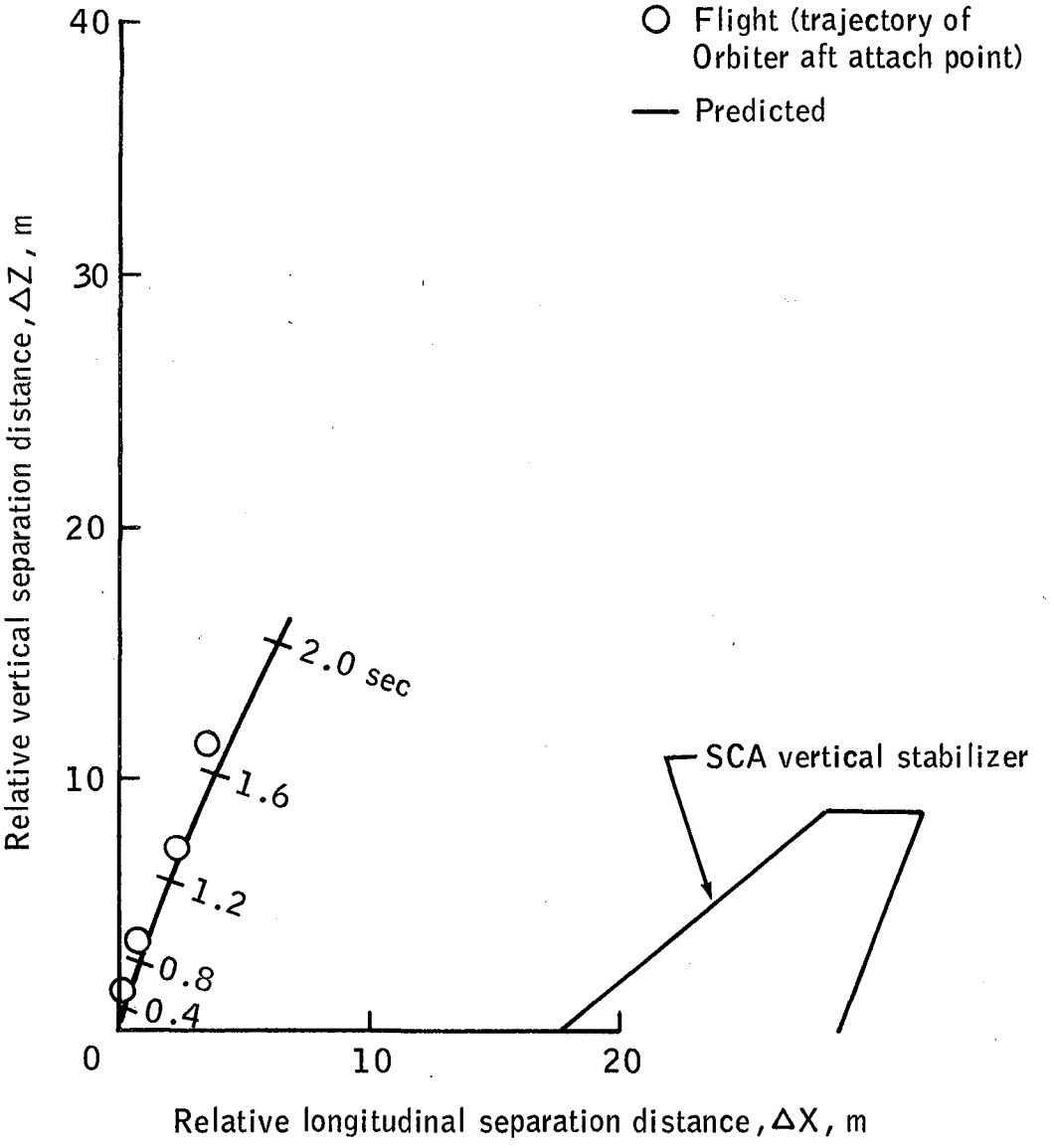

(h) Orbiter aft attach point separation trajectory. (Origin is fixed at aft attach point.)

Figure 18.- Concluded.

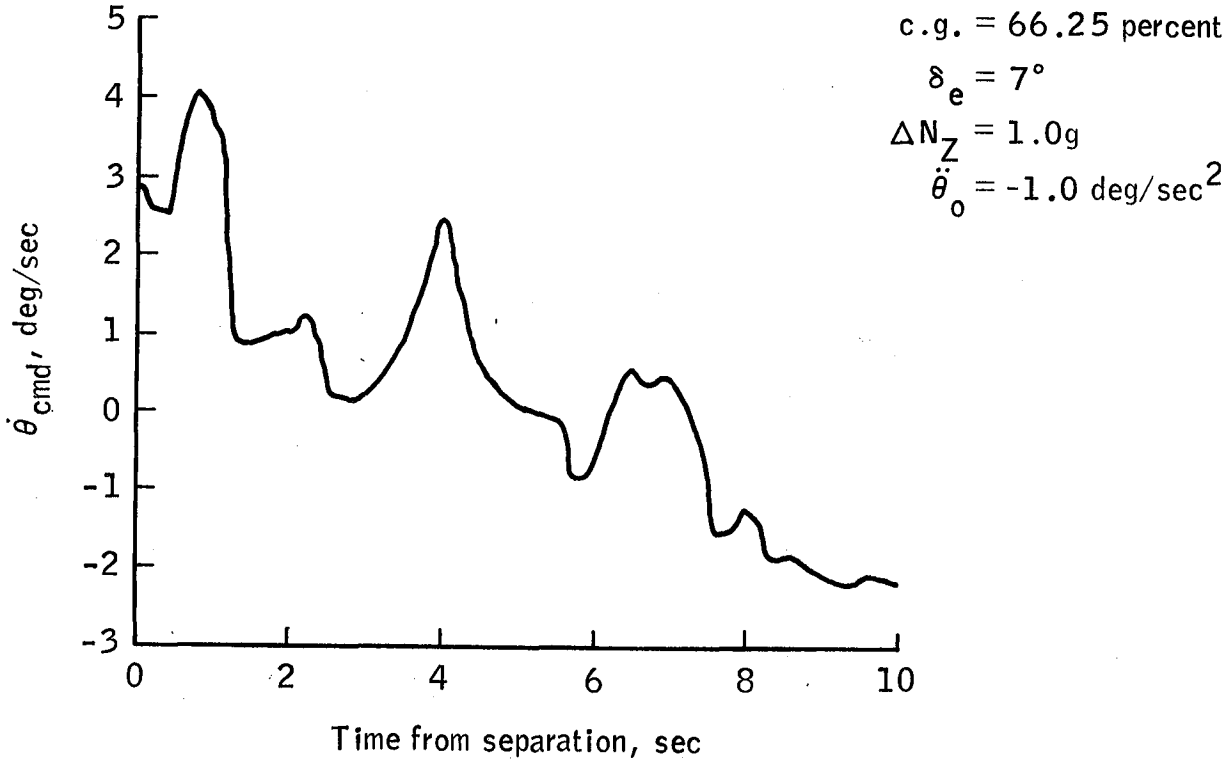

(a) Orbiter pitch rate command, $\dot{\theta}_{cmd}$, time history.

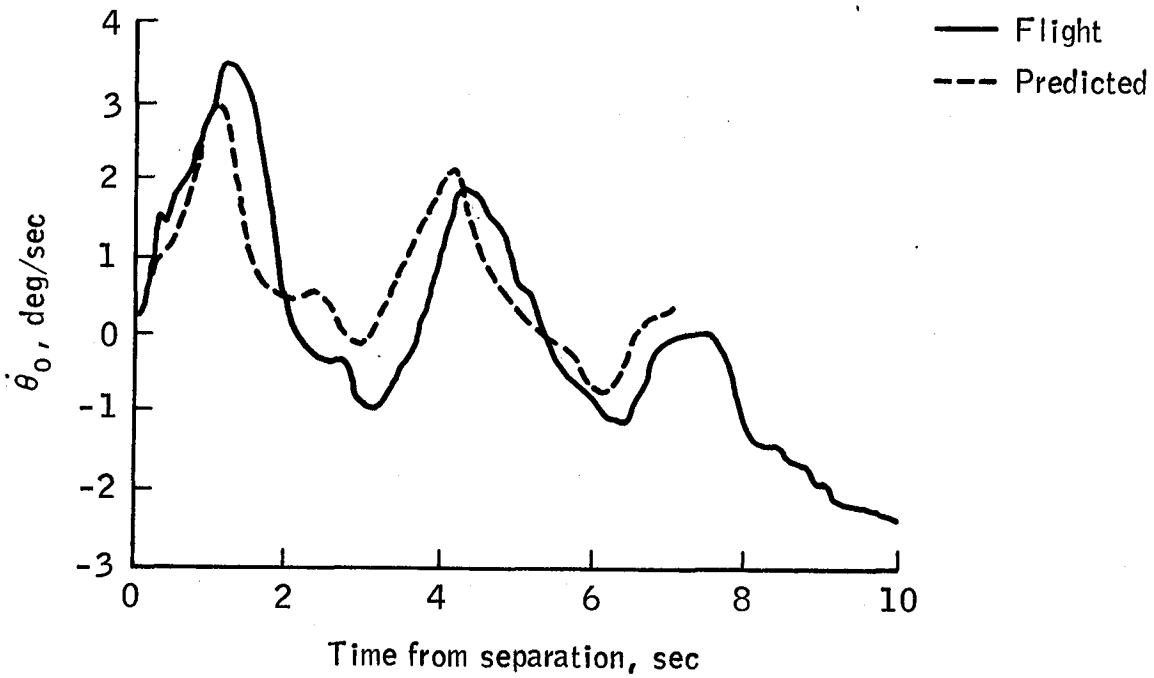

(b) Orbiter pitch rate, $\dot{\theta}_o$, time history.

Figure 19.- Free flight 5, tailcone off.

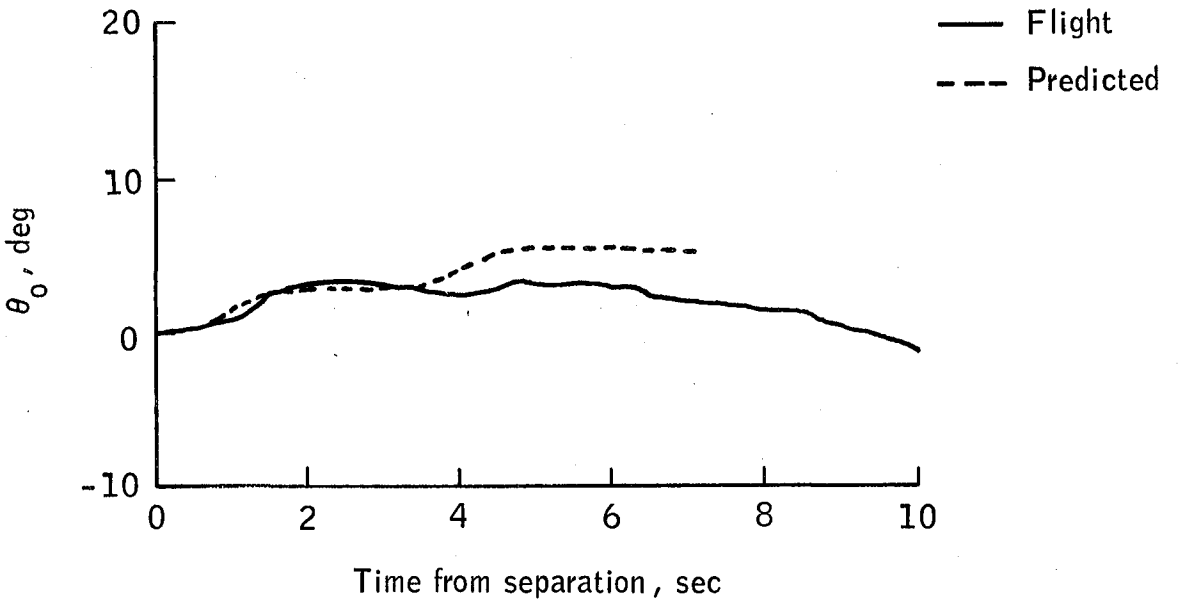

(c) Orbiter pitch attitude, θ_o, time history.

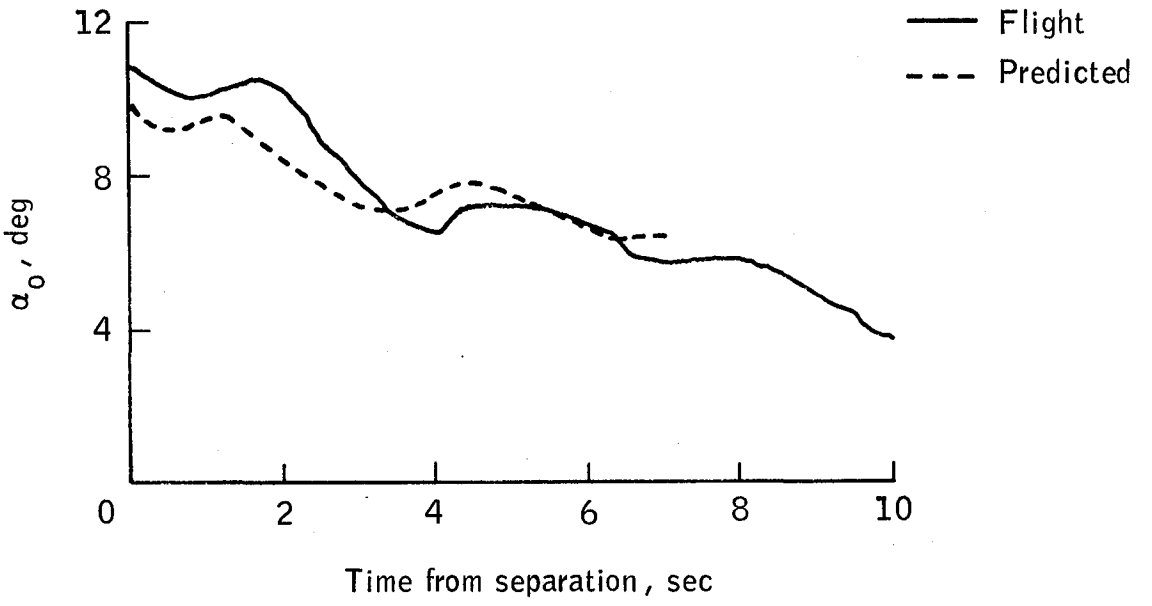

(d) Orbiter angle of attack, α_o, time history.

Figure 19.- Continued.

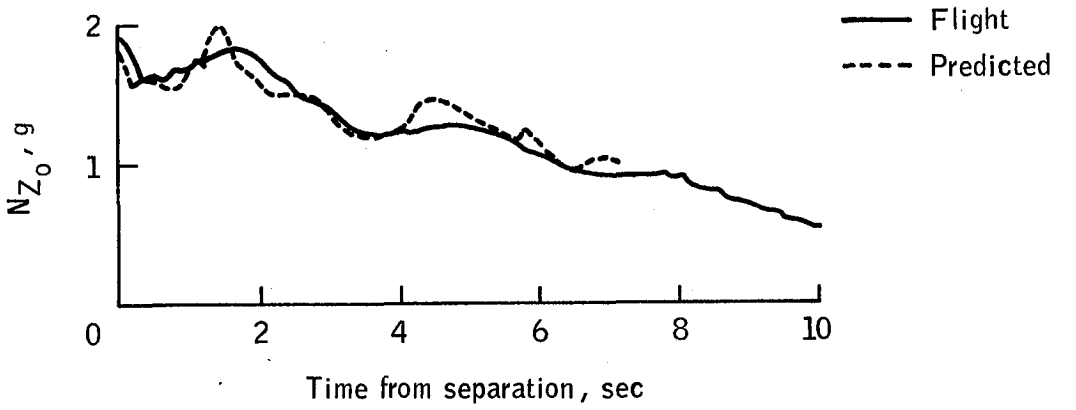

(e) Orbiter normal load factor, N_{Z_o}, time history.

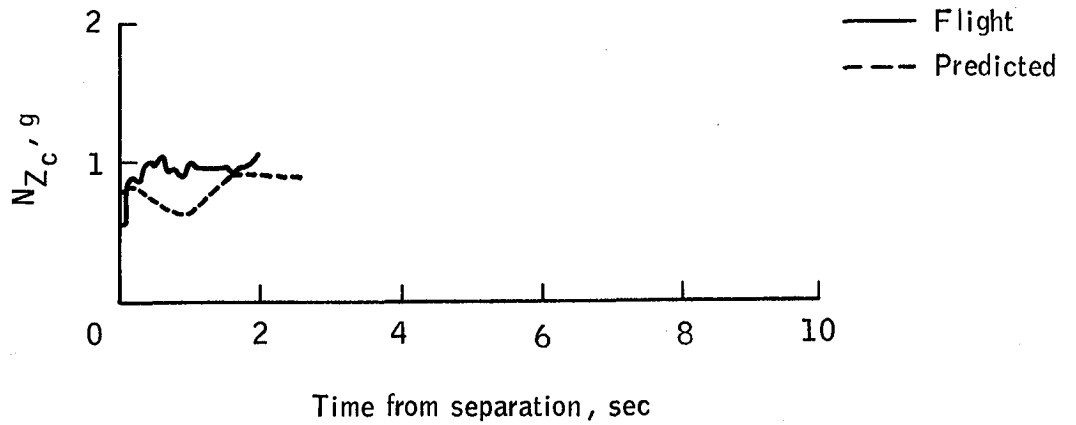

(f) SCA normal load factor, N_{Z_c}, time history.

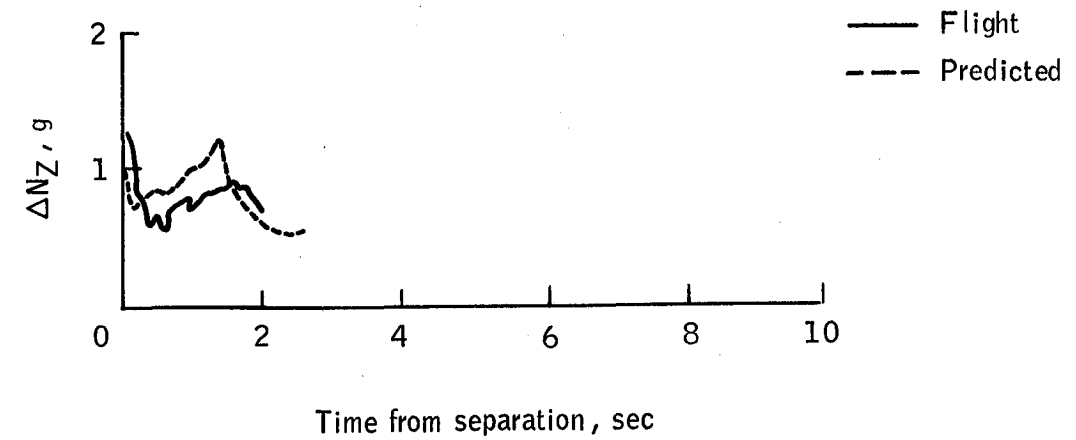

(g) Relative normal load factor, ΔN_Z, time history.

Figure 19.- Continued.

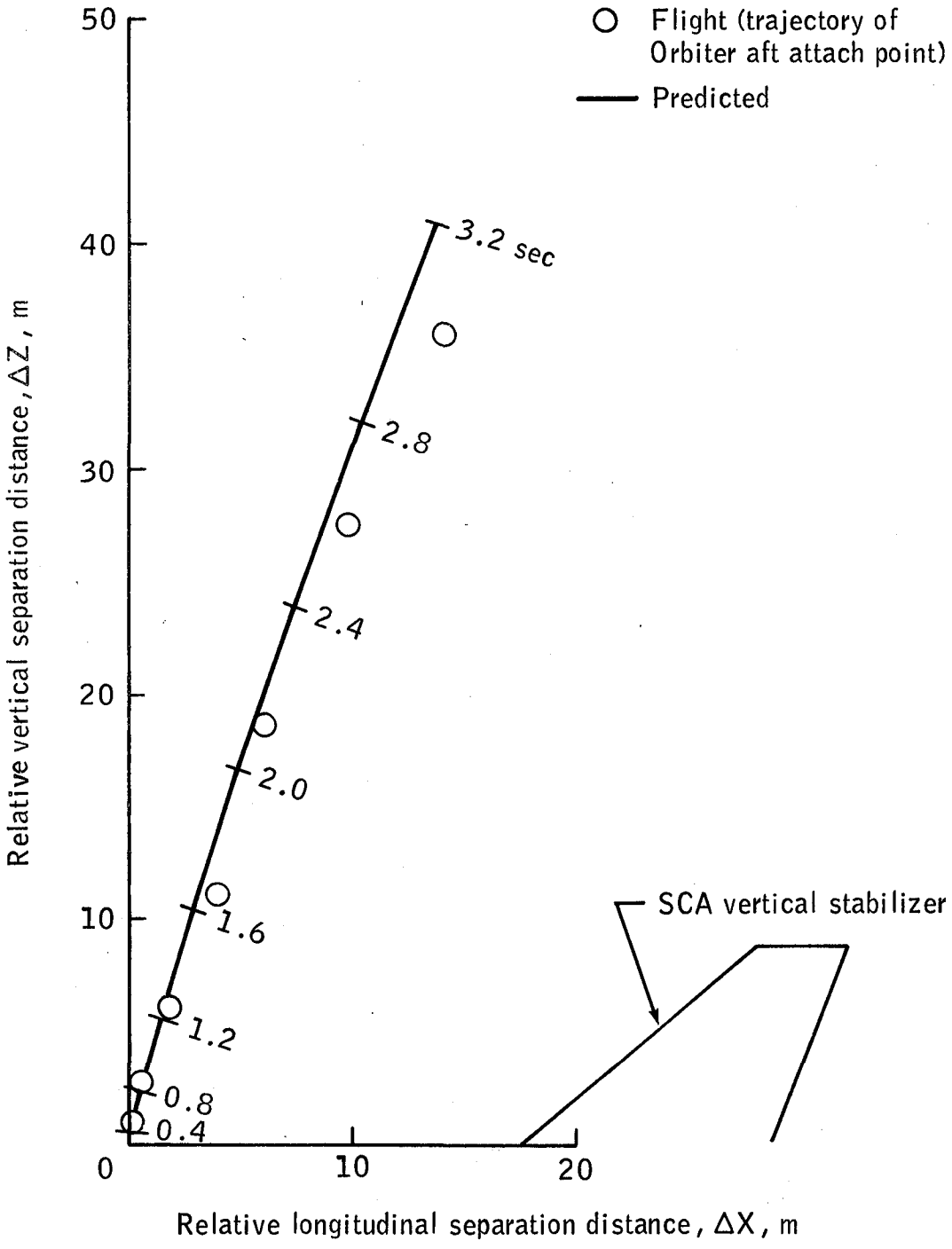

(h) Orbiter aft attach point separation trajectory. (Origin is fixed at SCA aft attach point.)

Figure 19.- Concluded.

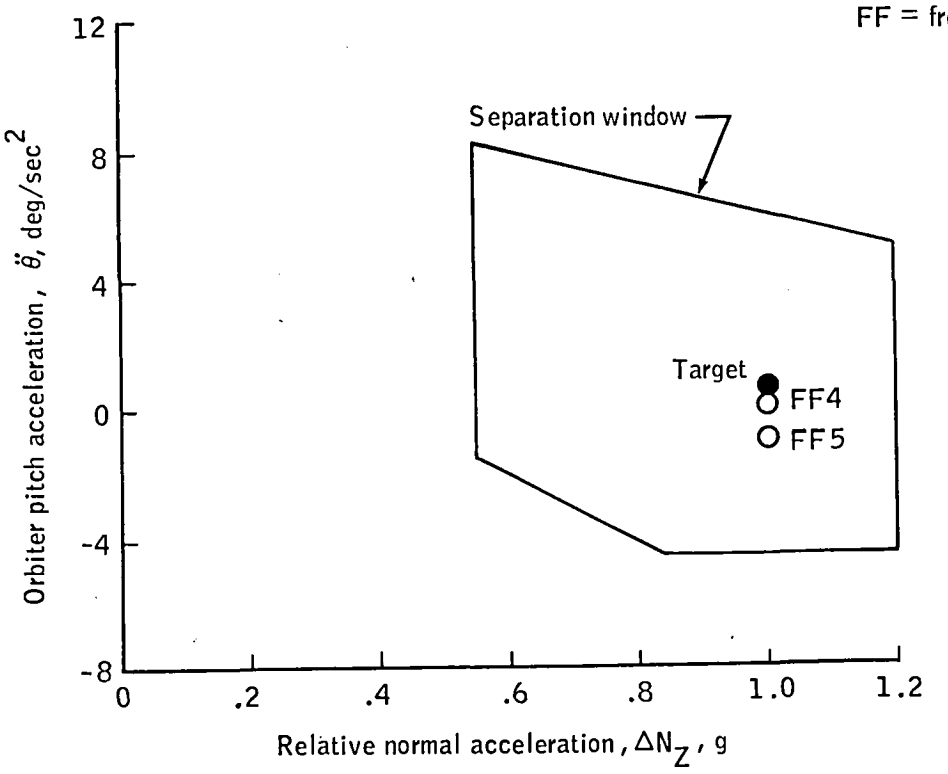

(a) Relative normal acceleration compared to Orbiter pitch acceleration.

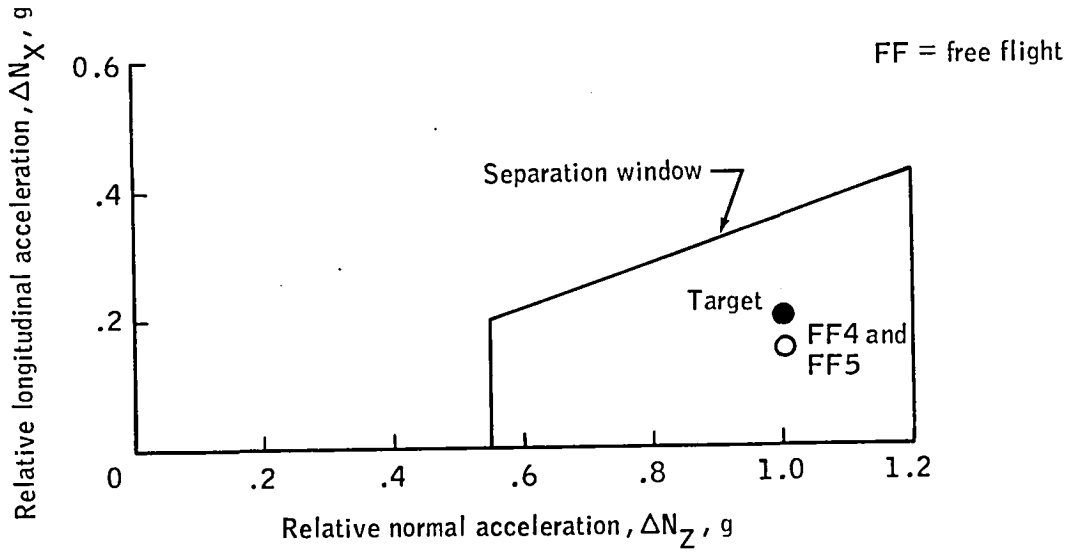

(b) Relative normal acceleration compared to relative longitudinal acceleration.

Figure 20.- Orbiter tailcone-off separation initial conditions.

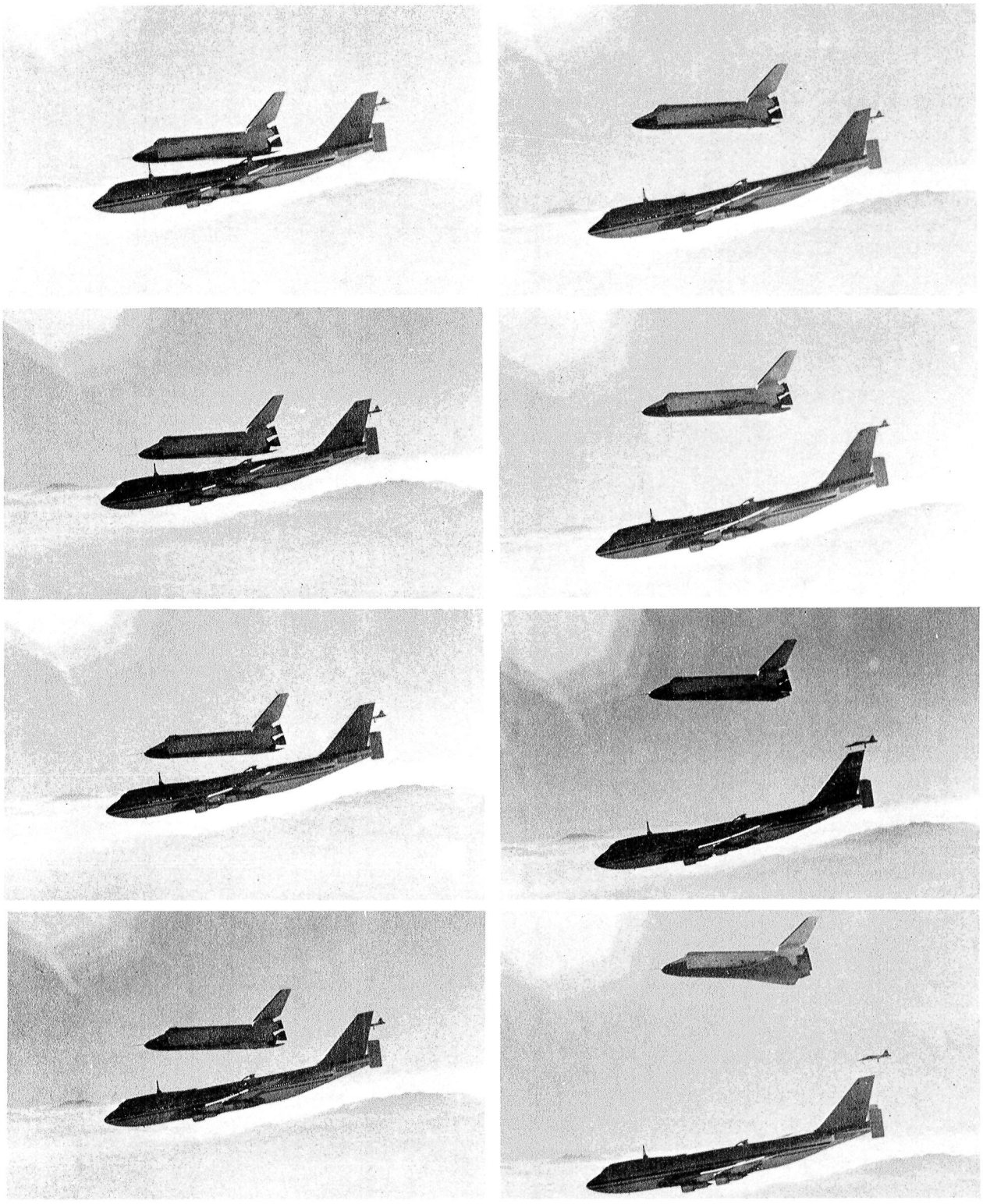

Figure 21.- Free flight 5, SCA/Orbiter tailcone-off separation trajectory (2 frames per second).

APPENDIX - GRACIE PROGRAM

The Ground Reduced Aerodynamic Coefficients and Instrumentation Errors (GRACIE) program was developed as a tool to aid in flight test verification of the Orbiter/Shuttle Carrier Aircraft (SCA) separation aerodynamic data base. The program calculates the force and moment coefficients of each vehicle in proximity to the other, using the load measurement system (LMS) data, the flight instrumentation data (α, β, body rates, accelerations, etc.), and the vehicle mass properties. The uncertainty in each coefficient is determined, based on the quoted instrumentation accuracies. (Units of measurement are those used in the software design.)

SYMBOLS

$[A]$ transformation matrix to change from SCA body axis to Orbiter body axis coordinate system

$$\begin{bmatrix} \cos i_o & 0 & -\sin i_o \\ 0 & 1 & 0 \\ \sin i_o & 0 & \cos i_o \end{bmatrix}$$

C vehicle aerodynamic coefficients

C coefficients

F vehicle forces

F load cell force components

$[G]$ transformation matrix to change from body axis to stability axis

$$\begin{bmatrix} -\cos \alpha_o & 0 & -\sin \alpha_o \\ 0 & 1 & 0 \\ \sin \alpha_o & 0 & \cos \alpha_o \end{bmatrix}$$

$[I]$ vehicle inertia matrix, slug-ft^2

$$\begin{bmatrix} I_{XX} & 0 & -I_{XZ} \\ 0 & I_{YY} & 0 \\ -I_{XZ} & 0 & I_{ZZ} \end{bmatrix}$$

i_o Orbiter incidence angle, deg

L attach strut forces as measured by the load measurement system, lb

ℓ vehicle reference length used for calculating vehicle moment coefficients, ft

M vehicle moments

m vehicle mass, slugs

N_X, N_Y, N_Z linear acceleration at vehicle center of gravity, g

p vehicle roll rate, deg/sec

$\dot{p}$ vehicle roll acceleration, deg/sec^2

q vehicle pitch rate, deg/sec

$\bar{q}$ dynamic pressure, lb/ft^2

$\dot{q}$ vehicle pitch acceleration, deg/sec^2

R vehicle position vector

r vehicle yaw rate, deg/sec

$\dot{r}$ vehicle yaw acceleration, deg/sec^2

S vehicle reference area, ft^2

T SCA thrust, lb

V velocity, ft/sec

W vehicle weight, lb

X,Y,Z rectangular Cartesian coordinates

α vehicle angle of attack, deg

β	vehicle angle of sideslip, deg
γ	vehicle flightpath angle, deg
ΔN_X, ΔN_Y, ΔN_Z	relative load factors, g
θ	vehicle pitch angle, deg
$\ddot{\theta}$	Orbiter instantaneous pitch acceleration, deg/sec^2
λ	tilt angle of forward strut, deg
$\boldsymbol{\rho}$	center of gravity (c.g.) relative position vector (ΔX, ΔY, ΔZ), ft
ρ	c.g. to attach strut moment arm, ft
ϕ	vehicle roll angle, deg
ψ	vehicle yaw angle, deg
$\boldsymbol{\omega}$	vehicle angular velocity vector - p,q,r
$\dot{\boldsymbol{\omega}}$	vehicle angular acceleration vector - $\dot{p},\dot{q},\dot{r}$

Subscripts:

A	axial
a	aft
c	SCA vehicle
c.g.	center of gravity
f	forward
D	drag
L	left
N	normal
o	Orbiter vehicle
R	right

Operator:

(')	uncertainty in designated coefficient

PROGRAM DESCRIPTION AND ASSUMPTIONS

The GRACIE program uses flight test data to determine aerodynamic coefficients and their corresponding uncertainties for comparison with wind tunnel predicted values. The program manipulates LMS forces, SCA body motions, vehicle configurations, and vehicle mass properties to output tabulated and plotted time histories of Orbiter proximity, SCA proximity, and mated vehicle aerodynamic force and moment coefficients, as well as relative normal load factor (ΔN_Z) and Orbiter instantaneous pitch acceleration ($\ddot{\theta}_o$). The LMS data, the SCA body motion data, and the vehicle configuration are obtained from a ground-recorded telemetry data tape on which all instrumentation calibrations have been recorded. The vehicle mass properties and the SCA predicted data time histories are input through subroutines because they require postflight calculations and are not recorded on the data tape.

The program performs three basic operations using the flight test data. The equations of motion and the aerodynamic uncertainty calculations are made with data retrieved from flight test instrumentation, and the predicted values of the coefficients are determined. The following sections describe these operations.

Equations of Motion

As a basis for calculating equations of motion, the mated vehicle is assumed to be a rigid body in motion with respect to a fixed coordinate system XYZ (fig. 22). Affixing a second set of axes to the carrier aircraft, with the origin (c) located at the carrier c.g., and observing its motion allows evaluation of the motion of any other point in the mated configuration, namely the Orbiter c.g., as well as the mated c.g. For example, the acceleration of the Orbiter c.g. (o) can be determined by knowing the relative position (ρ), the linear acceleration ($\ddot{R}$), angular rates (ω), and angular accelerations ($\dot{\omega}$) of the carrier c.g. (c).

$$\ddot{R}_o = \ddot{R}_c + \dot{\omega}_c \times \rho + \omega_c \times (\omega_c \times \rho) + \alpha_{o/c} + 2\omega_c \times V_{o/c}$$

However, the mated vehicle is assumed to be a rigid body; therefore, the relative velocities and accelerations between the c.g.'s are

$$\alpha_{o/c} = V_{o/c} = 0$$

Therefore,

$$\ddot{R}_o = \ddot{R}_c + \dot{\omega}_c \times \rho + \omega_c \times (\omega_c + \rho)$$

The total resultant or applied forces on either vehicle are then

$$F_{c\ \text{total applied}} = m_c \ddot{R}_c$$

$$F_{o\ \text{total applied}} = m_o \ddot{R}_o$$

and

$$F_{m\ \text{total applied}} = m_m \ddot{R}_m$$

Similar use of kinematics provides the equations for calculating the resultant moments (M) on each vehicle, i.e.

$$M_{c\ \text{total applied}} = [I]_c \dot{\omega}_c + \omega_c \times [I]_c \omega_c$$

$$M_{o\ \text{total applied}} = [I]_o \dot{\omega}_o + \omega_o \times [I]_o \omega_o$$

and

$$M_{m\ \text{total applied}} = [I]_m \dot{\omega}_m + \omega_m \times [I]_m \omega_m$$

where

$$\omega_o = [A]\omega_c, \quad \dot{\omega}_o = [A]_c \dot{\omega}$$

and

$$\omega_m = \omega_c, \quad \dot{\omega}_m = \dot{\omega}_c$$

From figure 23, the load cell outputs, expressed in the carrier body axis coordinate system, are as follows:

F_{f_Y} = forward side force

F_{f_Z} = forward vertical force (parallel to strut axis)

$F_{f_{X_7}}$, $F_{f_{Z_7}}$ = drag and vertical components of forward vertical strut force (carrier body axis coordinate system)

F_{L_X} = left aft drag force

F_{L_Z} = left aft vertical force

F_{R_X} = right aft drag force

F_{R_Y} = right aft side force

F_{R_Z} = right aft vertical force

where

$$F_{f_{X_7}} = F_{f_Z} \sin \lambda, \quad F_{f_{Z_7}} = F_{f_Z} \cos \lambda$$

and

$$\lambda = 88.27^\circ - \sin^{-1}\left[\frac{929.098 \sin\left(i_o + 2.734^\circ\right)}{1723336.5 - 1723333.7 \cos\left(i_o + 2.734^\circ\right)}\right]$$

Also shown in figure 23 are the moment arms ($\ell_1, \ell_2, \ldots, \ell_7$) from the Orbiter c.g. to each load cell attach point, based on the carrier body axis coordinate system. Using figure 23 in conjunction with figure 24, the moment arms are determined from the following relations, noting that the attach point locations are in the Orbiter body coordinate system:

$$\phi_f = \tan^{-1}\left(\frac{Z_{c.g._o} - Z_f}{X_{c.g._o} - X_f}\right)$$

$$\phi_a = \tan^{-1}\left(\frac{Z_{c.g._o} - Z_R}{X_R - X_{c.g._o}}\right)$$

$$\ell_f = \left(\frac{Z_{c.g._o} - Z_f}{\sin \phi_f}\right)$$

$$\ell_a = \left(\frac{Z_{c.g._o} - Z_R}{\sin \phi_a}\right)$$

$$\ell_1 = \ell_a \sin(\phi_a + i_o)/12$$

$$\ell_2 = \ell_a \cos(\phi_a + i_o)/12$$

$$\ell_3 = \ell_f \sin(\phi_f - i_o)/12$$

$$\ell_4 = \ell_f \cos(\phi_f - i_o)/12$$

$$\ell_5 = -(Y_L + Y_{c.g._o})/12$$

$$\ell_6 = (Y_R - Y_{c.g._o})/12$$

From figure 25, and using the Orbiter moment arms previously calculated, the position vector is

$$\rho = \begin{bmatrix} \ell_2 - \left(X_R - X_{c.g._{747}}\right)/12 \\ \left(Y_{c.g._o} - Y_{c.g._{747}}\right)/12 \\ \left(Z_{c.g._{747}} - Z_R\right)/12 - \ell_1 \end{bmatrix}$$

Notice that in figure 25, the attach point locations are in the carrier body axis coordinate system.

The following free body diagrams and corresponding equations of motion are used in calculating the aerodynamic force and moment coefficients of the mated vehicle, the SCA in proximity to the Orbiter, and the Orbiter in proximity to the SCA.

Mated vehicle aerodynamic coefficients.- Force coefficients (drag, side force, lift)

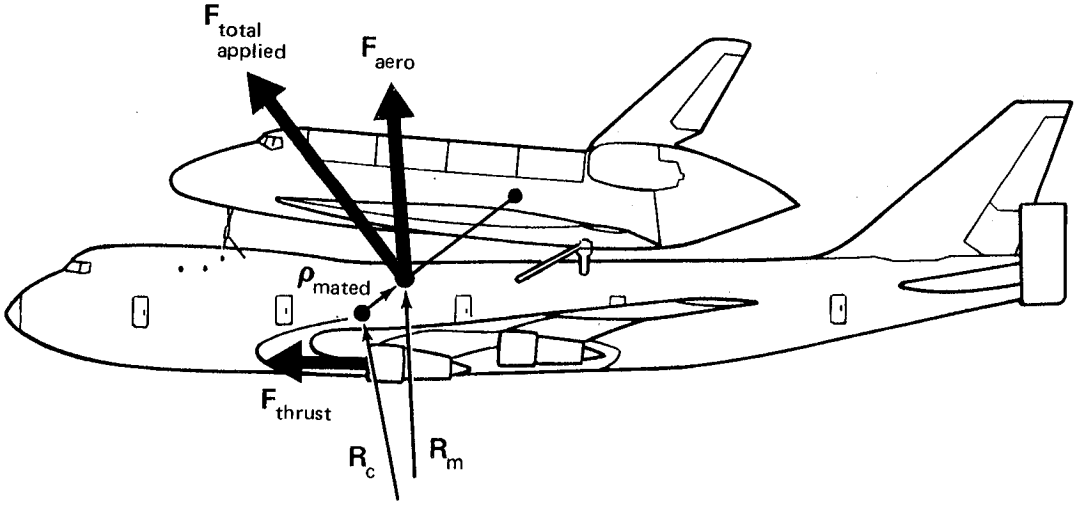

$$F_{\substack{\text{total} \\ \text{applied}}} = F_{aero} + F_{thrust}$$

$$F_{\substack{\text{total} \\ \text{applied}}} = m_m \ddot{R}_m = m_m \left[\ddot{R}_c + \dot{\omega}_c \times \rho_m + \omega_c \times \left(\omega_c \times \rho_m\right)\right]$$

$$F_{aero} = m_m \ddot{R}_m - F_{thrust}$$

$$C_{\substack{body \\ axis}} = \frac{F_{aero}}{\bar{q}S_c}$$

$$C_{\substack{stability \\ axis}} = [G]_c C_{\substack{body \\ axis}}$$

$[G]_c$ = Transformation matrix to change from carrier body axis to carrier stability axis

Mated vehicle aerodynamic coefficients.- Moment coefficients (rolling moment, pitching moment, yawing moment)

$$M_{\substack{total \\ applied}} = M_{aero} + M_{thrust}$$

$$M_{\substack{total \\ applied}} = [I]_m \dot{\omega}_c + \omega_c \times [I]_m \omega_c$$

$$M_{aero} = M_{\substack{total \\ applied}} - M_{thrust}$$

$$C_{moment} = \frac{M_{aero}}{\bar{q}S_c \ell_c}$$

Carrier aerodynamic coefficients (proximity).- Force coefficients (drag, side force, lift)

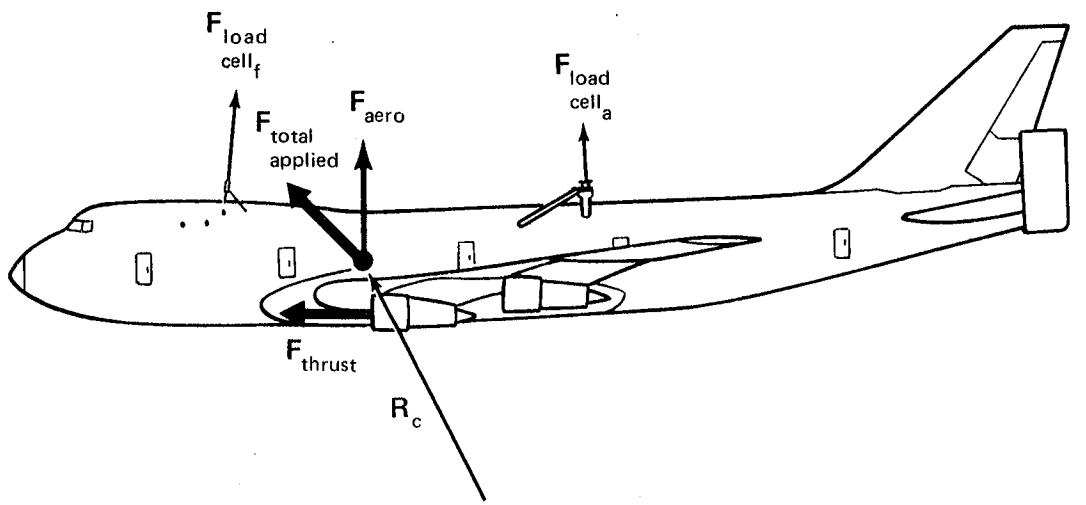

$$F_{\substack{\text{total}\\\text{applied}}} = F_{\text{aero}} + F_{\substack{\text{load}\\\text{cell}}} + F_{\text{thrust}}$$

$$F_{\substack{\text{total}\\\text{applied}}} = m_c \ddot{R}_c$$

$$F_{\substack{\text{load}\\\text{cell}}} = L_c = L_f + L_L + L_R$$

$$F_{\text{aero}} = m_c \ddot{R}_c - F_{\substack{\text{load}\\\text{cell}}} - F_{\text{thrust}}$$

$$C_{\substack{\text{body}\\\text{axis}}} = \frac{F_{\text{aero}}}{\bar{q} S_c}$$

$$C_{\substack{\text{stability}\\\text{axis}}} = [G]_c C_{\substack{\text{body}\\\text{axis}}}$$

Carrier aerodynamic coefficients (proximity).- Moment coefficients (rolling moment, pitching moment, yawing moment)

$$M_{\substack{\text{total}\\\text{applied}}} = M_{\text{aero}} + M_{\substack{\text{load}\\\text{cell}}} + M_{\text{thrust}}$$

$$M_{\substack{\text{total}\\\text{applied}}} = [I]_c \dot{\omega}_c + \omega_c \times [I]_c \omega_c$$

$$M_{\substack{\text{load}\\\text{cell}}} = \sum_{s=1}^{3} \left(\rho_{s_c} \times L_{s_c} \right)$$

$$M_{\text{aero}} = M_{\substack{\text{total}\\\text{applied}}} - M_{\substack{\text{load}\\\text{cell}}} - M_{\text{thrust}}$$

$$C_{\text{moment}} = \frac{M_{\text{aero}}}{\bar{q} S_c \ell_c}$$

Orbiter aerodynamic coefficients (proximity).- Force coefficients (drag, side force, lift)

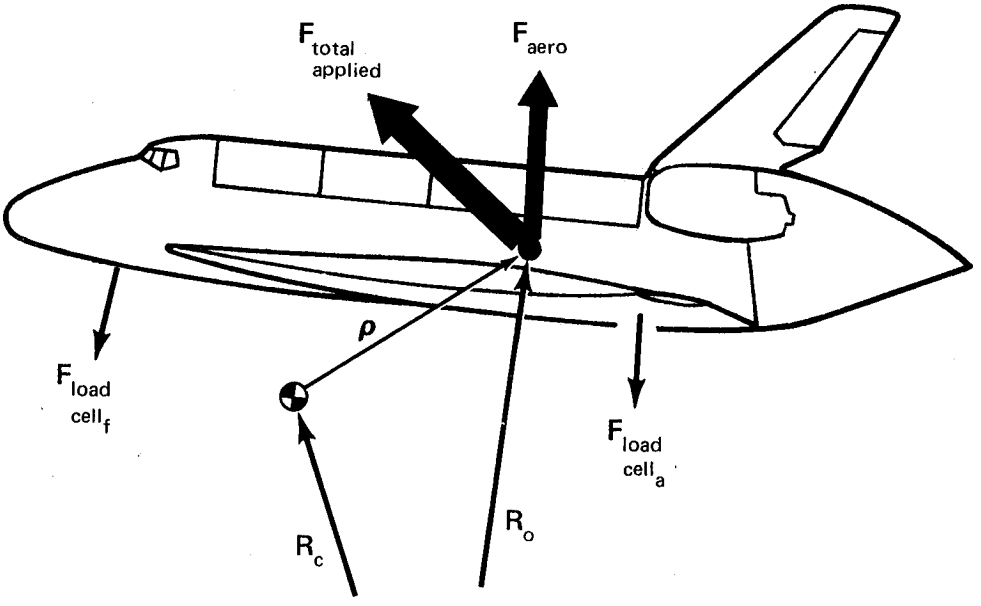

$$F_{\substack{total\\applied}} = F_{aero} + F_{\substack{load\\cell}}$$

$$F_{\substack{total\\applied}} = m_o \ddot{R}_o = m_o \left[\ddot{R}_c + \dot{\omega}_c \times \rho + \omega_c \times (\omega_c \times \rho) \right]$$

$$F_{\substack{load\\cell}} = L_o = L_f + L_L + L_R$$

$$F_{aero} = [A]\left(m_o \ddot{R}_o - L_o\right)$$

$$C_{\substack{body\\axis}} = \frac{F_{aero}}{\bar{q}\, S_o}$$

$$C_{\substack{stability\\axis}} = [G]_o\, C_{\substack{body\\axis}}$$

[A] = Transformation from carrier to Orbiter coordinate system at incidence angle i_o

Orbiter aerodynamic coefficients (proximity).- Moment coefficients (rolling moment, pitching moment, yawing moment)

$$M_{\substack{\text{total}\\\text{applied}}} = M_{\text{aero}} - M_{\substack{\text{load}\\\text{cell}}}$$

$$M_{\substack{\text{total}\\\text{applied}}} = [I]_o \dot{\boldsymbol{\omega}}_o + \boldsymbol{\omega}_o \times [I]_o \boldsymbol{\omega}_o$$

$$M_{\substack{\text{load}\\\text{cell}}} = \sum_{s=1}^{3} \left(\boldsymbol{\rho}_{s_o} \times \mathbf{L}_{s_o} \right)$$

$$M_{\text{aero}} = M_{\substack{\text{total}\\\text{applied}}} - M_{\substack{\text{load}\\\text{cell}}}$$

$$C_{\text{moment}} = \frac{M_{\text{aero}}}{\bar{q} S_o \ell_o}$$

Orbiter pitch acceleration:

$$\ddot{\theta} = \frac{M_{\text{aero}_Y}}{I_{YY_o}}$$

Relative load factors:

$$\Delta N_z = L_o \left(\frac{W_o + W_c}{W_o W_c} \right)$$

Aerodynamic Uncertainties

An integral part of the separation analysis is knowing the uncertainty associated with each coefficient and how that uncertainty affects the size of the separation window as well as the vehicle trajectory. Each aerodynamic coefficient is a function of i independent measurements, n_i, and the uncertainty of each measurement is Δn_i.

$$C = f(n_1, n_2, n_3, \ldots, n_i) \qquad (1)$$

The uncertainty in each calculated coefficient is obtained by using the following equation:

$$\Delta C = \left[\left(\frac{\delta C}{\delta n_1}\right)^2 (\Delta n_1)^2 + \left(\frac{\delta C}{\delta n_2}\right)^2 (\Delta n_2)^2 + \ldots + \left(\frac{\delta C}{\delta n_i}\right)^2 (\Delta n_i)^2\right]^{1/2} \qquad (2)$$

The uncertainties in the aerodynamic coefficients are based on the quoted accuracies of the load measurement system and the flight test instrumentation.

The uncertainty in the Orbiter force and moment coefficients are calculated as follows. The Orbiter aerodynamic forces are first calculated with respect to the SCA body coordinate system from the following equations:

$$C_X = \frac{m_o\left(N_X + \dot{q}\Delta Z - \dot{r}\Delta Y + qp\Delta Y - q^2\Delta X + rp\Delta Z - r^2\Delta X\right) - \Sigma F_X}{\bar{q}S_o}$$

$$C_Y = \frac{m_o\left(N_Y - \dot{p}\Delta Z + \dot{r}\Delta X - p^2\Delta Y + pq\Delta X + rq\Delta Z - r^2\Delta Y\right) - \Sigma F_Y}{\bar{q}S_o}$$

$$C_Z = \frac{m_o\left(N_Z + \dot{p}\Delta Y - \dot{q}\Delta X - p^2\Delta Z + pr\Delta X - q^2\Delta Z + qr\Delta Y\right) - \Sigma F_Z}{\bar{q}S_o}$$

From equation (2), the uncertainty in C_X is

$$N'_X = \left(\frac{m_o}{\bar{q}S_o}\right)^2 (\Delta N_X)^2$$

$$p' = \left[\frac{m_o(q\Delta Y + r\Delta Z)}{\bar{q}S_o}\right]^2 (\Delta p)^2$$

$$q' = \left[\frac{m_o(p\Delta Y - 2q\Delta X)}{\bar{q}S_o}\right]^2 (\Delta q)^2$$

$$r' = \left[\frac{m_o(p\Delta Z - 2q\Delta X)}{\bar{q}S_o}\right]^2 (\Delta r)^2$$

$\dot{p}'$ = negligible

$$\dot{q}' = \left(\frac{m_o \Delta Z}{\bar{q}S_o}\right)^2 (\Delta \dot{q})^2$$

$$\dot{r}' = \left(\frac{m_o \Delta Y}{\bar{q}S_o}\right)^2 (\Delta \dot{r})^2$$

$$\bar{q}' = \left[\frac{-m_o(N_X + \dot{q}\Delta Z - \dot{r}\Delta Y - qp\Delta Y - q^2\Delta X + rp\Delta Z - r^2\Delta X) + L_X}{\bar{q}^2 S_o}\right]^2 (\Delta \bar{q})^2$$

$$F'_{f_X} = \left(\frac{1}{\bar{q}S_o}\right)^2 \left(\Delta F_{f_X}\right)^2$$

$$F'_{L_X} = \left(\frac{1}{\bar{q}S_o}\right)^2 \left(\Delta F_{L_X}\right)^2$$

$$F'_{R_X} = \left(\frac{1}{\bar{q}S_o}\right)^2 \left(\Delta F_{R_X}\right)^2$$

$$\Delta C_X = \left(N'_X + p' + q' + r' + \dot{p}' + \dot{q}' + \dot{r}' + \bar{q}' + F'_{f_X} + F'_{L_X} + F'_{R_X}\right)^{1/2}$$

The uncertainty in C_Z is calculated similarly. The coefficients are then transformed into the Orbiter body axis coordinate system.

$$C_{A_o} = C_X \cos i_o - C_Z \sin i_o$$

$$C_{N_o} = C_X \sin i_o + C_Z \cos i_o$$

The uncertainties in these two coefficients are

$$\Delta C_{A_o} = \left[(\cos i_o)^2 (\Delta C_X)^2 + (\sin i_o)^2 (\Delta C_Z)^2\right]^{1/2}$$

$$\Delta C_{N_o} = \left[(\sin i_o)^2 (\Delta C_X)^2 + (\cos i_o)^2 (\Delta C_Z)^2\right]^{1/2}$$

Finally, these coefficients are transformed into the Orbiter stability axis coordinate system

$$C_{D_o} = C_{A_o} \cos(\alpha_c + i_o) + C_{N_o} \sin(\alpha_c + i_o)$$

$$C_{lift_o} = -C_{A_o} \sin(\alpha_c + i_o) + C_{N_o} \cos(\alpha_c + i_o)$$

and the uncertainties in the Orbiter coefficients of lift and drag are

$$\Delta C_{lift_o} = \Big\{\left[\cos(\alpha_c + i_o)\right]^2 (\Delta C_{A_o})^2 + \left[\sin(\alpha_c + i_o)\right]^2 (\Delta C_{N_o})^2 + \left[C_{A_o} \sin(\alpha_c + i_o) - C_{N_o} \cos(\alpha_c + i_o)\right]^2 (\Delta\alpha_c)^2\Big\}^{1/2}$$

$$\Delta C_{D_o} = \Big\{\left[\sin(\alpha_c + i_o)\right]^2 (\Delta C_{A_o})^2 + \left[\cos(\alpha_c + i_o)\right]^2 (\Delta C_{N_o})^2 + \left[C_{A_o} \cos(\alpha_c + i_o) + C_{N_o} \sin(\alpha_c + i_o)\right]^2 (\Delta\alpha_c)^2\Big\}^{1/2}$$

The uncertainty in the Orbiter side force coefficient, ΔC_{Y_o}, is found in the same way.

The Orbiter moment coefficients are based on the following equations:

$$C_{m_X} = \frac{\dot{p}_o I_{XX} + q_o r_o \left(I_{ZZ_o} - I_{YY_o}\right) + I_{XZ_o}\left(\dot{r}_o + p_o q_o\right)}{\bar{q} S_o b_o}$$

$$+ \frac{- F_{fZ}\rho_{fY} + F_{fY}\rho_{fZ} - F_{LZ}\rho_{LY} - F_{RZ}\rho_{fY} + F_{RY}\rho_{RZ}}{\bar{q} S_o b_o}$$

$$C_{m_Y} = \frac{\dot{q}_o I_{YY_o} + p_o r_o \left(I_{XX_o} - I_{ZZ_o}\right) + I_{XZ_o}\left(r_o^2 - p_o^2\right)}{\bar{q} S_o \bar{c}_o}$$

$$+ \frac{F_{fZ}\rho_{fX} - F_{fX}\rho_{fZ} + F_{LZ}\rho_{LX} - F_{LX}\rho_{LZ} + F_{RZ}\rho_{RX} - F_{RX}\rho_{RZ}}{\bar{q} S_o \bar{c}_o}$$

$$C_{m_Z} = \frac{\dot{r}_o I_{ZZ_o} + p_o q_o \left(I_{YY_o} - I_{XX_o}\right) - I_{XZ_o}\left(q_o r_o - \dot{p}_o\right)}{\bar{q} S_o b_o}$$

$$+ \frac{- F_{fY}\rho_{fX} + F_{fX}\rho_{fY} + F_{LX}\rho_{LY} - F_{RY}\rho_{RX} + F_{RX}\rho_{RY}}{\bar{q} S_o b_o}$$

Again using equation (2), the uncertainty in the Orbiter pitching moment is

$$\dot{q}' = \left(\frac{I_{YY_o}}{\bar{q} S_o \bar{c}}\right)^2 \left(\Delta \dot{q}\right)^2$$

$$p' = \left[\frac{r_o\left(I_{XX_o} - I_{ZZ}\right) + 2p_o I_{XZ_o}}{\bar{q}S_o\bar{c}}\right]^2 (\Delta p)^2$$

$$r' = \left[\frac{p_o\left(I_{XX_o} - I_{ZZ_o}\right) - 2r_o I_{XZ_o}}{\bar{q}S_o\bar{c}}\right]^2 (\Delta r)^2$$

$$\bar{q}' = \left[\frac{\dot{q}_o I_{YY_o} + p_o r_o\left(I_{XX_o} - I_{XZ_o}\right) + I_{XZ_o}\left(r_o^2 - p_o^2\right)}{\bar{q}^2 S_o\bar{c}}\right.$$

$$\left. + \frac{F_{fZ}\rho_{fX} - F_{fX}\rho_{fZ} + F_{LZ}\rho_{LX} - F_{LX}\rho_{LZ} + F_{RZ}\rho_{RX} - F_{RX}\rho_{RZ}}{\bar{q}^2 S_o\bar{c}}\right]^2 (\Delta\bar{q})^2$$

$$F'_{fZ} = \left(\frac{\rho_{fX}}{\bar{q}S_o\bar{c}}\right)^2 \left(\Delta F_{fZ}\right)^2$$

$$F'_{fX} = \left(\frac{\rho_{fZ}}{\bar{q}S_o\bar{c}}\right)^2 \left(\Delta F_{fX}\right)^2$$

$$F'_{LZ} = \left(\frac{\rho_{LX}}{\bar{q}S_o\bar{c}}\right)^2 \left(\Delta F_{LZ}\right)^2$$

$$F'_{LX} = \left(\frac{\rho_{LZ}}{\bar{q}S_o\bar{c}}\right)^2 \left(\Delta F_{LX}\right)^2$$

$$F'_{RZ} = \left(\frac{\rho_{RX}}{\bar{q}S_o\bar{c}}\right)^2 \left(\Delta F_{RZ}\right)^2$$

$$F'_{RX} = \left(\frac{\rho_{RZ}}{\bar{q}S_o\bar{c}}\right)^2 \left(\Delta F_{RX}\right)^2$$

$$\Delta C_{m_Y} = \left(\dot{q}' + p' + r' + \bar{q}' + F'_{fZ} + F'_{fX} + F'_{LZ} + F'_{LX} + F'_{RZ} + F'_{RX}\right)^{1/2}$$

The uncertainties in the rolling moment and the yawing moment are calculated similarly.

Analysis of the uncertainties in the SCA proximity and mated vehicle coefficients is performed in a like manner.

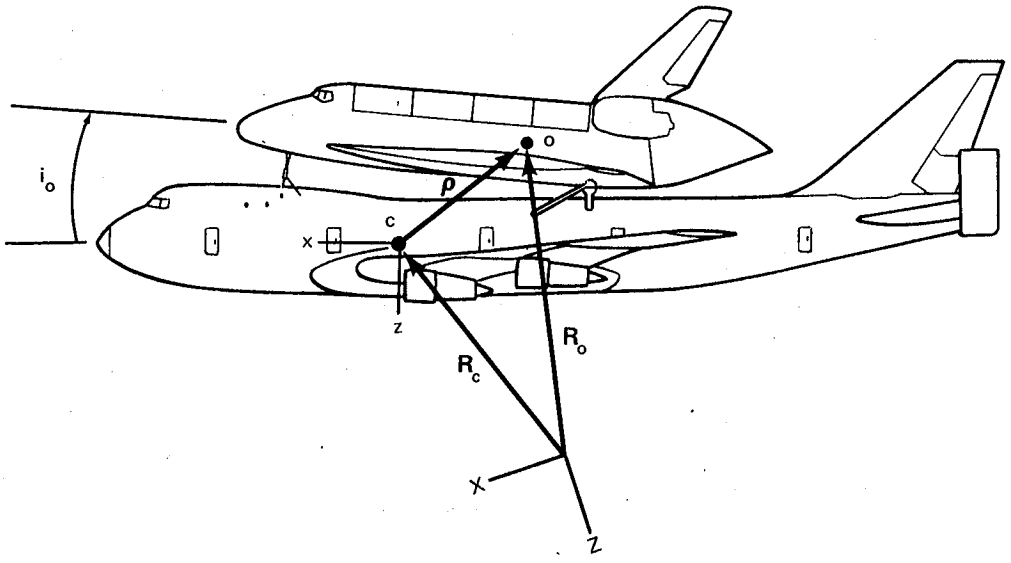

Figure 22.- Vehicle coordinate system.

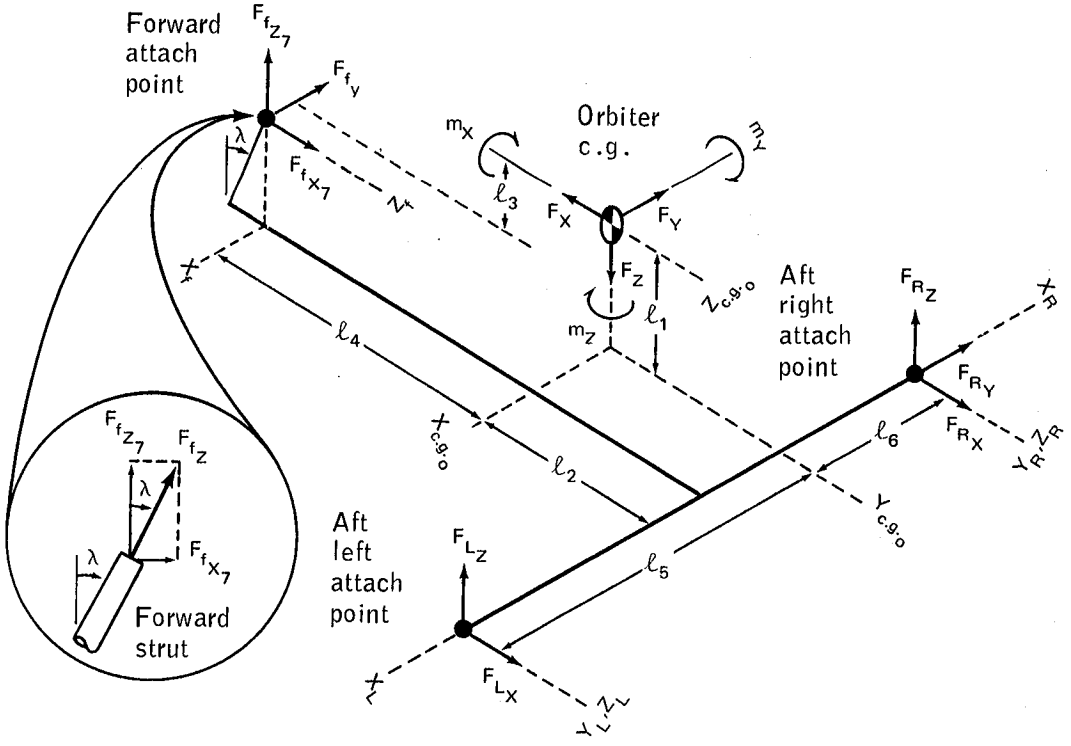

Figure 23.- Orbiter attach point geometry.

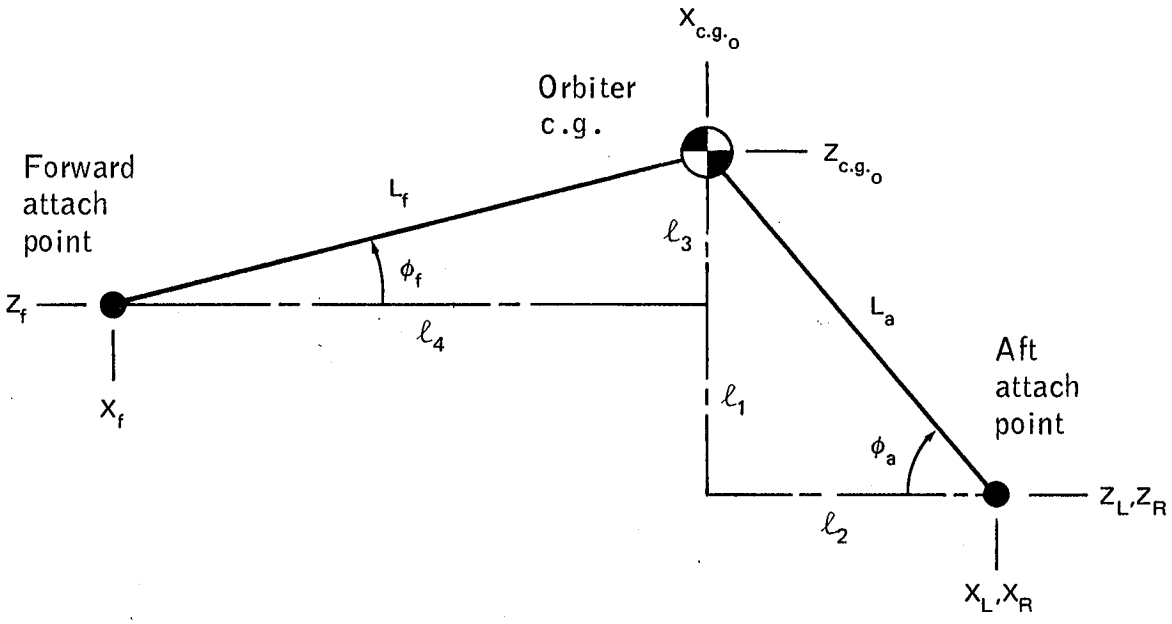

Figure 24.- Orbiter attach point moment arms.

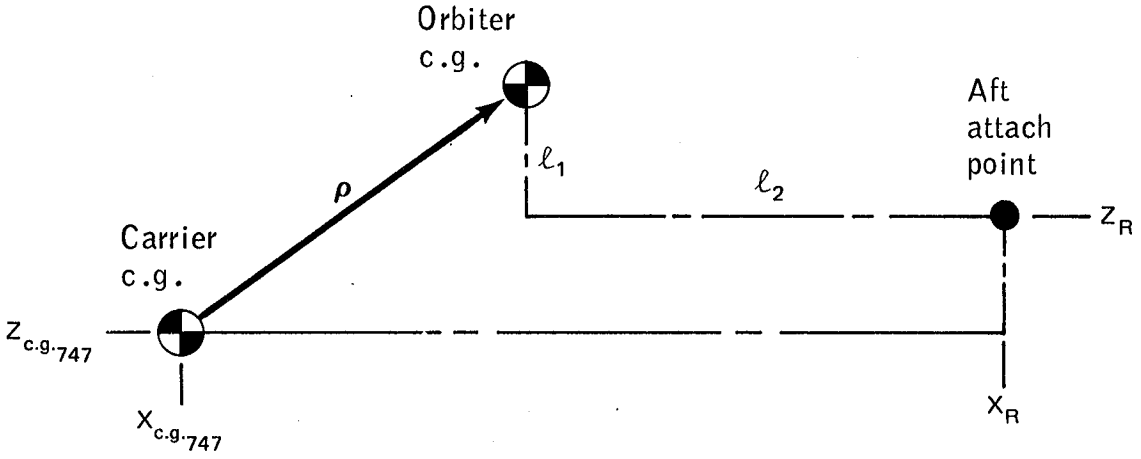

Figure 25.- Relative c.g. locations.

1. Report No.	2. Government Accession No.	3. Recipient's Catalog No.
NASA TM-58223		

4. Title and Subtitle	5. Report Date
ORBITER/SHUTTLE CARRIER AIRCRAFT SEPARATION: WIND TUNNEL, SIMULATION, AND FLIGHT TEST OVERVIEW AND RESULTS	May 1980
	6. Performing Organization Code: JSC-16711
7. Author(s): D. J. Homan, JSC, and D. E. Denison and K. C. Elchert, Rockwell International	8. Performing Organization Report No.
9. Performing Organization Name and Address: Lyndon B. Johnson Space Center, Houston, Texas 77058	10. Work Unit No.: 953-36-00-00-72
	11. Contract or Grant No.
12. Sponsoring Agency Name and Address: National Aeronautics and Space Administration, Washington, D.C. 20546	13. Type of Report and Period Covered: Technical Memorandum
	14. Sponsoring Agency Code

15. Supplementary Notes

16. Abstract

A summary of the approach and landing test phase of the Space Shuttle Program is given from the Orbiter/Shuttle Carrier Aircraft separation point of view. Material in the report covers the data and analyses used during the wind tunnel testing, simulation, and flight test phases in preparation for the Orbiter approach and landing tests. Predicted separation parameters are compared to actual flight data.

17. Key Words (Suggested by Author(s))	18. Distribution Statement
Test flights Space Shuttle Orbiter Wind tunnel Simulations Free flight Active-captive flight Captive-active flight Approach and landing tests	STAR Subject Category: 18 (Spacecraft Design, Testing, and Performance)

19. Security Classif. (of this report)	20. Security Classif. (of this page)	21. No. of Pages	22. Price*
Unclassified	Unclassified	87	$5.00

*For sale by the National Technical Information Service, Springfield, Virginia 22161

☆ U.S. GOVERNMENT PRINTING OFFICE: 1980—671-099/1610